Stony Brook University

Role of Sir3 N-terminus in Yeast Transcriptional Silencing

A Dissertation Presented

by

Peihua Yuan

To

The Graduate School

in Partial Fulfillment of the

Requirements

for the Degree of

Doctor of Philosophy

in

Biochemistry and Structural Biology

Stony Brook University

May 2008

Stony Brook University

The Graduate School

Peihua Yuan

We, the dissertation committee for the above candidate for the

Doctor of Philosophy degree,

hereby recommend acceptance of this dissertation.

Dr. Rolf Sternglanz, Dissertation Advisor

Distinguished Professor of Biochemistry and Cell Biology

Dr. Aaron Neiman, Chairperson of Defense

Associate Professor of Biochemistry and Cell Biology

Dr. Peter Gergen

Professor of Biochemistry and Cell Biology

Dr. Janet Leatherwood, Outside Member

Associate Professor of Molecular Genetics and Microbiology

This dissertation is accepted by the Graduate School

Lawrence Martin

Dean of the Graduate School

Abstract of Dissertation

Role of Sir3 N-terminus in Yeast Transcriptional Silencing

by

Peihua Yuan

Doctor of Philosophy

in

Biochemistry and Structural Biology

Stony Brook University

2008

This study focuses on the function of the Sir3 (Silencing information regulator) BAH (Bromo adjacent homology) domain which is located at the N-terminus of *Saccharomyces cerevisiae* Sir3 protein. Previous work has shown that the N-terminus of Sir3 is crucial for the function of Sir3 in transcriptional silencing. However, the precise biological role of the BAH domain is not fully understood.

My data show that the BAH domain, amino acids 1-214 of Sir3, can partially silence the *HM* loci in a *sir3*Δ strain as long as Sir1 is overexpressed. This BAH silencing requires the other silencing proteins, Sir1, Sir2 and Sir4. Chromatin-IP reveals that Sir3 N-terminal fragments spread from the silencers to the silenced loci, suggesting that the Sir3 BAH domain is sufficient to establish and maintain a heterochromatin state. The Sir3 BAH domain was found to bind to DNA and nucleosomes *in vitro*. This DNA and nucleosome binding capability probably contributes to silencing.

In an attempt to understand the role of the Sir3 BAH domain, I used mutagenesis to determine the specific residues within this domain that are required for the function of full-length Sir3 in silencing. A mutant library was constructed and screened for BAH mutations that affect silencing at telomeres. Ten mutants were obtained. All of them caused a telomeric silencing defect but *HMR* silencing was normal. All of them are *eso* (Enhancers of the *sir1* mutant) mutants in that their phenotype are greatly exacerbated by a *sir1*Δ mutation. A136T, C177R and S204P are the three most drastic *sir3* BAH mutations; they lead to a lack of *HML* silencing. According to the crystal structure of Sir3 BAH, these three residues are located around the same region of Sir3, implying this region is important for the function of the Sir3 BAH domain.

Table of Contents

List of Figures

List of Tables

Acknowledgements

I would like to thank my advisor, Dr. Rolf Strerglanz, for his guidance and help during my Ph.D study. He has taught and helped me in my research with great patient and kindness. From him, I have learned the manner of a devoted and energetic scientist and a knowledgeable and caring teacher. I am also very grateful to his useful and interesting suggestions about the English language, which made my life in graduate school more memorable.

I wish to thank Dr. Ann Sutton for her help and teaching. She has been always patient and helpful with my questions and problems in work. She worked hard to make our lab a pleasant and organized place for working and a warm family for all of the lab members to stay.

Thanks to Jessica J. Connelly, Vinaya Sampath and Xiaorong Wang for their friendship and all the inspiring suggestions and talks. Their thoughts and work directly contributed to my work related to *SIR3*. We are the “Sir3 BAH” team in the lab.

I would thank to Yao Yu for being both labmate and housemate, and sharing our experience in science and life. Thanks to Jie Ren for time we spent together on the same bench and for her great suggestions to my work. Thanks to Danielle DePeralta and Evelyn Prugar, the technicians in our lab, they have helped everybody in the lab and brought us laughter. Thanks to Chia-Lin Wang for his help

in work.

Thanks to the BSB program administrators, Mrs. Carol Juliano and Mrs. Beverly Pizza, for their help during my Ph.D studies. They have been always kind, patient and very helpful to me whenever I came to them with questions and requests.

I am thankful for my husband Yang Zhao. He gives me support, he's a team player, he stands beside me and he gives me a swift kick when I need it. He takes care of me, he loves me and he forgives me. We're not perfect, and we're not always going to get it right. But we do learn from our mistakes and we find new ways to make each other smile. He's my best friend. He's the person I want to talk to when things go wrong. He's the one I want to talk to when things go right. I am lucky and grateful. Thanks for the happiness and sadness we shared, sharing and will share.

I would thank to my mother for her love and support. Thanks to my cousin Jiang Hua for her friendship and helps. Thanks to my grandfather for his deep love and always thinks I am the best.

CHAPTER ONE

Background and Significance

I. Heterochromatin, nucleosome and histone

In eukaryotes, chromatin is found in two varieties: euchromatin and heterochromatin (Grunstein, 1998; Weiler *et al*., 1995). Originally, the two forms were distinguished cytologically by how darkly they stained - the former is lighter, while the latter stains darkly, indicating tighter packing. Heterochromatin is the higher-order chromatin structure, which is believed to serve several functions, from gene regulation to the protection of the integrity of chromosomes; all of these roles can be attributed to the dense packing of DNA, which makes it less accessible to protein factors that bind DNA or its associated factors (Merrick *et al*., 2006). Heterochromatin is stably inherited; when a cell divides the two daughter cells will typically contain heterochromatin within the same regions of DNA, resulting in epigenetic inheritance (Wallace *et al*., 2005).

The nucleosome is the fundamental repeating unit of chromatin, occurring generally every 157-240 bp (Figure 1). Nucleosomes package DNA into chromosomes inside the cell nucleus and control gene expression. The nucleosome core, the crucial part of the nucleosome, comprises an octamer, containing a single

histone H3-H4 tetramer and two histone H2A-H2B dimers, and 147 bp of DNA (Luger *et al*., 1997; Davey *et al*., 2002). Each of the four histones (H2A, H2B, H3, and H4) shares a very similar structural motif consisting of three alpha helices separated by loops. Histone H1 is the linker DNA between adjacent nucleosomes. There is about 50 bp of "linker DNA" that separates the core particles.

According to the crystal structure, the histone octamer likely interacts with the dsDNA every 10 bp. It has been shown that water molecules roughly double the number of histone-DNA interactions by acting as intermediates between atoms which would otherwise be too far apart to form hydrogen bonds (Davey *et al*., 2002). It is the flexibility in the formation of these water-mediated interactions which allows for the histone octamer to wrap a very wide variety of DNA sequences.

The end of each histone protein contains a tail of amino acid residues of different lengths, characteristic of that histone. The purpose of the tails are not totally clear at present, but they appear to contribute to the stability of the nucleosome (Brower-Toland *et al*., 2005) as well as to serve as docking sites for other proteins. The structure of the tails can be altered slightly by other enzymes in the nucleus and may play a significant role in the generation of a higher order chromatin structure (Luger *et al*., 1997).

Histones undergo posttranslational modifications which alter their interaction with DNA and nuclear proteins. The H3 and H4 histones have long tails protruding from the nucleosome which can be covalently modified at several places. These

modifications decorate the canonical histones (H2A, H2B, H3 and H4), as well as variant histones (such as H3.1, H3.3 and HTZ.1) (Berger, 2007).

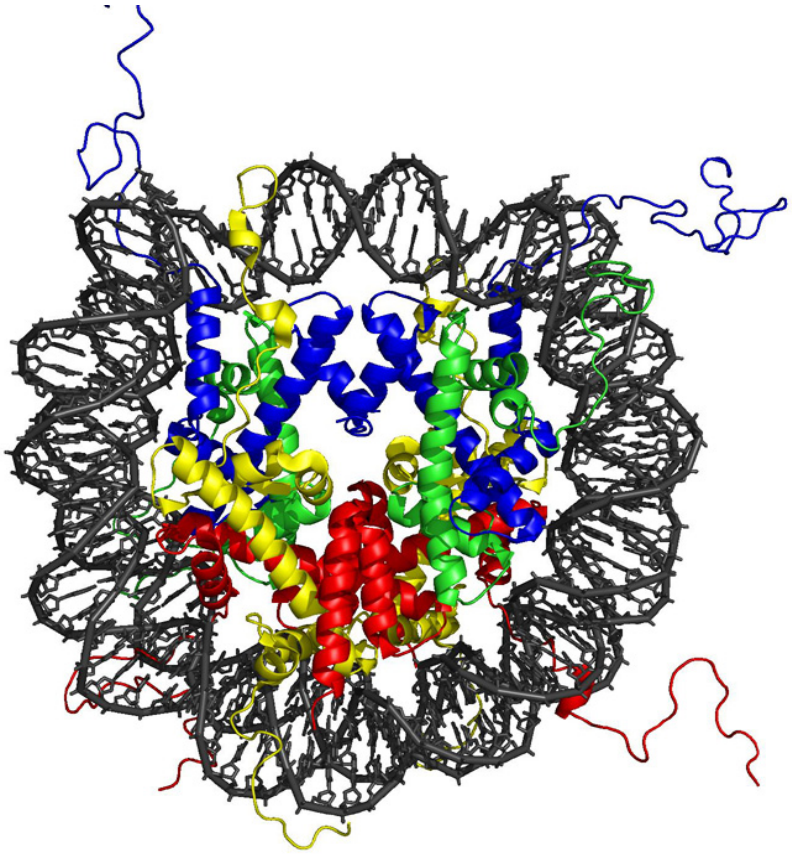

Figure 1: The crystal structure of the nucleosome core particle consisting of H2A (yellow), H2B (red), H3 (blue) and H4 (green) at 1.9 Å resolution. It shows the DNA double helix wound around the central histone octamer (PDB 1KX5).

Most modifications localize to the amino-(N-) and carboxy-(C-) terminal histone tails. Modifications of the tail include acetylation, phosphorylation, methylation, ubiquitylation and SUMOylation. The core of the histones can also be modified. Combinations of modifications are thought to constitute a code, the so-called "histone code" (Strahl *et al*., 2000; Jenuwein *et al*., 2001). Histone modifications act in diverse biological processes such as gene regulation, DNA

repair and chromosome condensation.

Histone acetylation emerges as a central switch that allows interconversion between permissive and repressive chromatin structures and domains. It is widely assumed that a particular histone acetylation patterns lead to altered folding of the nucleosomal fiber that renders chromosomal domains more accessible. As a consequence, the transcription machinery may be able to access promoters and hence initiate transcription more frequently. These principles are not only at the heart of transcriptional regulation but are also likely to govern other processes involving chromatin, including replication, site-specific recombination and DNA repair (Strahl *et al*., 2000).

II. Transcriptional silencing at *HM* loci and telomeres in *Saccharomyces cerevisiae*

In heterochromatin, nucleosomes are posttranslationally modified at specific sites and bind some non-histone chromatin proteins. Silencing of the mating-type loci, *HMR* and *HML*, and telomeres in *Saccharomyces cerevisiae* is a good model for studying heterochromatin formation. The Sir (silent information regulator) proteins are the structural proteins that regulate silent chromatin in *S. cerevisiae*. Nucleosomes in the silenced region are hypoacetylated, and the Sir proteins spread through this region to repress transcription (Rusche *et al*., 2002).

In *S. cerevisiae,* haploid cells are either one of two mating types, **a** or α. The

mating type is determined by the allele at the mating type locus *MAT*. *MAT***a** and *MAT*α encode regulatory proteins that, by affecting the expression of other genes, are responsible for the difference between the two mating types (Johnson, 1995). In addition to the *MAT* locus, all *S. cerevisiae* strains have unexpressed copies of mating type genes at two other loci, *HML* and *HMR*, located near the two telomeres on the same chromosome as *MAT* (Figure 2).

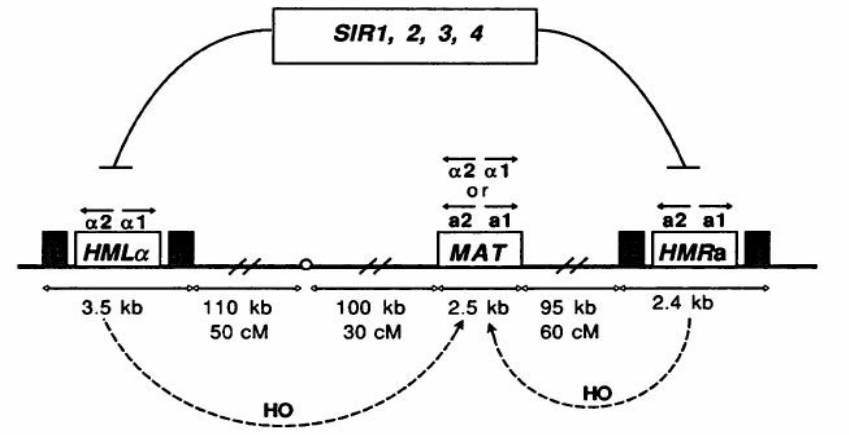

Figure 2: A schematic drawing of *Saccharomyces cerevisiae* chromosome III and the silenced *HM* loci. The three loci that contain the mating-type genes, *HML*, *MAT*, and *HMR*, are indicated. The *E* and *I* silencers flank *HML* and *HMR*. A double-stranded cleavage by the HO endonuclease initiates mating-type switching, which replaces the genes at *MAT* with copies of the genes at either *HML* or *HMR* (Laurenson *et al.*, 1992).

S. cerevisiae strains that express the HO endonuclease are able to switch mating types by replacing the allele at *MAT* with an allele copied from transcriptionally silent donor loci, *HML* and *HMR* (Figure 2). The silent *α1* and *α2* genes are usually found at the *HML* locus, and the silent *al* and *a2* genes are usually found at the *HMR* locus. *S. cerevisiae* strains which lack the HO gene, hence with stable mating types, still maintain transcriptionally repressed copies of mating-type

alleles at *HML* and *HMR*.

The *HM* loci are flanked by ~150 bp *cis*-acting elements, silencers *E* (essential) and *I* (important), both of which are located ~1 kb from the genes they regulate. The silencers function to initiate assembly of the SIR complex (Figure 3). They contain binding sites for the origin replication complex (ORC), repressor and activator protein 1 (Rap1), and ARS-binding factor (Abf1) (Lustig *et al*., 1998; Loo *et al*., 1995). Isolated binding sites for any of the silencer binding proteins, termed protosilencers, are unable to act as silencers on their own, but can function to enhance silencing by cooperating with intact, distant silencers (Boscheron *et al*., 1996). *HMR-E* is the best-characterized silencer. While mutations in any one of the protein-binding sites at the *HMR-E* locus have little effect on silencing (Brand *et al*., 1987; Kimmerly *et al*., 1988), a combination of mutations within the binding sites for ORC, Rap1 and Abf1 causes severe defects in *HMR* silencing (Kimmerly *et al*., 1988). The role of silencers is not limited to initiating silencing. Silencer *I*, for example, also serves as an insulator, separating active and inactive chromatin at *HML* (Bi *et al*., 1999).

Silencing at the *HM* loci requires the SIR complex, which is composed of Sir1, Sir2, Sir3 and Sir4 (Moazed *et al*., 1997). None of the *SIR* genes is essential for viability, but deletion of *SIR2*, *SIR3* or *SIR4* completely abolishes silencing, whereas disruption of *SIR1* partially reduces silencing.

In addition to the establishment of silent chromatin, the maintenance and stable

inheritance of the silenced state are also important for repression of the *HM* genes (Pillus *et al*., 1989). Sir2, Sir3 and Sir4 have been shown to be required for the maintenance of silent chromatin (Pillus *et al*., 1989). The mechanism by which Sir-mediated heterochromatin represses transcription is not well understood.

Telomeres are protein-DNA complexes formed at the end of chromosomes that are important for chromosome end stability and proper organization of chromosomes within the nucleus (Bryan *et al*., 1999; Zakian *et al*., 1996; Chikashige *et al*., 1997). In *S. cerevisiae*, telomeric DNA consists of TG_{1-3} repeats that are ~300 bp in length at the ends of chromosomes. These repeats are organized into a non-nucleosomal chromatin structure termed telosome (Wright *et al*., 1992). In some organisms, such as *S. cerevisiae, S. pombe, Drosophila* and humans, reporter genes placed near telomeres are repressed in a position-dependent manner, a phenomenon known as telomere position effect (TPE) (Levis *et al*., 1985; Gottschling *et al*., 1990; Nimmo *et al*., 1994; Baur *et al*., 2001).

Silencing at telomeres is similar to silencing at the *HM* loci (Figure 3). Telomere position effect requires most of the proteins required for silencing of the *HM* loci, except Sir1 and the ORC complex (Gottschling *et al*., 1990). Consequently, we treat silencing at the *HM* loci and telomeres as related phenomena, and "silenced chromatin" refers to both classes of silenced loci.

Compared with silencing at the *HM* loci, telomeric silencing is more sensitive to subtle changes in the level of silencing proteins (Aparicio *et al*., 1991). The

telomeres contain multiple Rap1-binding sites that recruit the SIR complex (Strahl-Bolsinger *et al*., 1997). Rap1 initiates silencing at telomeres by interacting through its C-terminal domain with Sir3 and Sir4, both of which are required for repression (Wotton *et al*., 1997). The association of Sir proteins with TG_{1-3} DNA repeats suggests that the Sir proteins may initially be recruited to the telomeric DNA (Bourns *et al*., 1998). Once assembled on telomeres, Sir proteins propagate over the nucleosomes to form a silent chromatin structure at the telomeres. Orc1, Abf1 and Sir1 are not required for the assembly of Sir proteins on the telomeres (Aparicio *et al*., 1991; Pillus *et al*., 1989).

III. Silencing initiation, spreading and maintains

Silenced chromatin formation occurs in discrete steps. First, the Sir proteins are recruited to the silencers or the telomeres. Then, Sir proteins spread throughout the target locus.

Sir proteins are recruited to silencers through a series of protein-protein interactions. Sir1 binds directly to Orc1 (Zhang *et al*., 2002; Triolo *et al*., 1996; Gardner *et al*., 1999) and enhances the probability of recruiting the other Sir proteins to the silencer. Sir1 localizes to silencers but does not spread throughout silenced regions (Rusche *et al*., 2002; Zhang *et al*., 2002).

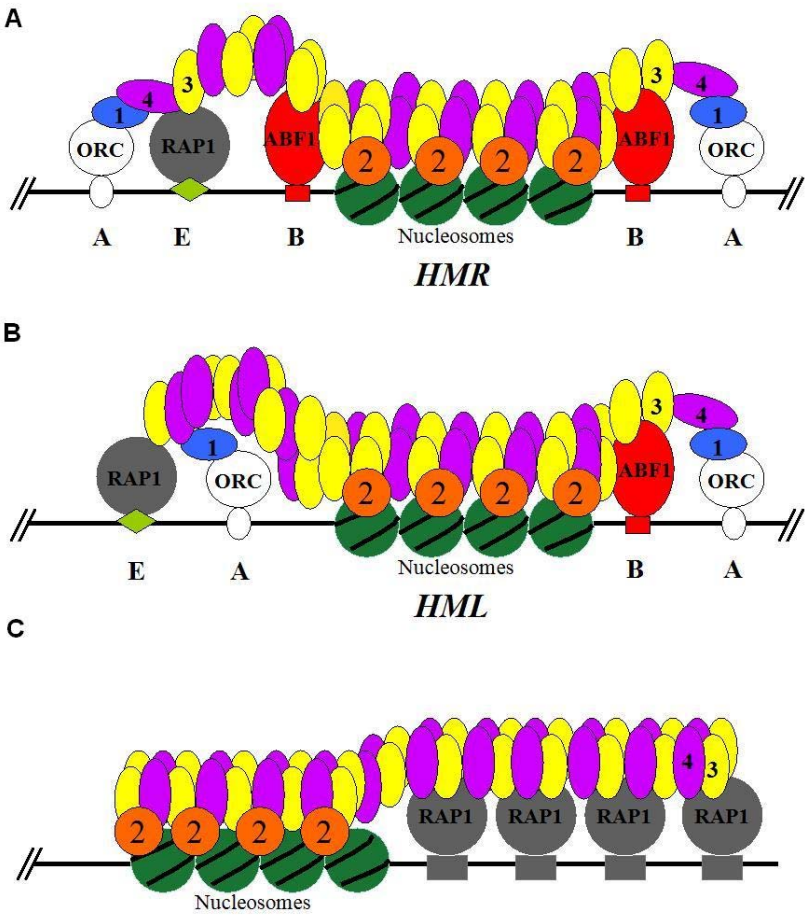

Figure 3: *HML*, *HMR* and telomere silencing. (A) *HMR* silencing. (B) *HML* silencing. (C) Telomeric silencing. The Sir proteins, Sir1 (1), Sir2 (2), Sir3 (3), and Sir4 (4) are colored and numbered as indicated.

The assembly of Sir proteins at silencers or telomeres exhibits a hierarchy of recruitment. Sir1 can be recruited to a silencer in the absence of any other individual Sir protein (Rusche *et al*., 2002). Sir4 is recruited to the silencer through its interactions with Sir1 (Triolo *et al*., 1996) and Rap1 (Moretti *et al*., 1994; Moretti *et al*., 2001). The recruitment of Sir4 to the silencer does not require Sir2 or Sir3 (Hoppe *et al*., 2002). Sir4 likely brings Sir2 to the silencer as a member of a Sir2-Sir4 complex (Ghidelli *et al*., 2001; Hoppe *et al*., 2002). Sir4 is also required to

recruit Sir3 to the silencer (Hoppe *et al*., 2002). Sir3 binds Rap1 (Moretti *et al*., 1994), Sir4 (Moazed *et al*., 1997) and also Abf1 as well (our unpublished data, a collaboration with D. Shore). Sir2 and Sir3 can each associate with the silencer in the absence of the other (Rusche *et al*., 2002). The catalytic activity of Sir2 is not required for its association, or the association of any other Sir protein, with the silencer (Hoppe *et al*., 2002).

The structure of silenced chromatin is determined by Sir proteins and histones. Chromatin immunoprecipitation studies reveal that Sir proteins spread inward from telomeres (Hecht *et al*., 1996; Lieb *et al*., 2001) and are also distributed throughout *HMR* and *HML* (Lieb *et al*., 2001; Zhang *et al*., 2002). At the silenced loci, the tails of histones H3 and H4 are unacetylated (Braunstein *et al*. 1993; Suka *et al*. 2001; Braunstein *et al*., 1996).

After Sir proteins have assembled at a silencer, they spread from the silencer to the gene that is to be silenced. Although Sir2 and Sir3 are not required for the other Sir proteins to associate with a silencer, they are required for the SIR complex to spread stably from the silencer (Rusche *et al*., 2002; Hoppe *et al*., 2002). The spreading of the SIR complex at telomeres has similar requirements (Luo *et al*., 2002). The ability of the Sir proteins to bind to the tails of histones H3 and H4 in nucleosomes enables the Sir proteins to spread across the chromosome. As described above, Sir3 and presumably Sir4 bind more efficiently to hypoacetylated histone tails than to fully acetylated tails (Carmen *et al*., 2002).

The NAD^+-dependent histone deacetylase activity of Sir2 is required for spreading of the Sir proteins (Rusche *et al*., 2002; Hoppe *et al*., 2002). This observation supports a mechanism for the spreading of Sir proteins that involves the sequential deacetylation of histone tails in nucleosomes along the chromosome. In this model, upon the recruitment of the Sir proteins to the silencers, Sir2 is brought into the proximity of its substrate, the acetylated lysines on the tails of histones H3 and H4 of a nearby nucleosome. The subsequent deacetylation of these tails by Sir2 creates a high-affinity binding site for Sir3 and Sir4, thus enabling the recruitment of additional Sir proteins to the nucleosomes flanking the silencers. This process positions the newly loaded Sir2 next to the acetylated tails of H3 and H4 on the next nucleosome. The sequential process of deacetylating neighboring nucleosomes and loading additional Sir proteins allows the Sir proteins to spread over several kilobases of DNA.

IV. Sir3 and the BAH domain

The structural role of Sir proteins in silenced chromatin is mediated by binding to histones. Sir3 and Sir4 bind residues 1-25 of histone H3 and 15-34 of histone H4 *in vitro* (Hecht *et al*., 1995). Although Sir3 and Sir4 are present in approximately equimolar amounts (Cockell *et al*., 1995), only Sir3 is limited for the propagation of telomeric silencing (Renauld *et al*., 1993). In SIR^+ cells, TPE represses genes up to 4 kb from the telomere, while in cells overexpressing *SIR3*, telomeric repression

extends roughly 20 kb from the telomeric TG_{1-3} repeats, coinciding with the spread of Sir3 along the repressed chromatin (Hecht *et al*., 1996; Renauld *et al*., 1993). The propagation of Sir3 is presumably mediated by its interaction with nucleosomes (Hecht *et al*., 1995; Onishi *et al*., 2007).

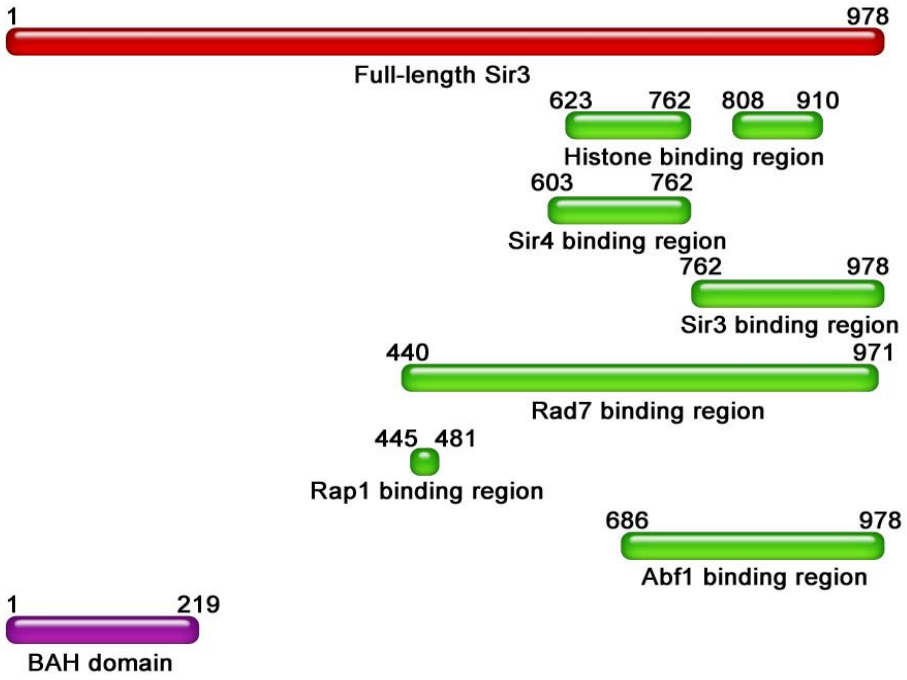

Figure 4: A schematic picture of Sir3 and its protein interaction regions (Gotta *et al.*, 1998). All the interaction regions already known are outside the Sir3 BAH domain. However, the Sir3 BAH domain is required for silencing.

Like Sir4, Sir3 has no known enzymatic activity. It plays a structural role in the assembly of silenced chromatin. Sir3 is recruited to the silencer separately from the Sir2-Sir4 complex. Recombinant Sir3 binds both nucleosomes and DNA *in vitro* (Georgel *et al*., 2001). As shown in Figure 4, Sir3 can bind histones, Sir4, Rap1, Rad7and Sir3 itself (Gotta *et al*., 1998).

The N-terminus of Sir3 shares 50% identity with Orc1N (Figure 5A). Orc1 is the largest subunit of the six-subunit ORC complex and it is essential for cell growth. The N-terminus of Orc1 is not essential for cell growth; the expression of Orc1 lacking its N-terminus complements an *ORC1* deletion. The N-terminus of Orc1 binds to the C-terminus of Sir1 (Triolo *et al*., 1996). Without the N-terminus of Orc1, *HMR* and *HML* silencing is weakened, just as it is with deletion of *SIR1*.

The high conservation in sequence between the N-terminus of Orc1 and Sir3 suggest that the role the N-terminus of Sir3 plays in silencing at the *HM* loci may be similar to that of Orc1N. In support of this idea, the N-terminus of Orc1 can functionally replace the N-terminus of Sir3 in the context of *HM* loci silencing. Expression of an Orc1$^{1\text{-}231}$-Sir3$^{241\text{-}978}$ chimera is sufficient to restore mating in a strain deleted for *SIR3* (Bell *et al*., 1995).

This N-terminal region of Orc1 (aa 1-219) includes a bromo-adjacent homology (BAH) domain. The Sir1-binding domain of Orc1 lies within the Orc1 BAH domain (Figure 6). The BAH domain of Orc1 interacts with the C-terminus of Sir1, and this interaction is important for recruiting other Sir proteins to the *HM* loci as Sir1 also interacts with Sir4 (Triolo *et al*., 1996). The N-terminal region of Sir3 (aa 1-219) also contains a BAH domain.

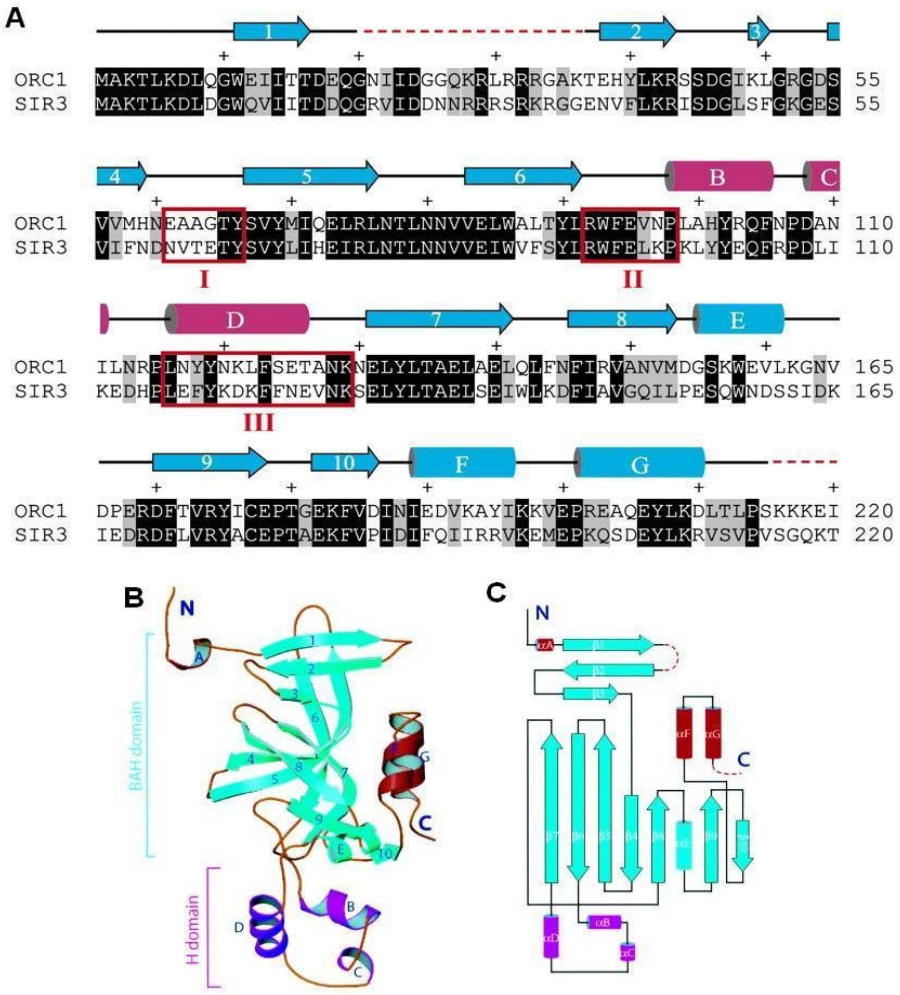

Figure 5: The alignment of Orc1 and Sir3 BAH sequences and the crystal structure of Orc1 BAH domain. (A) Alignment of Orc1 and Sir3 BAH sequences. Orc1 BAH secondary structures, with those in the H-domain shown in red, are indicated above the sequences. Dashed red lines indicate disordered regions. Three Sir1-interacting Orc1 segments are enclosed in red boxes (Hsu *et al.*, 2005). (B) The crystal structure of Orc1 BAH domain is shown in a ribbon representation. (C) Topology diagram showing the fold of the structure of Orc1 BAH domain. The core of the structure consists mainly of β-strands and is colored cyan. The H domain is shown in magenta, and N- and C-terminal helices are shown in red (Zhang *et al.*, 2002).

BAH domain is named because it bears similarity to a region within chicken polybromo-1 protein that is found next to a bromo domain. In addition to Sir3 and Orc1, other BAH domain containing proteins include: Rsc1 and Rsc2, components

of the RSC chromatin remodeling complex in *S. cerevisiae*; Dnmt1, a DNA methyltransferase found in higher eukaryotates that is responsible for the majority of DNA methylation in the cell; and ASH1, a SET domain containing protein in *D. melanogaster* that is involved in maintaining active transcription of many genes (Callebaut *et al*., 1999; Goodwin *et al*., 2001).

A BAH domain is often present in conjunction with other well-defined domains that are involved in chromatin function, such as bromo-domains that bind acetyl-lysines of N-terminal histone tails, PHD fingers and methyl-DNA-binding domains (Callebaut *et al*., 1999). The structure suggests that the BAH domain has at least two functions. First, it can serve as a scaffold for harboring specific protein-protein interaction modules. Secondly, a number of *sir3* mutations that affect silencing mapped to its core BAH domain, suggesting a direct role for the BAH domain in interacting with key components of chromatin, such as histones.

The human Orc1 BAH domain is not required for nuclear localization of Orc1 or association of Orc1 with other ORC subunits. However, the BAH domain in human Orc1 facilitates its ability to activate replication origins *in vivo* by promoting association of ORC with chromatin; the BAH domain may also affect the selective degradation of human Orc1 (Noguchi *et al*., 2006). These data suggest possible functions of the Sir3 and Orc1 BAH domains in *S. cerevisiae*.

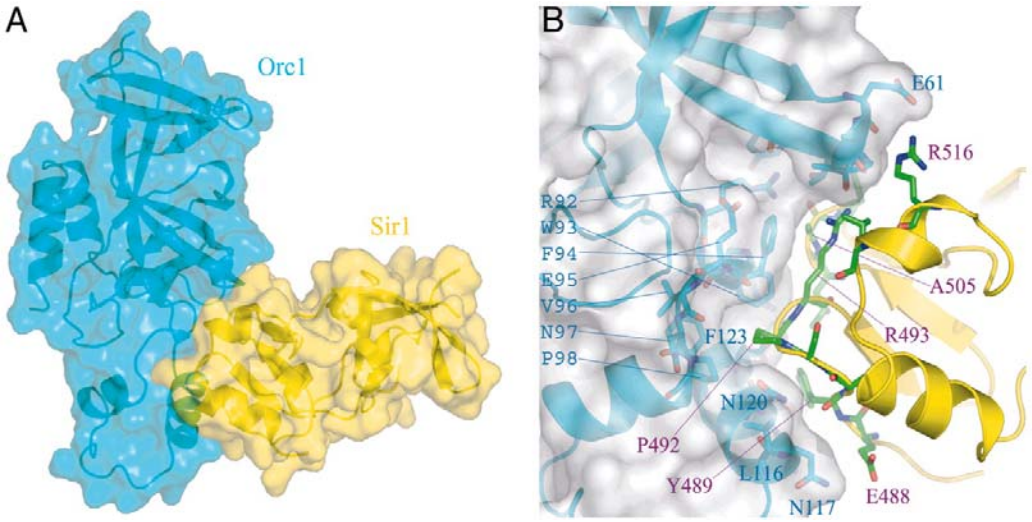

Figure 6: Cocrysctal of Orc1^{BAH}-Sir1C complex. (A) A surface representation of the Orc1^{BAH}–Sir1^{C} complex (cyan and yellow). (B) A detailed view of the protein interface. Orc1 BAH is shown in cyan and Sir1C is shown in yellow (Hsu *et al.*, 2005).

In the yeast Orc1^{BAH}, the H domain is a small non-conserved helical domain (Figure 5B and 5C). It is required for the silencing function of Orc1 (Zhang *et al*., 2002). The cocrystal structure presents the precise identification of Sir1-interaction regions within the H-domain (Figure 6). Specifically, Sir1 packs into a hydrophobic pocket formed by six residues on the Orc1 BAH domain surface. Three of the Orc1 amino acids that form this pocket (N120, F123, and S124) are from the H domain, but the other three (W93, F94, and P98) are outside the H domain in a loop linking a β-strand and an α-helix in Orc1^{BAH} (Hou *et al*., 2002).This Sir1 binding region in Orc1 is not well conserved in the Sir3 BAH domain, explaining why Sir3 does not bind to the C-terminus of Sir1.

A binding partner for the Sir3 N-terminal BAH domain has not yet been published. However, the C-terminus of Sir3 is not sufficient to complement

silencing in a *sir3*Δ strain. Moreover, several point mutations in the N-terminal domain of Sir3 suppress silencing-deficient mutants in Rap1 and the N-terminus of histones H3 and H4, although there is no evidence that the Sir3 BAH domain can interact directly with these proteins (Hecht *et al*., 1995; Johnson *et al*., 1990; Liu *et al*., 1996). All these data suggest that the Sir3 BAH domain plays an important role in silencing.

V. Overview of thesis

We have undertaken a study of the Sir3 BAH domain in order to further characterize its silencing roles. In this dissertation I present evidence that the Sir3 BAH domain can partially silence the *HM* loci, but only with overexpression of *SIR1*. The data from my random mutagenesis screen demonstrate that the region around A136, C177 and S204 of Sir3 is important for its function. The Sir3 BAH domain can bind to DNA and nucleosomes, and spread along the chromosome to maintain heterochromatin. Certain histone mutations can suppress the weak *sir3* mutants in the BAH domain. Also, a mutational analysis suggests that the extreme N-terminus might play a role in maintaining the structure of the Sir3 protein.

CHAPTER TWO

Sir3 BAH Silencing

I. Introduction

A previous study showed that the N-terminal fragment of Sir3 (aa 1-503) was capable of suppressing the anti-silencing effect of Sir4C expression (Gotta *et al*., 1998), suggesting that this region of Sir3 was capable of folding into a functional domain. Our lab has shown that the N- and C-terminal fragments of Sir3, when co-expressed, complement a *sir3*Δ, suggesting that the N-terminus of Sir3 is capable of providing its silencing role on its own (J. Connelly unpublished).

Previous studies have reported that several interesting *sir3* mutants within BAH domain, including the substitution of residue 205 from aspartic acid to asparagine (D205N). Four positions of histone H4 (N-terminal residues 16, 17, 18, and 19) were known to be crucial for silencing. *HML* and *HMR* are efficiently repressed when these positions are occupied by basic amino acids but are derepressed when substituted with glycine. In a suppressor screen, *sir3* W86R and *sir3* D205N were isolated as extragenic suppressors of an H4 K16G mutation. They did not allow efficient mating in a strain with an H4 N-terminal deletion (aa 4-19), however (Johnson *et al*., 1990). In another independent screen, *sir3* D205N and *sir3*

S31L were identified as suppressors of the telomeric silencing defects conferred by missense mutations within the Rap1p C-terminal tail domain (aa 800-827). Each *SIR3* suppressor was also capable of suppressing a *rap1* allele which deletes 28 amino acids of the C-terminal tail, but none of the suppressors restored telomeric silencing to a 165 amino acids truncation allele (Liu and Lustig, 1996). These data suggest that the N-terminus of Sir3 contributes silencing function. We were very interested in the D205N mutant, since it was identified in two independent screens.

In an attempt to understand the role of the BAH domain of Sir3 in silencing, a former graduate student, J. Connelly, undertook a study on the first 380 amino acids of Sir3 fused to a C-terminal LexA tag. Her data suggested that this fragment of Sir3 could at least partially silence *HMR* and *HML* in the complete absence of *SIR3* (Connelly *et al*., 2006). Comparing with untagged $Sir3^{1-380}$ fragments, silencing was enhanced by the LexA tagged $Sir3^{1-380}$ fusion protein, probably due to the ability of LexA to dimerize. Moreover, these tags had to be C-terminally fused, as an N-terminal LexA fusion to $Sir3^{1-380}$ gave no silencing. Data of J. Connelly also indicted that overexpression of *SIR1* enhances $Sir3^{1-380}$ silencing and allows both Sir3 and Orc1 N-terminal fragments to silence *HML* in the absence of *SIR3*. It has been reported previously that a recombinant $Ocr1^{BAH}$ forms a folded domain *in vitro* (Zhang *et al*., 2002). We thought the same would be true for Sir3. Because the $Sir3^{1-380}$ includes the BAH domain, we thought that the silencing by this Sir3 N-terminal fragment might be due to the BAH domain. In the following study, we

used Sir3$^{1-214}$ as a BAH domain and tested its silencing function.

II. Results

1. The Sir3 BAH domain could silence *HML* and *HMR* in the absence of full-length Sir3

Sir3$^{1-214}$-LexA and Sir3$^{1-214\ D205N}$-LexA were expressed from a plasmid in a *MAT***a** *sir3*Δ strain (JCY3) or a *MAT***α** *sir3*Δ strain (JCY4) and mating was assayed both qualitatively and quantitatively to assess silencing at *HML* and *HMR*, respectively. Expression of full-length Sir3 from a similar plasmid was capable of restoring silencing at *HML* and *HMR*, while expression of LexA alone did not. The data show that the BAH fragment by itself could not restore silencing at either of *HM* loci (Figure 7A and B).

It was known that overexpression of *SIR1* led to a restoration of silencing of several mating defective mutants (Stone *et al*., 1991) and it enhanced silencing by Sir3$^{1-380}$. Therefore, we sought to determine if extra *SIR1* would allow Sir3 BAH silencing. A series of plasmids encoding BAH fragments, C-terminally tagged with LexA, were co-expressed with *SIR1* in a *MAT***a** *sir3*Δ strain (JCY3) or a *MAT***α** *sir3*Δ strain (JCY4) and mating was assayed both qualitatively and quantitatively to assess silencing at *HML* and *HMR*, respectively. The results are presented in Figure 7.

A

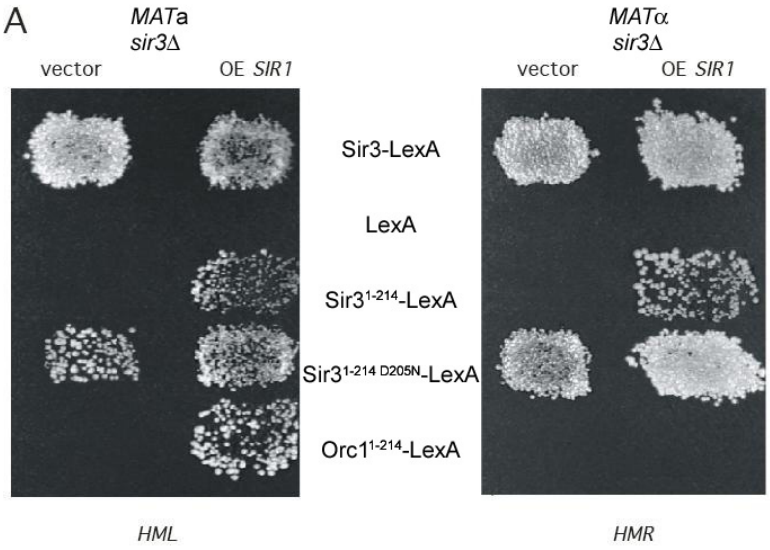

B

	W303-1a *sir3Δ*		W303-1b *sir3Δ*	
	vector	OE *SIR1*	vector	OE *SIR1*
Sir3-LexA	1	1.1	1	2.2
LexA	$<10^{-6}$	$<10^{-6}$	$<10^{-6}$	$<10^{-6}$
Sir3$^{1-214}$-LexA	$<10^{-6}$	2.8×10^{-2}	$<10^{-6}$	2.6×10^{-2}
Sir3$^{1-214\ D205N}$-LexA	5.1×10^{-3}	1.6×10^{-1}	6.7×10^{-1}	9.5×10^{-1}
Orc1$^{1-214}$-LexA	$<10^{-6}$	4.0×10^{-2}	$<10^{-6}$	$<10^{-6}$

Figure 7: BAH silencing at ***HM*** loci. Sir3$^{1-214}$-LexA and Orc1$^{1-214}$-LexA can partially silence ***HML*** and Sir3$^{1-214}$-LexA can silence ***HMR*** in the absence of ***SIR3***, as long as Sir1 is overexpressed. Sir3$^{1-214\ D205N}$-LexA can silence both ***HM*** loci, even without Sir1 overexpression. The indicated strains were transformed with plasmids expressing Sir3-LexA, LexA, Sir3$^{1-214}$-LexA, Sir3$^{1-214\ D205N}$-LexA or Orc1$^{1-214}$-LexA, and co-transformed with either a Sir1-overexpressing plasmid (OE ***SIR1***) or a vector. Mating was measured qualitatively by patch mating (A) and quantitatively (B), to assess silencing at the indicated locus.

SIR1 overexpression caused BAH fragments to silence *HML* and *HMR*. Both Sir3$^{1-214}$-LexA and Orc1$^{1-214}$-LexA could silence *HML* in a significant fraction of cells, but only if *SIR1* was overexpressed (Figure 7A). It should be emphasized that silencing by Orc1$^{1-214}$-LexA occurred in the absence of any Sir3 protein whatsoever.

HMR also could be partially silenced by Sir3$^{1-214}$-LexA, but not by Orc1$^{1-214}$-LexA, again only when *SIR1* was overexpressed (Figure 7B). There was no silencing by LexA alone.

As described above, the *sir3* D205N allele was known to improve silencing of certain H4 and *rap1* mutants. Since residue D205 resides within Sir3^{BAH}, we tested the effect of the D205N mutation on silencing by this protein. We found that Sir3$^{1-214\ D205N}$-LexA greatly improved silencing at *HML* and *HMR*, when compared to wild type Sir3$^{1-214}$-LexA, and even gave some silencing without extra Sir1 (Figure 7A and B).

2. BAH silencing required Sir1, Sir2, Sir4, Ard1 and the H4 N-terminal tail

Having identified a unique silencing function for the BAH domains of Sir3 and Orc1, we sought to determine if this silencing was dependent on the other Sir proteins and on NatA, the enzyme that acetylates the N-terminal Ala residues of Sir3 and Orc1 (Geissenhöner *et al*., 2004; Wang *et al*., 2004). Plasmids expressing Sir3$^{1-214}$-LexA, Orc1$^{1-214}$-LexA or Sir3$^{1-214\ D205N}$-LexA were co-transformed with a plasmid that overexpressed *SIR1* into *MAT***a** strains with a deletion of *SIR3* and deletions of *SIR1* (JCY8), *SIR2* (JCY42), *SIR4* (JCY17) or *ARD1* (XRY2; *ARD1* codes for the catalytic subunit of NatA). We assessed silencing at *HML* by patch mating. Deletion of *SIR2* or *SIR4* abolished silencing by all three BAH proteins, as

did deletion of *SIR1* in the absence of the Sir1 overexpressing plasmid (Figure 8). We conclude that silencing by each BAH domain depends on the usual silencing proteins (Sir1, Sir2, and Sir4). Figure 8 also shows that Sir3$^{1-214}$-LexA and Orc1$^{1-214}$-LexA could not silence in an *ard1*Δ strain, and Sir3$^{1-214\ D205N}$-LexA silencing was diminished by the *ard1*Δ mutation. Thus, acetylation of the N-termini of Sir3^{BAH} and Orc1^{BAH} is required for them to act in silencing. This is expected, given that NatA is known to acetylate full-length Sir3 and Orc1, and that Sir3 must be N-terminally acetylated in order to function fully (Geissenhöner *et al*., 2004; Wang *et al*., 2004).

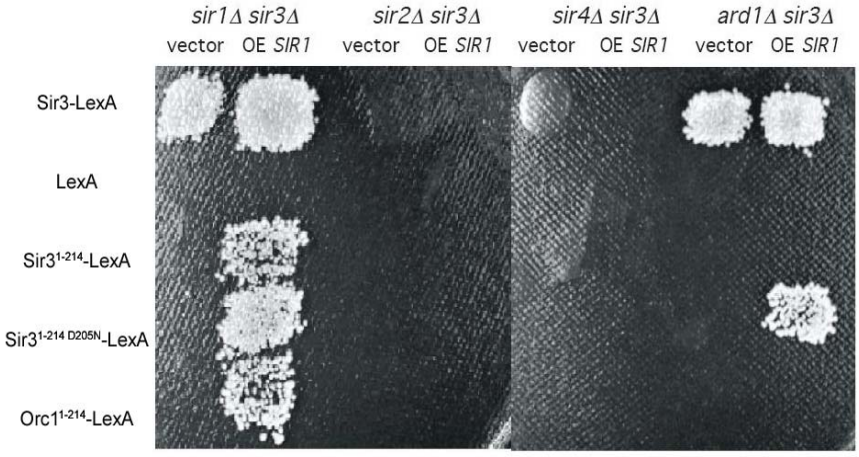

Figure 8: Silencing by the Sir3 BAH domain depended on ***SIR1***, ***SIR2***, ***SIR4*** and ***ARD1***. The indicated strains were transformed with plasmids expressing Sir3-LexA, LexA, Sir3$^{1-214}$-LexA, Sir3$^{1-214\ D205N}$-LexA or Orc1$^{1-214}$-LexA, and co-transformed with either a Sir1-overexpressing plasmid (OE ***SIR1***) or a vector. Mating was measured qualitatively by patch mating. It should be noted that Sir3$^{1-214\ D205N}$-LexA gives some silencing in an ***ard1*** mutant as long as Sir1 is overexpressed.

Finally, we checked whether the N-terminus of H4, known to bind to the Sir3 C-terminal region (Carmen *et al*., 2002; Liou *et al*., 2005), was required for Sir3$^{1-214}$

or Sir3$^{1-380}$ silencing. As mentioned above, previous studies showed that residues in the N-terminus of H4 were important for silencing. An H4 deletion, removing amino acids 4-14, reduced mating efficiency, whereas deletion of amino acids 4-23 abolished mating at *HML* (Durrin *et al*., 1991). N-terminal residues 16, 17, 18, and 19 of H4 are crucial to silencing. *HM* silencing was abolished when these positions were substituted with glycine (Johnson *et al*., 1990). *sir3* W86R and *sir3* D205N were isolated as the suppressors of H4 K16G mutations which provided a link between Sir3 BAH domain and a component of chromatin (Johnson *et al*., 1990).

In this experiment, we only tested the *sir3* alleles which could give BAH silencing with a normal level of Sir1. Plasmids encoding Sir3-LexA (positive control), LexA (negative control), Sir3$^{1-214\ D205N}$-LexA, Sir3$^{1-380}$-LexA, Sir3$^{1-380\ D205N}$-LexA proteins were introduced into *sir3*Δ derivatives of strains with deletions of the H4 N-terminus, deletions of either amino acids 4-14 (PYY7 and PYY8) or 4-23(PYY9 and PYY10). The results indicated that with full-length H4, Sir3$^{1-214\ D205N}$-LexA, Sir3$^{1-380\ D205N}$-LexA could cause a weak silencing at *HML*, and Sir3$^{1-214\ D205N}$-LexA, Sir3$^{1-380\ D205N}$-LexA and Sir3$^{1-380}$-LexA could partially silence *HMR* (Figure 9). When residues 4-14 of H4 were deleted, there was no *HML* silencing with the BAH fragments. For unknown reason, in my experiments even full-length Sir3 could not cause any *HML* silencing with the deletion of H4 4-14, which was not consistent with the previous results (Durrin *et al*., 1991). On the other hand, full-length Sir3 could silence *HMR* with the deletion of H4 4-14. And Sir3$^{1-214}$

^{D205N}-LexA, Sir3$^{1-380}$-LexA also gave some weak silencing at *HMR*. It was not clear why Sir3$^{1-380\ D205N}$-LexA showed more sensitivity to the H4 deletion than WT Sir3$^{1-380}$-LexA. With the deletion of H4 amino acids 4-23, none of the Sir3 N-terminus fragments were functional; even full-length Sir3 could not restore any mating ability. In conclusion, mutations in the H4 N-terminus affected Sir3^{BAH} silencing.

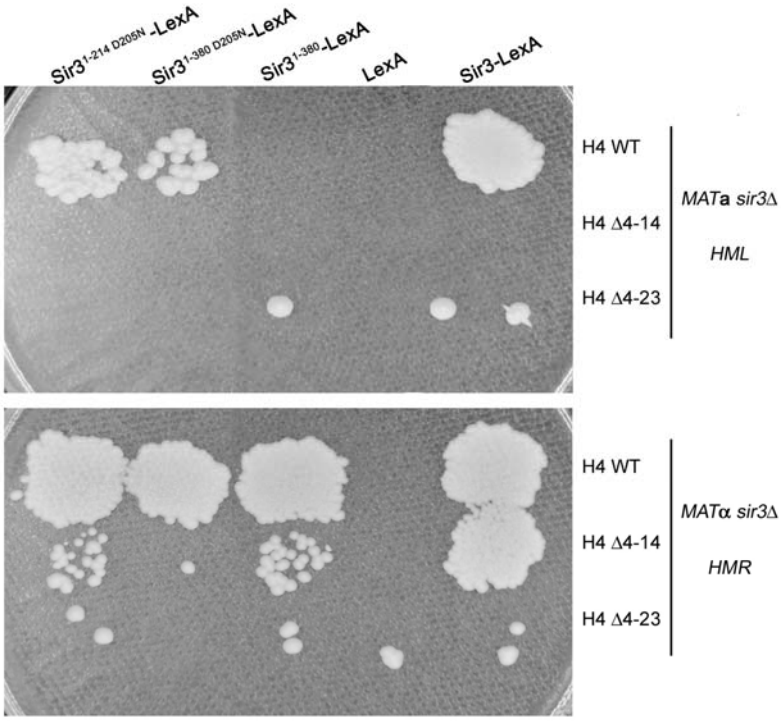

Figure 9: Silencing by the N-terminal fragments of Sir3 depended on N-terminus of H4. Plasmids encoding Sir3-LexA (positive control), LexA (negative control), Sir3$^{1-214\ D205N}$-LexA, Sir3$^{1-380}$-LexA, and Sir3$^{1-380\ D205N}$-LexA proteins were introduced into *sir3*Δ derivatives of strains with full-length H4(PYY5 and PYY6) or deletions of the H4 N-terminal residues either 4-14 (PYY7 and PYY8)or 4-23(PYY9 and PYY10). In this experiment, Sir1 was at a normal level.

3. Sir3$^{1-380}$ was present at the silencer and spreads into the *HMR* locus

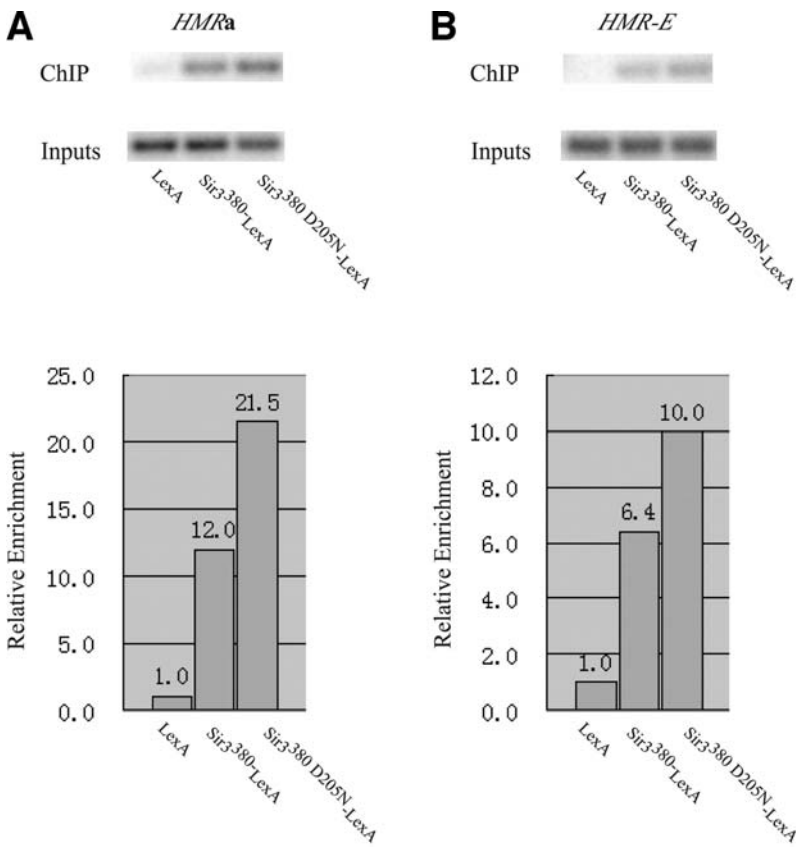

Figure 10: Chromatin immunoprecipitation localized $Sir3^{1-380}$-LexA to the *HMR* locus. Chromatin was immunoprecipitated from a *sir3*Δ strain expressing $Sir3^{1-380}$-LexA, $Sir3^{1-380\ D205N}$-LexA or LexA, each in the presence of the *SIR1* overexpressing plasmid pES13B. An antibody to LexA was used. Enrichment of LexA is shown for (A) the *HMR* locus itself (in the *a1* gene), and (B) the *HMR-E* silencer.

Since the $Sir3^{1-214}$ proteins gave Sir-dependent silencing, it seemed likely that they would spread from the silencers to the silenced loci, just as is seen with Sir2, Sir3 and Sir4 in a wild-type cell when all the full-length Sir proteins are present. To monitor the presence of $Sir3^{BAH}$ at both the *HMR-E* silencer and in the *HMR* silenced region (*HMR***a**), chromatin immunoprecipitation with an antibody to the LexA tag was used to immunoprecipitate Sir3 N-terminal fragments tagged with LexA. In order to increase the fraction of silenced cells, in this experiment a longer

piece, Sir3$^{1-380}$-LexA, was used and *SIR1* was also overexpressed. *MAT***α** *sir3*Δ cells expressing Sir3$^{1-380}$-LexA or Sir3$^{1-380\ D205N}$-LexA were cross-linked and chromatin was sheared to a mean length of 500 bp. A control strain, *MAT***α** *sir3*Δ expressing LexA, was also tested to determine the contribution of the LexA tag.

As seen in Figure 10, Sir3$^{1-380}$-LexA was greatly enriched at both the *HMR-E* silencer and at the *HMR* locus itself. The D205N mutant was even better than WT, which is consistent with the mating results. These data suggested that Sir3$^{1-380}$-LexA had the ability to support the localization and spreading of the SIR complex at *HMR*. Therefore, it could be concluded that Sir3 N-terminus was associated with the locus that it silenced and could promote the spreading of the SIR complex.

4. D205K mutant could also enhance BAH silencing.

The D205N mutation led to stronger BAH silencing. This change was from a negative charged residue to a neutral residue. There remained a question: what would happen if D205 was substituted by a positive charge residue? Would this substitution cause a weaker silencing or better silencing?

The *sir3* D205K mutation was created by site-directed PCR mutagenesis. Full-length Sir3^{D205K}-LexA was constructed and telomeric silencing was tested in a *sir3*Δ strain (XRY16). The result indicated that the D205K mutant could restore telomeric silencing as well as WT Sir3 (Figure 11A), which suggested that D205K could not weaken silencing in context of full-length Sir3. Later, we made a Sir3$^{1-214}$

^{D205K}-LexA plasmid and measured BAH silencing at *HMR* (JCY4) by semi-quantitative mating assay (Figure 11B). The D205K mutant could silence a significant fraction of yeast cells, as well as D205N. The data indicated that D205K could enhance silencing, just like D205N.

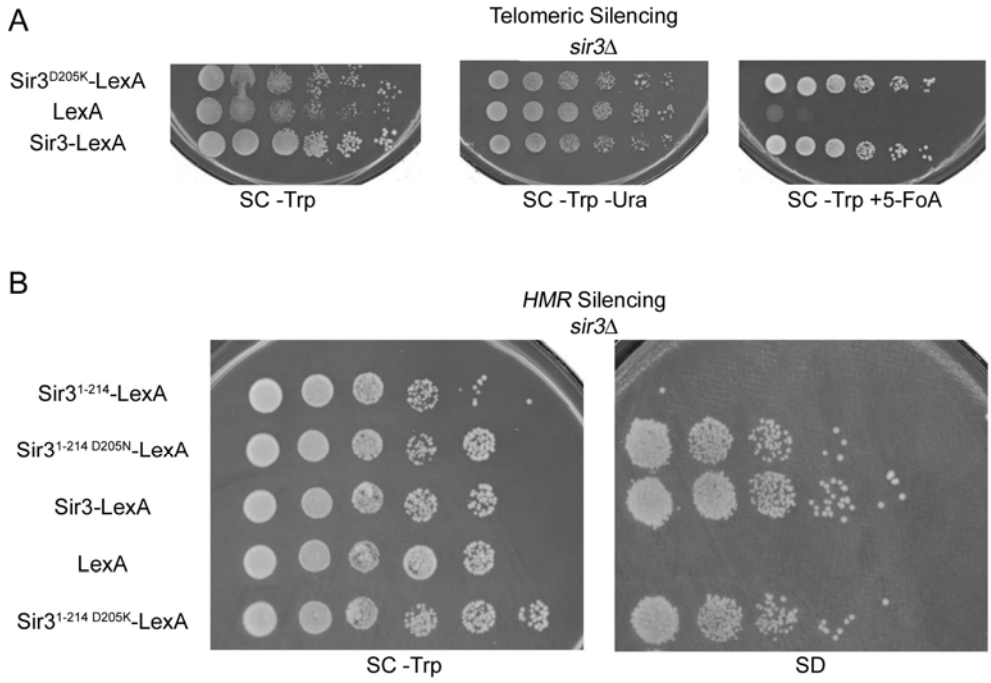

Figure 11: The *sir3* D205K mutant could enhance the BAH silencing. (A) Telomeric silencing assay. The indicated strain (XRY16) was transformed with plasmids expressing full-length Sir3-LexA, LexA, and Sir3^{D205K}-LexA. Silencing was assessed by spot dilution. The D205K mutant could restore telomeric silencing as well as WT Sir3. (B) BAH silencing at *HMR*. The indicated strain (JCY4) was transformed with plasmids expressing Sir3-LexA, LexA, Sir3$^{1-214}$-LexA, Sir3$^{1-214\ D205N}$-LexA or Sir3$^{1-214\ D205K}$-LexA. Silencing was measured by semi-qualitative mating assay. The D205K mutant could silence a significant fraction of yeast cells, as well as D205N.

III. Discussion

Previous studies have demonstrated that mutations in the N-terminal region of Sir3 interfered with its silencing function (Stone *et al*., 2000; Wang *et al*., 2004).We

have shown that short N-terminal fragments of Sir3 (aa 1-214), lacking any of the known protein-interacting domains of full-length Sir3, give Sir1-, Sir2-, and Sir4-dependent silencing in a measurable fraction of cells. This silencing is greatly increased, and in some cases totally dependent, on overexpression of full-length Sir1 or upon introduction of the hypermorphic *sir3* D205N mutation. Similarly, the Orc1$^{1\text{-}214}$ fragment can also give silencing, at least at *HML*, as long as Sir1 is overexpressed. Since the BAH domain can silence in the absence of full-length Sir3, it suggests that the BAH domain possesses the essential silencing features of the full-length protein, including (i) the ability to be recruited to the silent chromatin, and (ii) spreading along the silenced region.

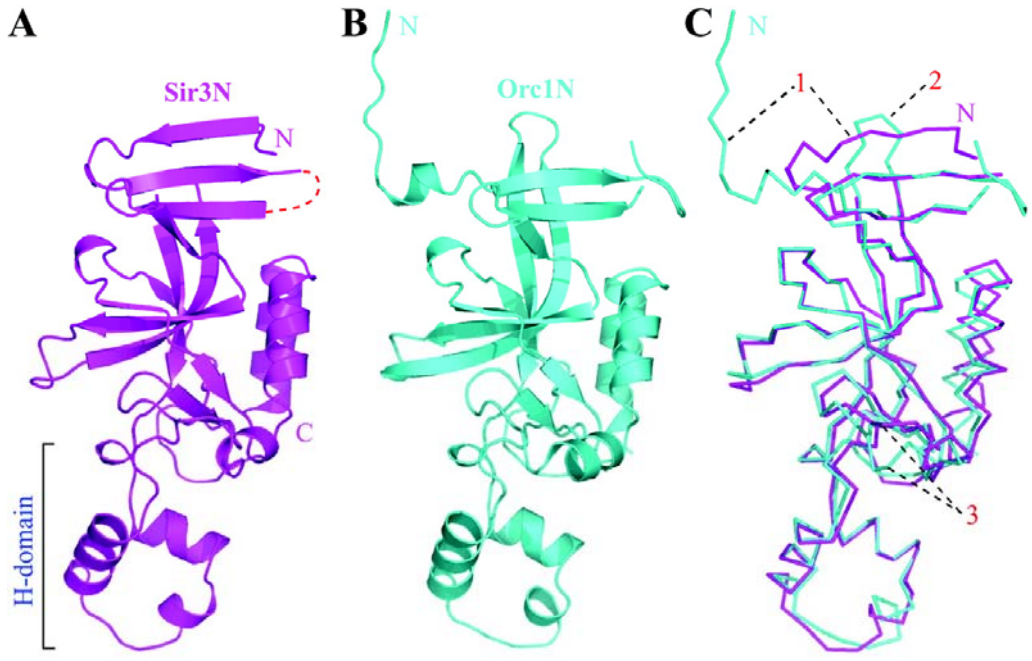

Figure 12: Structure of Sir3^{BAH} (J. Connelly *et al.*, 2006). (A) Structure of Sir3^{BAH} shown in a ribbon representation (PDB: 2FVU). The red dashed line denotes the disordered segment in the structure. The H domain is indicated by a left bracket. This is the domain of Orc1^{BAH} known to bind to the C-terminal OIR of Sir1. (B) Structure of Orc1^{BAH}

(PDB: 1M4Z) viewed from the same direction as in A. (C) Superposition of the $Sir3^{BAH}$ and $Orc1^{BAH}$ backbone structures. Numbers 1, 2, and 3 point to the three regions that differ the most between the two structures.

One possibility is that the Sir3 BAH domain can be recruited to silent chromatin through association with other Sir proteins. However, no interaction partner was observed in the two-hybrid searches by using $Sir3^{BAH}$ as bait (work of J. Connelly), which suggests that the Sir3 BAH domain probably can bind to nucleosomes by itself.

Our collaborators have determined the crystal structure of $Sir3^{BAH}$ (aa 1-219), which is illustrated in Figure 12. The structure of $Sir3^{BAH}$ indicates that the protein surface is quite negatively charged (calculated pI of 5.3 for residues 1 to 219 and pI of 6.0 for full-length Sir3). Thus, the charge distribution in $Sir3^{BAH}$ makes it favorable for interaction with the highly positively charged N-terminal tails of histones.

In chapter four, I present some evidence for the $Sir3^{BAH}$-nucleosome interaction, which can contribute to understanding BAH silencing. Sir3 is not conserved in higher eukaryotes, but the BAH domain is present from yeast to human. Studying the role of Sir3 BAH domain in yeast transcriptional silencing may reveal an evolutionarily conserved mechanism for chromatin association.

CHAPTER THREE

Sir3 BAH Random Mutagenesis Screen

I. Introduction

The N-terminus of Sir3 is essential for its silencing function at *HML, HMR* and telomeres (Gotta *et al*., 1998; Onishi *et al*., 2007). The expression of Sir3 lacking its N-terminus in a *sir3*Δ strain fails to complement the silencing defect (Gotta *et al*., 1998). However, we know little about the function of the N-terminus of Sir3, other than the fact the N-terminus of Sir3 contains a BAH domain (aa 1-219). In an attempt to investigate the role of the $Sir3^{BAH}$, we were interested in determining if there are any specific residues or regions in this domain which are important for silencing. Identification of these residues or regions would help us to figure out the role of the N-terminus of Sir3 in silencing. We used random PCR mutagenesis and gap repair to construct a *sir3* mutant library. Mutations in Sir3 were confined to the first 250 amino acids of the protein. This library was screened for mutants that fail to complement the telomeric silencing of a *sir3* deletion.

We look for *sir3* mutant plasmids that do not restore silencing to a *sir3*Δ strain. Plasmid pPY41 (Sir3-LexA) was constructed as described in Figure 13. It was used for gap repair in a yeast strain PYY4 with a *sir3*Δ. Strain PYY4 contains a *URA3*

reporter gene for measuring telomeric silencing, as well as a *LacZ* reporter gene used in two-hybrid analysis to screen for loss of full-length Sir3 protein.

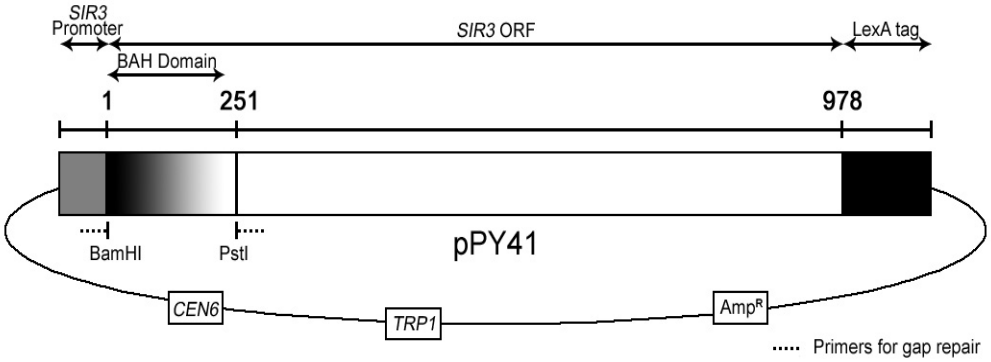

Figure 13: Plasmid (pPY41) used for gap repair. A LexA tag was fused at the C-terminus of full-length Sir3. Two primers were designed to amplify the first 753 bp of *SIR3*. Each primer was 50 bp. The BamHI site was just upstream of the *SIR3* start codon, and a PstI site was at 753 bp inside *SIR3*. Both of them were unique to pPY41, which could be used to linearize pPY41 and remove the BAH domain.

Random mutagenesis PCR was used to create a *SIR3* fragment spanning the first 753 bp. The BAH domain was then removed from pPY41 by BamHI and PstI, resulting in a linearized plasmid. The PCR product and the linearized pPY41 were co-transformed into PYY4 to construct a *SIR3* mutant library through gap repair (Figure 14A).

Full-length Sir3 with a LexA tag can interact with GAD-Rad7$^{94\text{-}565}$ to activate the *LacZ* gene and cause cells turn blue in a β-gal assay (Paetkau *et al*., 1994). Thus, nonsense mutations within *SIR3* that abolished the Sir3-Rad7 interaction could be detected by co-transformation of the *sir3* mutant library with pPY17 (GAD-Rad7$^{94\text{-}565}$) and checking for loss of *LacZ* reporter activation. These β-gal$^-$

candidates were eliminated from study (Figure 14B).

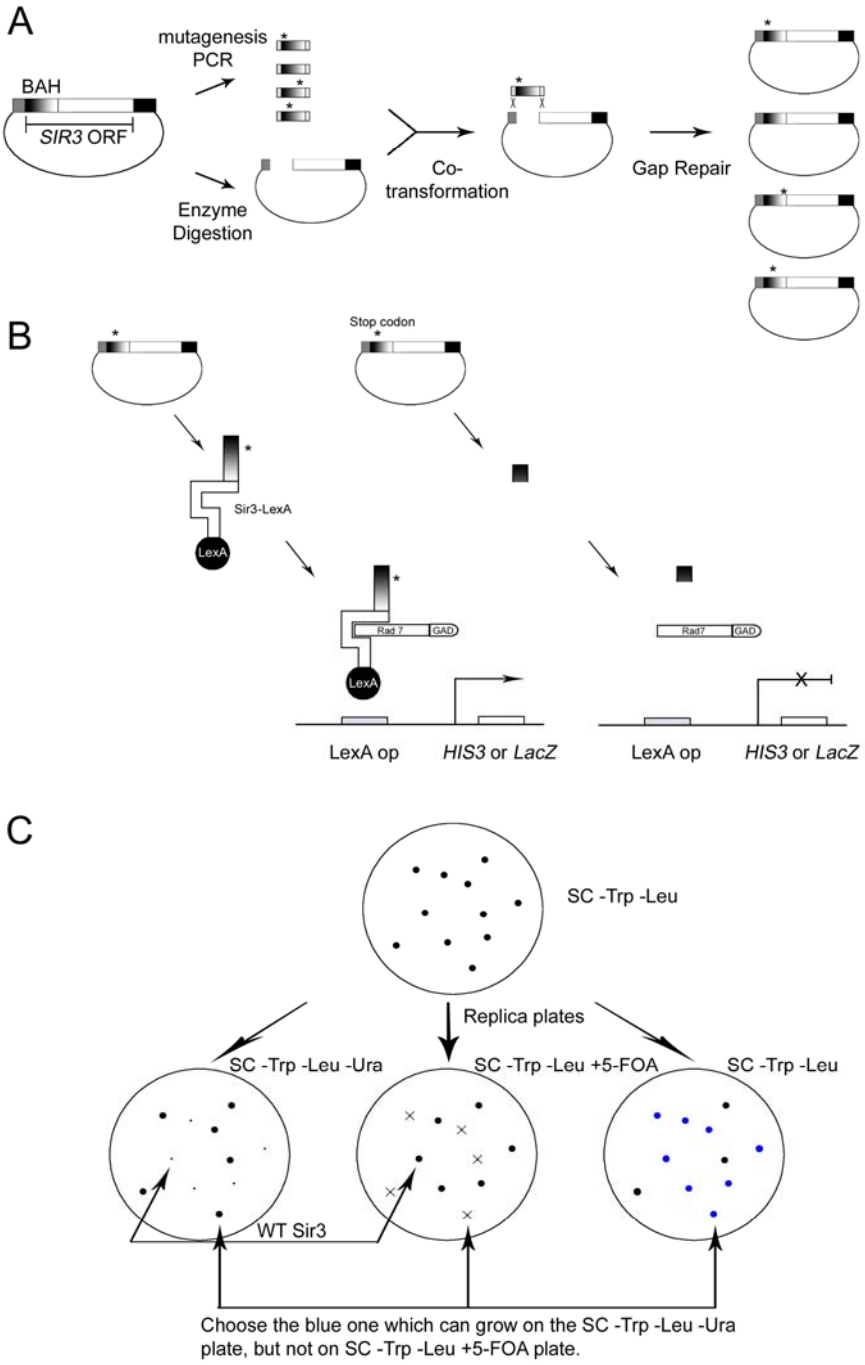

Figure 14: Procedure for Sir3 BAH random mutagenesis screen. (A) The gray bars represent the *SIR3* promoter region. The black-and-white gradient bars represent the mutagenized Sir3 BAH region. The white bars represent the rest of *SIR3* ORF. The black bars represent LexA tag, and the stars represent mutations. In the yeast cell, linearized pPY41 and

mutagenesized PCR fragments were recombined through a 50 bp overlap region on each side. Finally, complete plasmids containing mutations in the BAH domain were created. (B) GAD-Rad7$^{94-565}$ was used for two hybrid tests, which can get rid of nonsense mutations of Sir3 BAH. (C) The large spots represent good growth of colonies on the plate, the tiny spots represent poor growth of colonies on the plate and the crosses represent no growth on plate. The constructs that failed to complement a *sir3* deletion (no growth on 5-FOA plate but good growth on –Ura plate), but still gave a positive two-hybrid signal (blue colonies), were kept as candidates

Telomeric silencing of the remaining candidates was then tested by an *URA3* reporter gene. The *URA3* reporter gene placed proximal to telomeric sequences was transcriptionally repressed, and this telomeric silencing, observed as sensitivity to 5-FOA, was abolished in a *sir3* null mutant (Aparicio *et al.* 1991). Resistance to 5-FOA is a measure for silencing of the telomere-positioned *URA3* gene, because cells expressing *URA3* are sensitive to 5-FOA and only silenced cells are resistant and able to form colonies. If a mutation was made that affected the silencing ability of *SIR3*, then the yeast could grow well on a -Ura plate but not grow on 5-FOA plate. The constructs that failed to complement a *sir3* deletion, but still gave a positive two-hybrid signal, were kept as candidates (Figure 14C).

II. Results

1. A series of mutants in Sir3 BAH domain were obtained from the random mutagenesis screen

In the Sir3 BAH random mutagenesis screen, 24,000 transformants were

screened and finally eight single mutations were obtained, including N80D, F94L, A136T, C177R, A181V, S204P, Y207C, and K209R.

Except Y207C, all the other seven single mutations showed a complete telomeric silencing defect after retransformation into a *sir3*Δ strain, which was consistent with the phenotypes observed in the random mutagenesis screen. Y207C only gave a partial telomeric silencing defect.

An A2V mutation was obtained three times from the screen, but always combined with other point mutations. Site-directed PCR mutagenesis was used to get the single point mutation of A2V (work of H. Huang). A2V could not restore any telomeric silencing.

Based on the crystal structure of $Orc1^{BAH}$ (Figure 6; Hsu *et al*., 2005), α-helix D in the H domain contributes to its interaction with Sir1. Although there was no evidence to show that $Sir3^{BAH}$ could interact with any part of Sir1, we were still very interested in the corresponding region in the Sir3 BAH domain. An F123P mutation was created by site-directed PCR mutagenesis (work of J. Kilecki) which was would lead to a disruption of the α-helix. The point mutation F123P in the context of Sir3-LexA also gave a telomeric silencing defect phenotype.

The LexA tag sometimes affects Sir3 silencing function. In order to mimic the natural condition, we swapped all the single point mutations to an untagged Sir3 plasmid: pXR58. Full-length *SIR3* plasmids with various point mutations were *CEN*-based low-copy plasmids and driven by the native *SIR3* promoter. Telomeric

silencing was retested in a *sir3*Δ strain: XRY16 (Figure 15). We tested whether the *sir3* mutants were defective in telomeric silencing by plating a dilution series of transformants on 5-FOA containing medium to monitor silencing. On the 5-FOA plates, good growth means good silencing. Control transformants of a *sir3*Δ mutant strain showed no growth with vector only and good growth with a WT *SIR3* plasmid which meant that the WT Sir3 plasmid could complement the genomic deletion of *SIR3*.

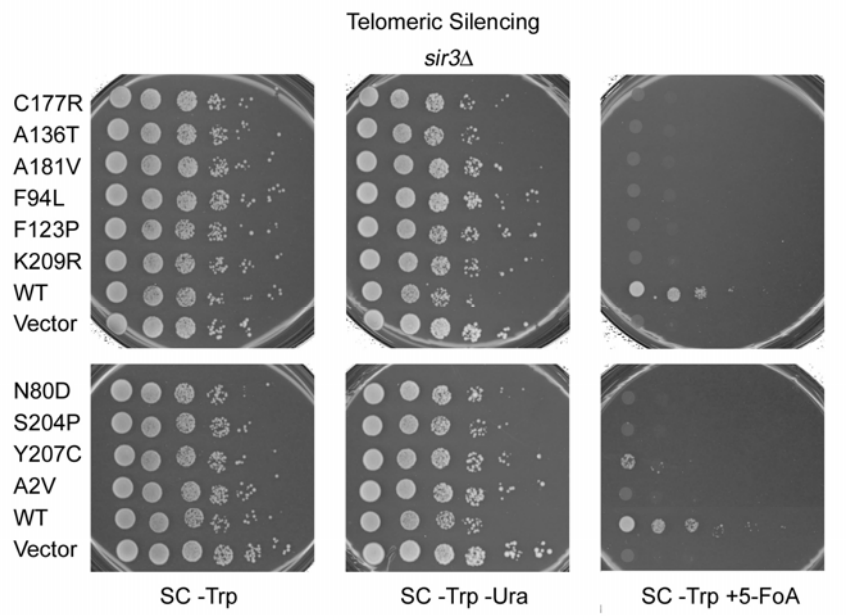

Figure 15: Telomeric silencing of ***sir3*** mutants from mutagenesis screen. The plasmids encoding full-length Sir3 with mutations indicated in the figure were transformed into a ***sir3***Δ strain with an ***URA3*** reporter gene at telomere (XRY16). WT Sir3 could restore telomeric silencing, and vector could not. Except Y207C, all other mutations cause complete telomeric silencing defects.Y207C only led partial silencing defects.

However, all the mutants from screen could not silence the telomere. Y207C led to a very weak silencing at telomere. F123P also caused a telomeric silencing defect. The data from the untagged plasmids were very similar to that found with

the LexA tagged plasmids. This suggests that the LexA tag had no effects on the Sir3 function in this screen.

2. Silencing of *sir3* mutants at *HM* loci

In the following study, we tested the silencing functions at *HML* and *HMR* of the *sir3* mutants obtained from the screen or from site-directed mutagenesis. A series of plasmids encoding full-length Sir3 with mutations were transformed into the *sir3*Δ strains (JCY3 and JCY4) to assess silencing at *HM* loci (Figure 16). All the *SIR3* constructs used in this experiment were *CEN*-based low-copy plasmids, driven by its own promoter and had no tag. Data showed that A136T, C177R and S204P had severe defects at *HML*, and N80D also had partial defects at *HML*. A2V, F94L, F123P, A181V, Y207C and K209R could restore silencing at *HML* as well as WT Sir3. At *HMR*, only A136T, C177R and S204P showed partial defects, and all other mutants led to normal silencing just like WT Sir3.

Based on the silencing function, we classified these mutants into four categories. Category "strong" represented no telomeric silencing function, a severe defect at *HML* and even a partial defect at *HMR*. A136T, C177R and S204P belonged to this category. N80D belonged to the "moderate" category, because it did not cause a big defect at *HML* and *HMR*. Category "weak" represented no telomeric silencing function but normal silencing at *HML* and *HMR.* A2V, F94L, F123P, A181V, and K209R were in this category. The "weakest" category only had

one mutant, Y207C, which only gave partial silencing at the telomere. The silencing of these *sir3* mutants are summarized in Table 1.

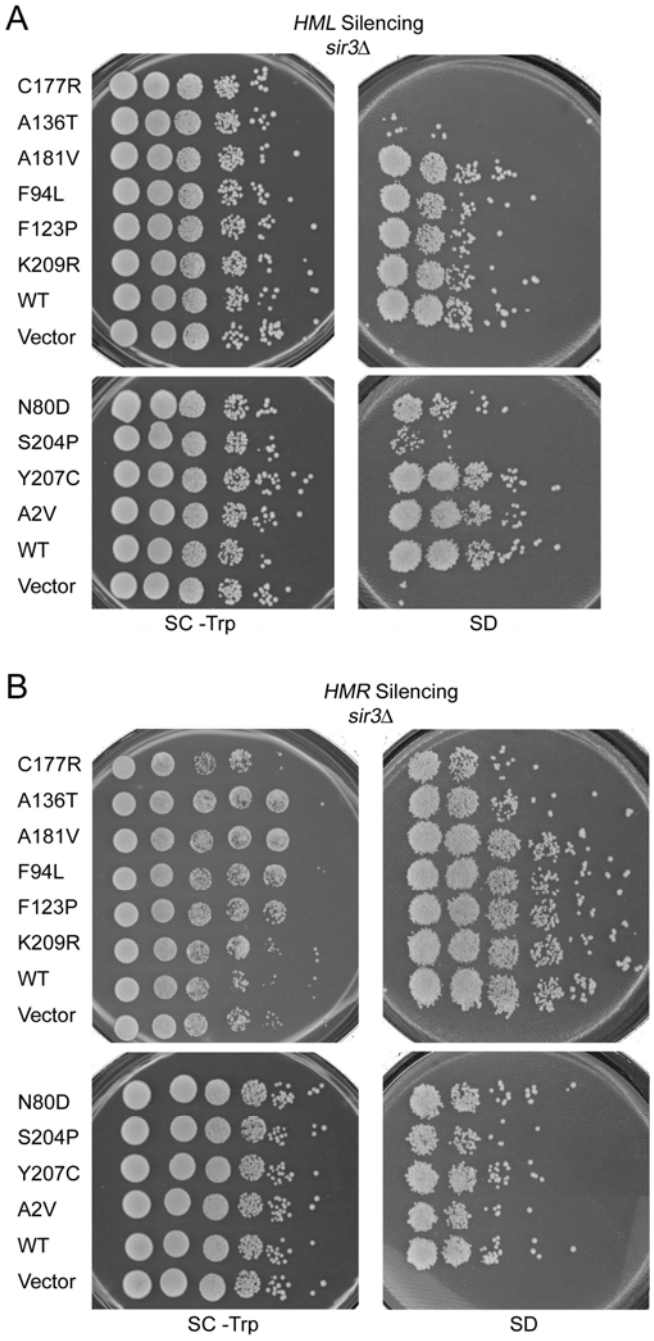

Figure 16: Silencing of ***sir3*** mutants from mutagenesis screen at ***HML*** and ***HMR***. The plasmids encoding full-length Sir3 with mutations indicated in the figure were transformed into a ***MAT*****a** ***sir3***Δ strain, JCY3 (A) or a ***MAT*****α** ***sir3***Δ strain, JCY4 (B). A136T, C177R and S204P had severe defects

at ***HML***, and N80D also had partial defects at ***HML***. A2V, F94L, F123P, A181V, Y207C and K209R could restore silencing at ***HML***, like WT Sir3. At ***HMR***, A136T, C177R and S204P only showed partial defects, and all other mutants led to silencing similar to WT Sir3.

3. The *eso* silencing phenotype of *sir3* mutants at *HM* loci

Previous work identified an unusual collection of *sir3* mutant alleles in a genetic screen for enhancers of the *sir1*Δ mutant mating-defective phenotype, which were called *eso* mutants (Stone *et al*., 2000). These *sir3-eso* mutants exhibited little or no mating defects alone, but the *sir1*Δ *sir3-eso* double mutants were essentially nonmating. Sequence analysis showed that eight of the nine *sir3-eso* alleles had mutations within the BAH domain (Figure 21C, Stone *et al*., 2000).

In my work, we investigated whether the *sir3* mutants I obtained were also *eso* mutants. A series of plasmids encoding full-length Sir3 (no LexA tag) with mutations were transformed into a *MAT***a** *sir1*Δ *sir3*Δ strain (JCY8) or a *MAT***α** *sir1*Δ *sir3*Δ strain (JCY9). *HML* and *HMR* silencing was assessed by semi-quantitative mating experiments (Figure 17). All the *SIR3* constructs used in this experiment were *CEN*-based low-copy plasmids and driven by the *SIR3* promoter. The result showed that WT Sir3 still could restore silencing at both *HM* loci. With a *sir1*Δ *sir3*Δ strain background, none of the *sir3* mutants could cause any silencing at either *HML* or *HMR*, even the weakest mutant Y207C. Thus, a *sir1* deletion could drastically enhance the phenotype of these *sir3* point mutants; thus they are *sir3-eso* mutants.

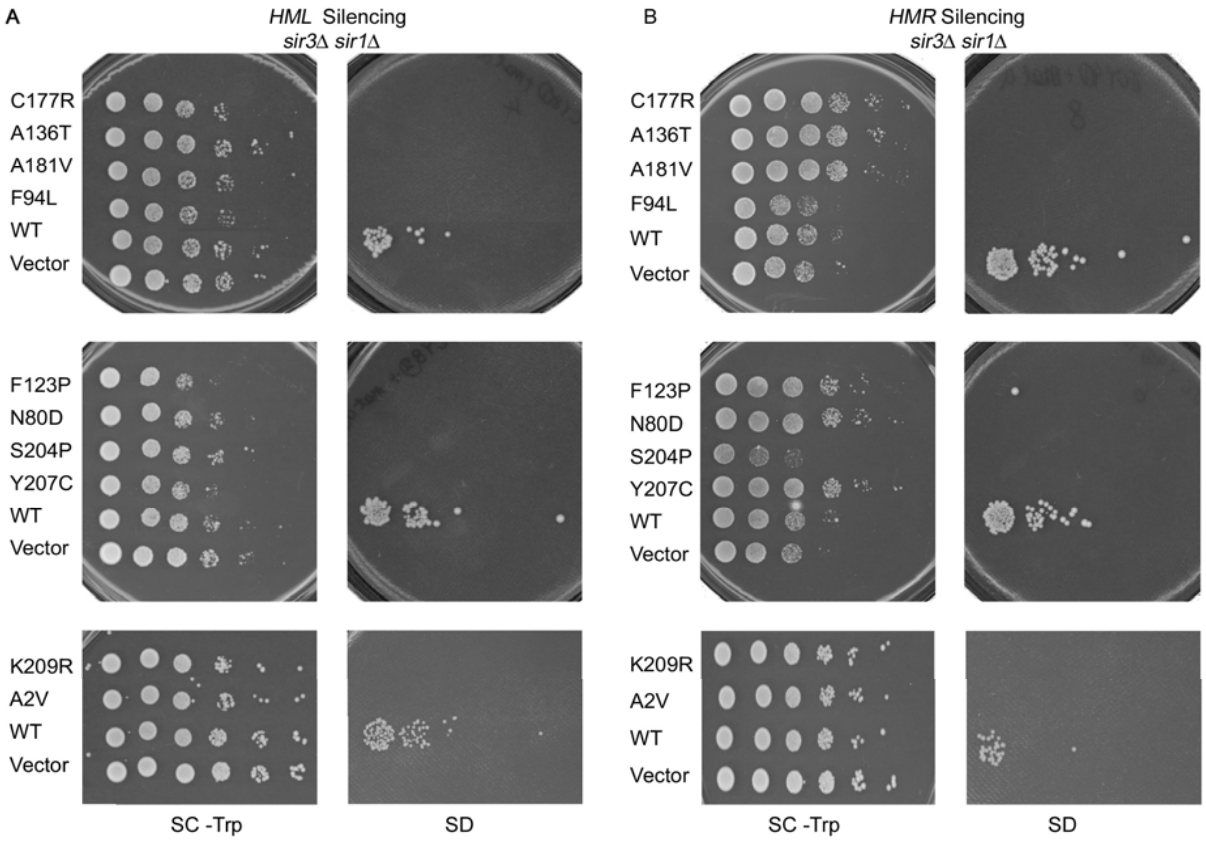

Figure 17: The *eso* silencing phenotype of *sir3* mutants at *HM* loci. A series of plasmids encoding full-length Sir3 (no LexA tag) with mutations were transformed into *sir1*Δ *sir3*Δ double deletion strains (JCY8 and JCY9). *HML* (A) and *HMR* (B) silencing was assessed by semi-quantitative mating experiments. No *sir3* mutants could cause any silencing at either *HML* or *HMR*, just like the empty vector.

These results suggest a genetic interaction between Sir3 and Sir1. As mentioned before, overexpression of *SIR1* can suppress the mating defect associated with certain *sir3* alleles (Stone *et al.,* 1991). However, there is no evidence to indicate that the Sir3 BAH domain can interact with any part of Sir1.

4. Some of the *sir3* mutants caused dominance at telomere

We next determined whether the *sir3* mutants were dominant or recessive. Telomeric silencing was measured by 5-FOA resistant assay in a WT *SIR3* strain (RS1045) with an *URA3* reporter gene at telomere. The plasmids encoding the mutant Sir3 proteins indicated in Figure 18 were transformed into RS1045. All the plasmids were *CEN*-based low-copy plasmids and driven by the *SIR3* promoter. A dilution series of transformants were plated on 5-FOA medium to monitor silencing. Control transformants of a *SIR3* strain showed good growth with both vector and with WT *SIR3* plasmids (Figure 18A and B).

We found that LexA fusion *sir3* mutants (data not shown) and untagged *sir3* mutants (Figure 18) showed some different dominant effects. When the C-terminus of Sir3 was fused with a LexA tag, only S204P, C177R and A136T alleles exhibited significant telomeric silencing defects, which meant they were dominant over the WT Sir3. N80D showed partial telomeric silencing defects. Other mutants led to a good telomeric silencing, which inferred that they could not exhibit any dominance at telomere. However, when there was no tag fused with Sir3, expect for Y207C, all of the mutants exhibited drastic silencing

defects at telomere (Figure 18). Even the weakest mutant Y207C gave very little repression. Thus, using the untagged protein all the mutants were dominant or semi-dominant.

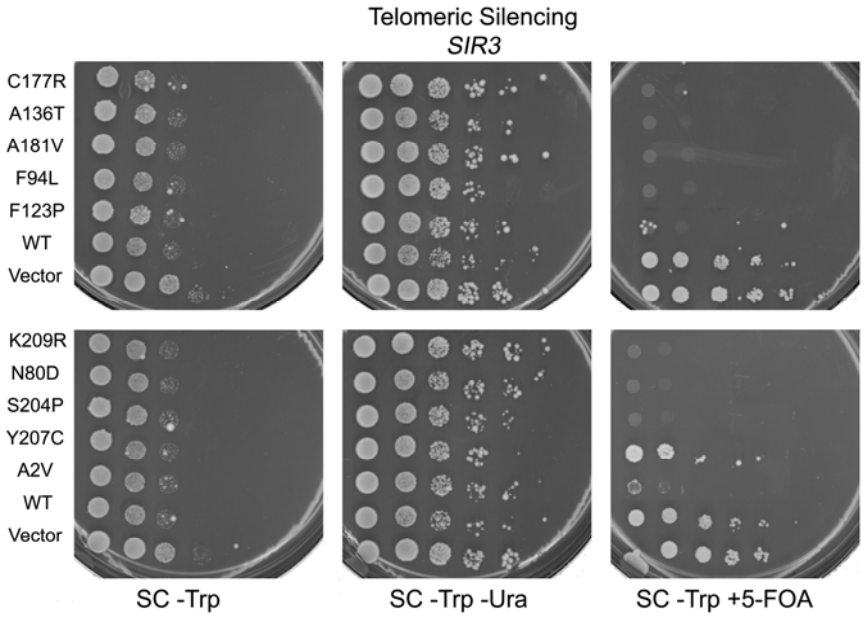

Figure 18: Dominance test of *sir3* mutants at telomere. Telomeric silencing was measured by 5-FOA resistance in a WT *SIR3* strain (RS1045) with *URA3* reporter gene at telomere. The plasmids encoding the mutant Sir3 proteins indicating in figure were transformed into RS1045. Expect Y207C, most of the mutants exhibited drastic silencing defects at telomere.

Sir3 can multimerize though its C-terminus. The mutations in the BAH domain causing dominant telomeric silencing defects would presumably form nonfunctional Sir3 multimers with WT Sir3, thereby interfering with silencing at telomeres. When the C-terminus of Sir3 was fused with a LexA tag, the tag probably weakened Sir3 binding affinity with other proteins. Therefore, Sir3-LexA with weak mutations could not compete with natural Sir3.

5. Protein levels of *sir3* mutants

The reason for silencing defects of these *sir3* alleles might not come from the nonfunctional mutations, but be due to the low levels of the Sir3 proteins. To exclude this possibility, a western blot was used to examine the Sir3 expression levels from the series of plasmids used in the previous experiments.

Plasmids encoding various *sir3* mutants were transformed into a *MAT***a** *sir3*Δ strain (JCY3), which was used to assess the *HML* silencing. Antibody for the Sir3 N-terminus was used to detect full-length Sir3 (Figure 19).

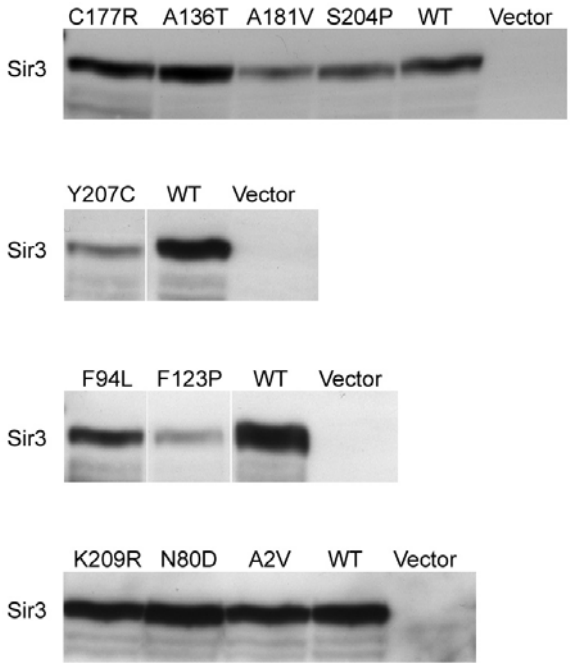

Figure 19: Western blot to examine the protein levels of *sir3* mutants. Plasmids encoding corresponding *sir3* mutants were transformed into a ***MAT*a** *sir3*Δ strain (JCY3). Antibody for the Sir3 N-terminus was used to detect full-length Sir3. Three strong mutants, A136T, C177R and S204P, had approximately the same protein levels as the WT Sir3 plasmid. F94L, N80D, K209R and A2V mutants also showed the same protein level as WT. A181V, Y207C and F123P seemed lower than WT but the proteins were still detectable.

The input control indicated that the protein loading amounts of WT and the

mutant *sir3* were approximately equal (data not shown). Three strong mutants, A136T, C177R and S204P, had approximately the same protein levels as WT Sir3 plasmid. F94L, N80D, K209R and A2V weak mutants also showed the same protein levels as WT. A181V, Y207C and F123P seemed lower than WT plasmid, but they were still detectable. The data suggested that all the mutants would not cause a big drop in protein levels.

III. Discussion

From the sequence alignment, we found that eight of ten amino acids for which mutations we obtained were conserved between $Sir3^{BAH}$ and $Orc1^{BAH}$ (Figure 20). The remaining two also showed similarity. According to the structure, N80 was situated in an unstructured region which was absent in the crystal structure (Figure 20). The structures of the region around N80 show significant conformational differences between $Sir3^{BAH}$ and $Orc1^{BAH}$.

Based on the structure, we classified all the mutations into three groups (Figure 21).

Group one contains six mutations. They are A136T, C177R, A181V, S204P, Y207C and K209R. All three strong mutants belong to this group. In Figure 21, they are labeled in red. As mentioned above, the D205N mutant could strengthen silencing. This residue is in α-helix F. There is a groove between α-helix F and the core domain of the BAH. Mutations in group one are located around the groove. The distance of Cα atoms between K209 and A136 is 5.15Å (Figure

21B), which is the approximate distance between helix F and the core domain.

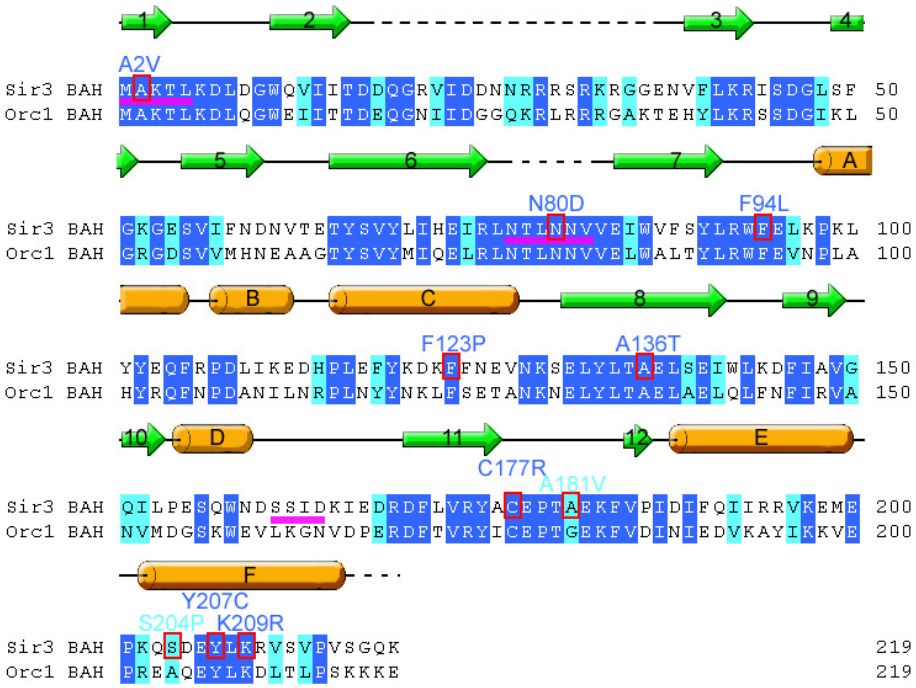

Figure 20: Alignment of Sir3^{BAH} and Orc1^{BAH} sequences and the secondary structure of Sir3 BAH domain. Residues identical between Sir3 and Orc1 are showed in blue, and similar residues are colored in cyan. The positions of mutations are labeled in red boxes. The secondary structure of the Sir3 BAH domain is indicated above the sequences. Orange cylinder represents α-helix and green arrow represents β-sheet. Dashed lines indicate disordered regions. Purple lines indicate the regions with significant conformational differences between Sir3^{BAH} and Orc1^{BAH} (Zhang *et al.*, 2002); even these residues are identical between the two proteins.

Group two contains the mutations in the extreme N-terminus. In Figure 21, it is labeled in orange. A former graduate student in our lab, X. Wang, discovered that the extreme N-terminus of Sir3 is very important for its function. In my work, I also got an A2V mutant. In yeast, after translation the first methionine is cleaved and this alanine becomes to the first residue of the mature Sir3 protein. Comparing to the structure of Orc1^{BAH}, the Sir3 extreme N-terminus has a significantly different conformation (Figure 12C). It might

explain why the Orc1 and Sir3 BAH domains have different silencing effects.

Group three contains two mutations: F94L and F123P. As shown in Figure 21, these two blue residues are situated in the H domain. In the Orc1, F94 and F123 are important for the association with Sir1. In Sir3, mutations in these two residues caused a silencing defect. Therefore, we think the H domain of the BAH might be very important for protein function.

A136T, C177R and S204P are the strongest mutations. S204 is in the α-helix F (Figure 22A), and the substitution with P breaks the α-helix and probably causes a big structural change in this region. A136 is in the middle of β-sheet 8, and C177 is located at the loop between β-sheet 11 and 12 (Figure 22A). These two residues are in the core domain of $Sir3^{BAH}$. The distance of Cα between S204 and A136 is 10.33Å, the distance of Cα between A136 and C177 is 7.83Å, and the distance of Cα between S204 and C177 is 16.33Å (Figure 22C). In conclusion, we think A136, C177 and S204 are not very close to each other. However, the locations of these three mutations belong to the same region of Sir3. They all are located in the groove between helix F and the core domain (Figure 22A and B). We think these three residues should play the same role in the function of the Sir3 BAH domain.

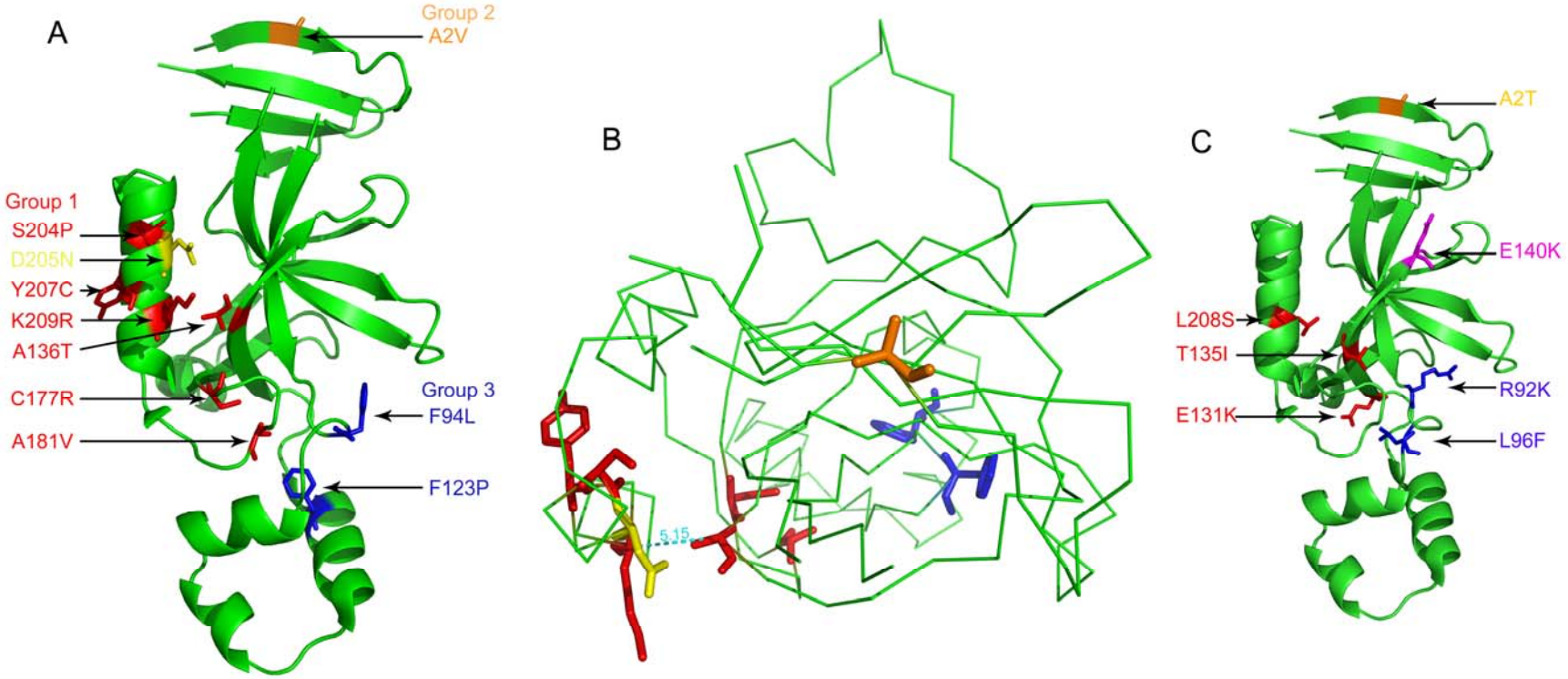

Figure 21: Locations of the mutations in this study are indicated in the structure of Sir3 BAH domain. (A) The crystal structure is shown in a ribbon representation. Position of group one mutants are colored in red, group two in orange and group three in blue. D205 is in yellow. (B) View of the structure from a different orientation and shown in backbone. The distance of Cα between K209 and A136 is 5.15Å, which is labeled in cyan. (PDB: 2FVU) (C) Locations of ***eso-sir3*** mutants. Except R30K (in a disorder region) and S813F (at the C-terminus), the rest seven ***sir3-eso*** mutants identified cluster within the BAH domain labeled with different colors (Stone ***et al.***, 2000).

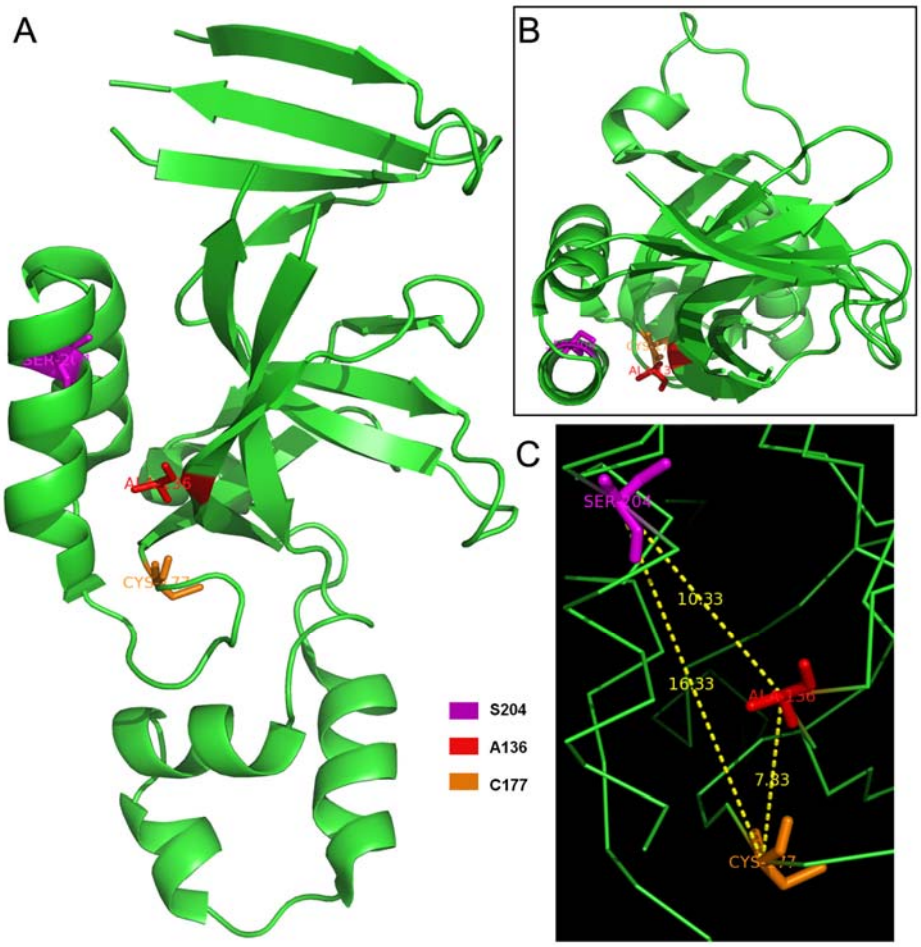

Figure 22: Locations of three drastic mutations in the Sir3^{BAH} structure. (A) The crystal structure is shown in a ribbon representation. S204 is colored in purple, A136 is in red, and C177 is in orange. (B) Top view of the structure in ribbon. (C)A Detailed view of the positions of three strongest mutations. The structure is in a backbone representation. The distance of Cα between S204 and A136 is 10.33Å, the distance of Cα between A136 and C177 is 7.83Å, and the distance of Cα between S204 and C177 is 16.33Å. (PDB: 2FVU)

Genotype	Telomere *sir3Δ*	*HML sir3Δ*	*HMR sir3Δ*	*HML sir3Δ sir1Δ*	*HMR sir3Δ sir1Δ*	Dominant at Telomere	Expression Levels	Category
A2V	-	+++	+++	-	-	Yes	+++	weak
N80D	-	++	+++	-	-	Yes	+++	moderate
F94L	-	+++	+++	-	-	Yes	+++	weak
F123P	-	+++	+++	-	-	Yes	++	weak
A136T	-	-/+	++	-	-	Yes	+++	strong
C177R	-	-/+	++	-	-	Yes	+++	strong
A181V	-	+++	+++	-	-	Yes	++	weak
S204P	-	-/+	++	-	-	Yes	+++	strong
Y207C	-/+	+++	+++	-	-	Yes	++	weakest
K209R	-	+++	+++	-	-	Yes	+++	weak
WT	+++	+++	+++	+++	+++	-	+++	
Null	-	-	-	-	-	-	-	

Table 1: Summary of mutations from the Sir3 BAH random mutagenesis screen. Plasmids encoding full-length Sir3 carrying various mutations were transformed into yeast strains. Yeast strains, XRY16 (***sir3***Δ, telomeric ***URA3***) and RS1045 (***SIR3***, telomeric ***URA3***) were used for telomeric silencing; JCY3 (***MAT*****a**, ***sir3***Δ) and JCY8 (***MAT*****a**, ***sir3***Δ***sir1***Δ) were used for ***HML*** silencing; JCY4 (***MATα***, ***sir3***Δ) and JCY9 (***MATα***, ***sir3***Δ***sir1***Δ) were used for ***HMR*** silencing. An anti-Sir3 antibody was used to detect the protein levels of the mutants in an ***MAT*****a** ***sir3***Δ strain (JCY3) by western blotting. +++=Good silencing; ++ to - =Different levels of defective silencing.

CHAPTER FOUR

Sir3 BAH Domain Association with Nucleosomes and DNA

I. Introduction

Full-length Sir3 has been shown to interact with Rap1, Sir4, and histone H3 and histone H4 N-terminal tails, and these interactions are thought to be responsible for the recruitment of Sir3 to the silent *HM* loci. Interestingly, the Sir3 regions involved in these interactions are located outside the BAH domain (also beyond the first 380 residues). The Sir3 BAH domain alone can silence a fraction of cells at *HM* loci (Chapter Two). Furthermore, point mutations in the BAH domain can weaken or abolish silencing (Chapter Three). These data suggest that the N-terminus of Sir3 plays an important role in transcriptional silencing and that it has the ability to function when separated from the rest of the protein. A natural question to ask is what protein-protein interactions recruit the Sir3 BAH domain to the silent chromatin.

The BAH domain is a module found in several chromatin associated proteins (Callebaut *et al*., 1999) and the D205N mutation within this domain of Sir3 suppresses the loss of silencing due to mutations in the histone H4 tail (Johnson *et al*., 1990). Given these observations, we reasoned that this domain might interact

with the nucleosomes. Nucleosome binding was inferred by a decrease in the mobility of the nucleosomes upon addition of $Sir3^{1-380}$ in a gel retardation assay (work of J. Connelly). It was previously reported that full-length Sir3 bound to DNA (Georgel *et al*., 1999). Our lab also discovered that $Sir3^{1-380}$ binding to a 146 bp DNA fragments in a gel retardation assay (work of J. Connelly).

II. Results

1. $Sir3^{1-214\ D205N}$ interacted with both nucleosomes and DNA

In order to test whether $Sir3^{1-214}$ bound to oligonucleosomes or DNA, we performed *in vitro* experiments using recombinant $Sir3^{1-214}$-His purified from *E. coli* and oligonucleosomes from yeast. To obtain oligonucleosomes, chromatin was isolated and partially digested with micrococcal nuclease, and oligonucleosomes were size fractionated on a gel filtration column (Figure 23). Two pooled fractions were used for binding assays (Figure 23A, labeled A and B): fraction A had oligonucleosomes with approximately 2 to 5 nucleosomes, and fraction B had mono- and dinucleosomes. Binding was assessed by a standard gel shift assay.

The results of this experiment are shown in Figure 23B. The addition of $Sir3^{1-214}$-His did not affect oligonucleosome mobility, whereas the addition of $Sir3^{1-214\ D205N}$-His led to a decrease in mobility. As mentioned previously, the D205N mutant could restore silencing to certain silencing mutants. C-terminal tagged $Sir3^{1-214}$-GST and $Sir3^{1-214\ D205N}$-GST were also tested in this assay. As with

the His-tagged proteins, only the Sir3$^{1\text{-}214\ D205N}$-GST protein had the ability to retard the mobility of the oligonucleosomes (data not shown). These results show that the D205N mutant greatly increased the ability of Sir3$^{1\text{-}214}$ to bind to oligonucleosomes.

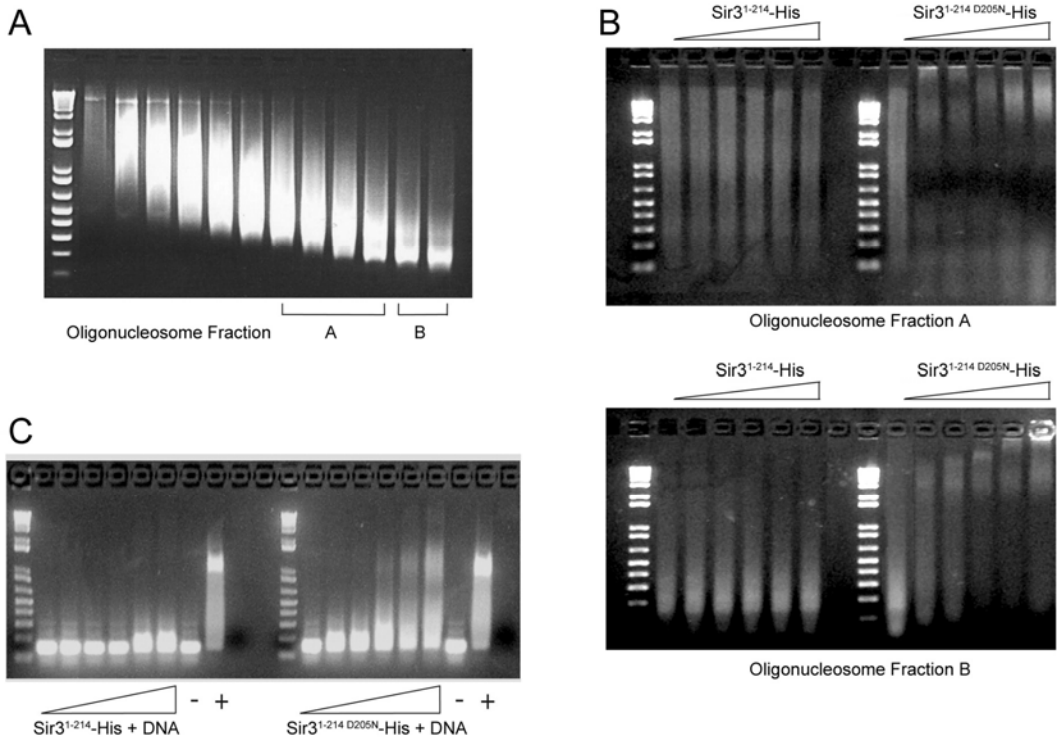

Figure 23: Oligonucleosomes and DNA binding ability of Sir3$^{1\text{-}214\ D205N}$-HIS. (A) Oligonucleosomes were isolated from yeast and size fractionated by gel filtration. Fractions were collected, and a portion of each fraction was electrophoresed on an agarose gel. The ethidium bromide-stained gel is shown. (B) Pooled oligonucleosome fractions A and B, or a 146 bp fragment of DNA (C), were incubated with increasing amounts of recombinant Sir3$^{1\text{-}214}$-His or Sir3$^{1\text{-}214\ D205N}$-His. In panel C, the lanes labeled – have a negative control with no protein added (identical to the first lane in the ramp), and the lanes labeled + have a positive control using recombinant Sir3$^{1\text{-}380}$-His.

We also examined whether Sir3$^{1\text{-}214}$ fragments could associate with DNA. We tested Sir3$^{1\text{-}214}$-His and Sir3$^{1\text{-}214\ D205N}$-His binding to DNA using a gel shift assay with a 146 bp DNA fragment (a gift from R. Xu). Just as with oligonucleosomes,

Sir3$^{1-214}$-His did not shift DNA, whereas Sir3$^{1-214\ D205N}$-His bound DNA and retarded its mobility at protein concentrations equivalent to those seen for nucleosomes (Figure 23C). Similar to the His-tagged proteins, only the Sir3$^{1-214\ D205N}$-GST protein had the ability to decrease the mobility of the DNA (data not shown). These data showed that the D205N gain-of-function mutation found within the BAH domain of Sir3 allowed the BAH domain of Sir3 to associate with nucleosomes through an interaction with DNA. Interestingly, the Sir3$^{1-380}$-His protein bound to both oligonucleosomes and DNA even without the D205N mutation (Figure 23 and data not shown).

2. Sir3$^{1-253}$ and Sir3$^{1-219}$ bound to DNA

One possible reason why the Sir3$^{1-214}$ fragment did not to bind to DNA and nucleosomes is because Sir3$^{1-214}$ is smaller than the real BAH domain and might be partially unfolded. Therefore, we thought it might be better to use longer fragments which could fold better *in vitro*.

Since Sir3$^{1-380}$ showed a significant DNA and nucleosome binding ability but Sir3$^{1-214}$ had no binding ability, we designed a middle-size fragment, Sir3$^{1-253}$ for DNA binding experiments. Sir3$^{1-253}$-His, Sir3$^{1-253\ A2V}$-His, Sir3$^{1-253\ D205N}$-His, Sir3$^{1-253\ A136T}$-His, Sir3$^{1-253\ C177R}$-His and Sir3$^{1-253\ S204P}$-His were purified from *E. coli*. A2V, A136T, C177R and S204P mutants were obtained from the BAH mutagenesis screen (Chapter Three). A136T, C177R and S204P were the three

strongest mutants which led to both telomeric and *HML* silencing defects. A 1.3-kilobase DNA fragment containing the *HMR-E* region was generated by PCR (As with the 146 bp fragment shown in Figure23C, $Sir3^{1\text{-}214\ D205N}$ could bind to this 1.3-kilobase DNA fragment, but $Sir3^{1\text{-}214}$ could not). DNA binding ability of the $Sir3^{1\text{-}253}$ was assessed by a gel retardation assay (Figure 24). 2~20 μg recombinant proteins were used in the reactions and the agarose gel was stained by ethidium bromide (Figure 24A). DNA input without any proteins was loaded as a control. All the $Sir3^{1\text{-}253}$-His fragments showed very significant DNA binding ability, even those with the strongest mutations leading to silencing defects. And the D205N mutant had no better binding than WT. It was not surprising because $Sir3^{1\text{-}380\ D205N}$ also showed an equal binding ability to $Sir3^{1\text{-}380}$ (work of J. Connelly). DNA binding capabilities of $Sir3^{1\text{-}253}$-His were also checked on a native PAGE gel with ^{32}P-labeled PCR products (Figure 24B). 10 μg of protein was used in each reaction. The result also suggested that all the $Sir3^{1\text{-}253}$-His fragments had the same DNA binding capabilities.

Further, nitrocellulose filter binding assay was used to quantify the fraction of bound input DNA. The nitrocellulose membrane can bind protein and protein-DNA complex, but not free DNA. The amount of radiolabeled DNA stuck to the nitrocellulose is quantified by measuring the amount of radioactivity on the filter using a scintillation counter or phosphoimager. A 1.3-kilobase DNA fragment of *HMR-E* was generated by PCR with ^{32}P-labeling. $Sir3^{1\text{-}253}$-His, $Sir3^{1\text{-}253\ A2V}$-His,

Sir3$^{1\text{-}253\ D205N}$-His, Sir3$^{1\text{-}253\ A136T}$-His, Sir3$^{1\text{-}253\ C177R}$-His and Sir3$^{1\text{-}253\ S204P}$-His from *E. coli* were pre-mixed with DNA fragments in solution and then loaded to the membrane. Concentrations of proteins were indicated as Figure 25. 10 µl of protein was used for each reaction.

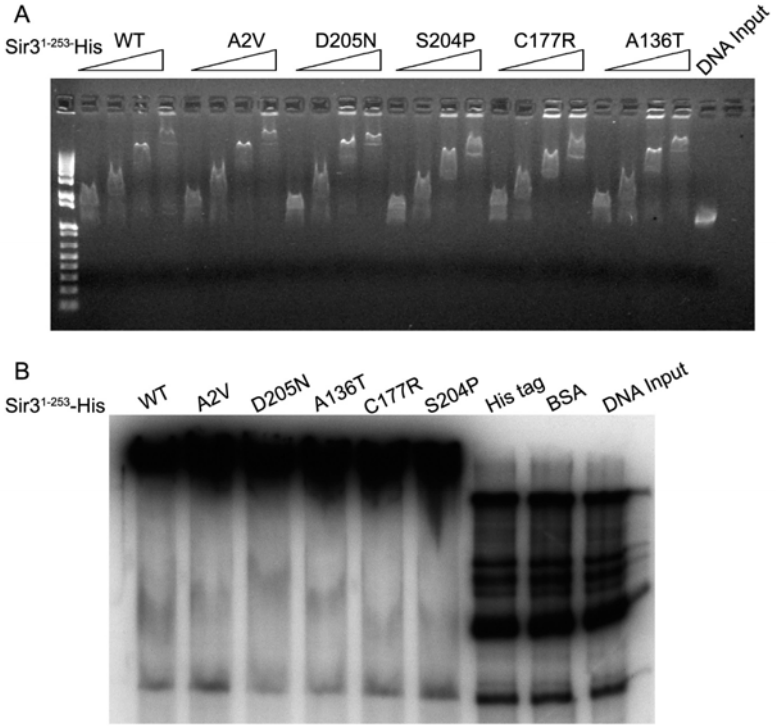

Figure 24: Sir3$^{1\text{-}253}$ bound to DNA. Sir3$^{1\text{-}253}$-His, Sir3$^{1\text{-}253\ A2V}$-His, Sir3$^{1\text{-}253\ D205N}$-His, Sir3$^{1\text{-}253\ A136T}$-His, Sir3$^{1\text{-}253\ C177R}$-His and Sir3$^{1\text{-}253\ S204P}$-His were purified from *E. coli*. A 1.3-kilobase DNA fragment containing the *HMR-E* region was generated by PCR. 2~20 µg recombinant proteins were used in the reactions and DNA binding abilities were assessed by a gel retardation assay in a ethidium-bromide-stained agarose gel(A) and a native PAGE gel (B). DNA input without any protein was loaded as a control. All the Sir3$^{1\text{-}253}$-His fragments showed very significant DNA binding abilities.

The results from filter binding experiments were very similar to that from gel retardation assay. All the Sir3$^{1\text{-}253}$-His fragments showed a dosage-dependent DNA binding ability (Figure 25A). A2V, D205N, A136T, C177R and S204P mutations all

had the same the binding capability in context of $Sir3^{1-253}$-His. Figure 25B showed the quantitative result from a phosphoimager. BSA was used as a negative control which had a very low background. WT, A2V, D205N, A136T, C177R and S204P all exhibited the same DNA binding ability.

$Sir3^{1-253}$ is larger than the BAH domain. Later, a shorter piece, $Sir3^{1-219}$ fragment was chosen for binding tests, since the crystal structure showed this fragment could form a folded BAH domain. To be consistent with nucleosome binding results (shown later), $Sir3^{1-219}$ was also tagged with GST at the C-terminus.

$Sir3^{1-219}$-GST, $Sir3^{1-219\ D205N}$-GST and $Sir3^{1-219\ A2Q}$-GST were purified from *E. coli*. *sir3* A2Q mutant was identified by our lab (Wang *et al*., 2004). It caused telomeric and *HML* silencing defects. A2Q was a stronger mutation than A2V which was obtained in the mutagenesis screen. A 1.3-kilobase DNA fragment of *HMR-E* was generated by PCR. DNA binding ability was assessed by a gel retardation assay, as before (Figure 24). 0~30 μg recombinant proteins were used in the reactions and the agarose gel was stained by ethidium bromide (Figure 26A). GST itself could not shift any DNA fragment, even at the highest concentration. $Sir3^{1-219}$-GST could decrease the mobility of DNA. $Sir3^{1-219\ D205N}$-GST had a slightly better affinity than WT, whereas $Sir3^{1-219\ A2Q}$-GST had a worse binding capability than WT.

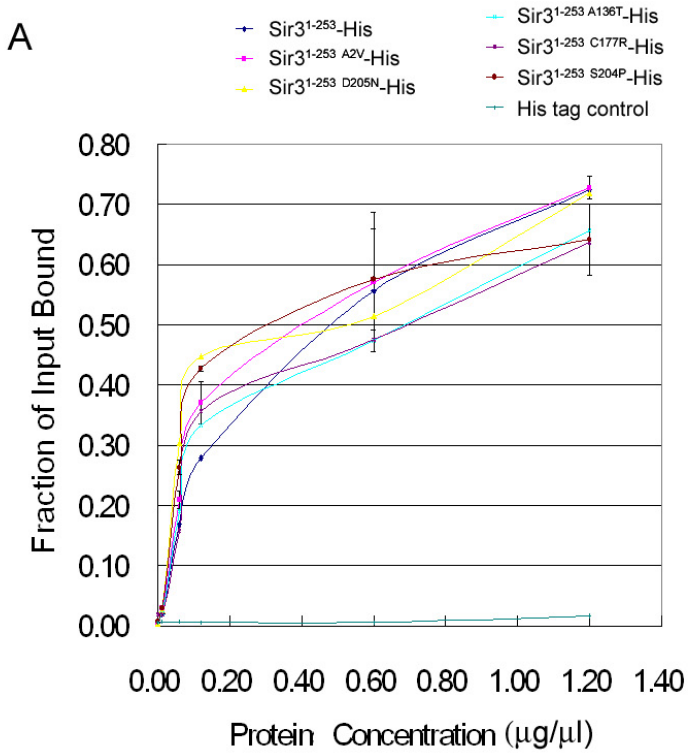

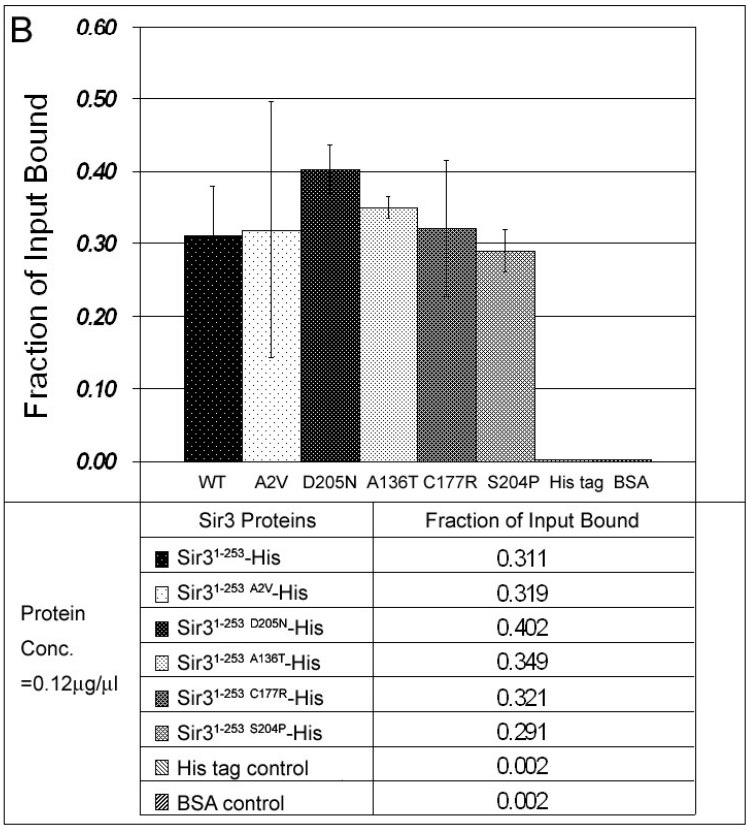

Protein Conc. =0.12µg/µl

Sir3 Proteins	Fraction of Input Bound
Sir3 1-253 -His	0.311
Sir3 1-253 A2V -His	0.319
Sir3 1-253 D205N -His	0.402
Sir3 1-253 A136T -His	0.349
Sir3 1-253 C177R -His	0.321
Sir3 1-253 S204P -His	0.291
His tag control	0.002
BSA control	0.002

Figure 25: The fractions of bound DNA with $Sir3^{1-253}$-His were quantified by nitrocellulose filter binding assay. A 1.3-kilobase DNA

fragment of *HMR-E* was generated by PCR with ^{32}P-labeling. Sir3$^{1-253}$-His, Sir3$^{1-253\ A2V}$-His, Sir3$^{1-253\ D205N}$-His, Sir3$^{1-253\ A136T}$-His, Sir3$^{1-253\ C177R}$-His and Sir3$^{1-253\ S204P}$-His from *E. coli* were mixed with DNA fragments in solution and then loaded to the membrane. Concentrations of protein are indicated in the figure. 10 µl of protein was used for each reaction. The amount of radiolabeled DNA stuck to the nitrocellulose was quantified by measuring the amount of radioactivity on the filter using a scintillation counter (A) or phosphoimager (B). Shown here are averages and standard deviation from duplicate reactions from one of many experiments.

In Figure 26A, DNA shown on the upper part of the agarose gel was not due to the real shift by Sir3 fragments, but from the contamination DNA in the protein preparation. To exclude this background, 1.3-kilobase DNA fragments of *HMR-E* labeled with ^{32}P were used for the same assay. DNA mobility was examined by phosphoimager (Figure 26B). The data indicated the same result of DNA mobility as the ethidium-bromide-stained gel and showed that upper band in the ethidium-bromide-stained gel (Figure 26A) was due to DNA in the Sir3 protein preps.

The DNA binding of Sir3$^{1-219}$-His was also detected by gel retardation assay. It resulted in some DNA smears at a high protein concentration (data not shown), which was very similar to the Sir3$^{1-219}$-GST fragment. A DNA fragment of *ADH1* promoter region (1.5 kb) was also used in the gel retardation assay. No difference was observed between *HMR-E* fragments and *ADH1* promoter fragments (data not shown).

Compared with Sir3$^{1-253}$, Sir3$^{1-219}$ exhibited a weak DNA binding ability. Therefore, there were two possible functions for the Sir3 region between residue

220 and 253: (i) this region could help folding of the BAH domain *in vitro*; (ii) this region might contribute to association with DNA.

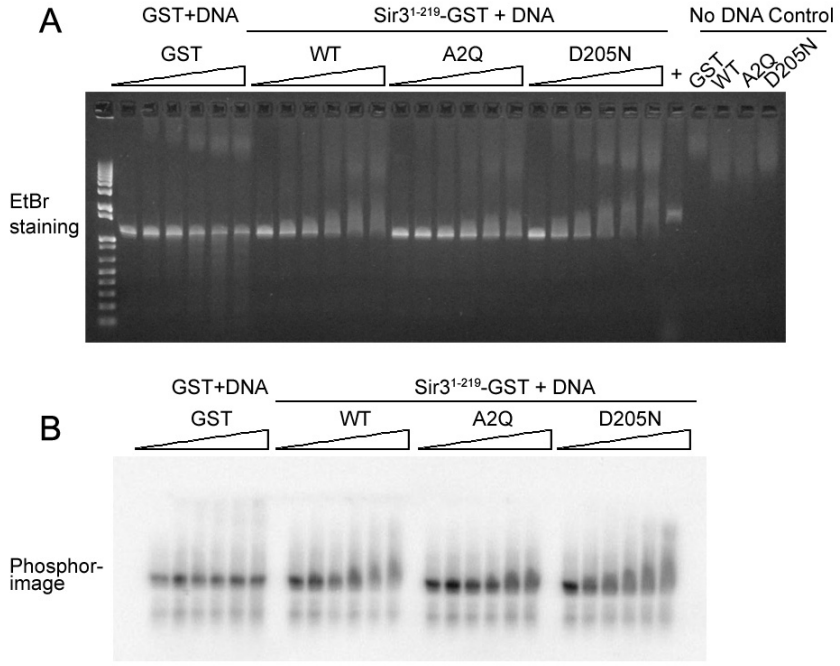

Figure 26: Sir3$^{1-219}$-GST bound to DNA. Sir3$^{1-219}$-GST, Sir3$^{1-219\ D205N}$-GST and Sir3$^{1-219\ A2Q}$-GST were purified from *E. coli*. A 1.3-kilobase DNA fragment of *HMR-E* was generated by PCR. DNA binding ability was assessed by a gel retardation assay. 0~30 µg recombinant proteins were used in the reactions and DNA mobility was assessed by ethidium bromide staining (A) or phosphoimager (B). GST was used as a negative control. The plus sign indicates the positive control, Sir3$^{1-214\ D205N}$-GST with DNA. Sir3$^{1-219}$-GST could decrease the mobility of DNA. Sir3$^{1-219\ D205N}$-GST had a slightly bigger affinity than WT, whereas Sir3$^{1-219\ A2Q}$-GST had a worse binding capability than WT.

These data suggested that the reason of D205N mutant could have DNA binding ability in context of Sir3$^{1-214}$ might be just because it could stabilize the structure of the recombinant Sir3 fragment. When a longer piece of Sir3 was used, all the recombinant proteins could fold well enough and be able to bind DNA. A2Q, A136T, C177R and S204P mutants caused silencing defects in context of full-length

Sir3. However, all of them could bind to DNA as well as WT in context of $Sir3^{1-253}$. These data suggested that the DNA binding ability of the Sir3 BAH domain might not be its key function.

3. $Sir3^{1-219}$ could bind to nucleosomes

Nucleosomes are made up of DNA and the histone octamer. $Sir3^{1-214\ D205N}$ could decrease the mobility of nucleosomes. But WT $Sir3^{1-214}$ never exhibited nucleosome binding ability. Therefore, a longer piece, a $Sir3^{1-219}$ fragment, was chosen for testing the nucleosome binding ability.

Enriched nucleosomes were isolated from yeast. Figure 27 showed protease K digestion products of the enriched nucleosomes. The bright bands at 150 bp, 300 bp, 450 bp were the DNA fragments corresponding to mono-, di- and tri-nucleosomes. The data suggested that the enriched nucleosomes mainly contained oligonucleosomes with approximately 1 to 3 nucleosomes. Recombinant proteins of $Sir3^{1-219}$-GST were purified from *E. coli*. A standard GST pull-down assay was used to assess the nucleosome binding ability. Histone H3 which bound to the $Sir3^{1-219}$-GST was detected by western.

$Sir3^{1-219}$-GST exhibited the nucleosome binding capability, but not at the lowest concentration (Figure 28), while $Sir3^{1-219\ D205N}$-GST still gave some binding at this concentration (Figure 28). The data meant that the D205N mutant could bind to nucleosomes more tightly than WT.

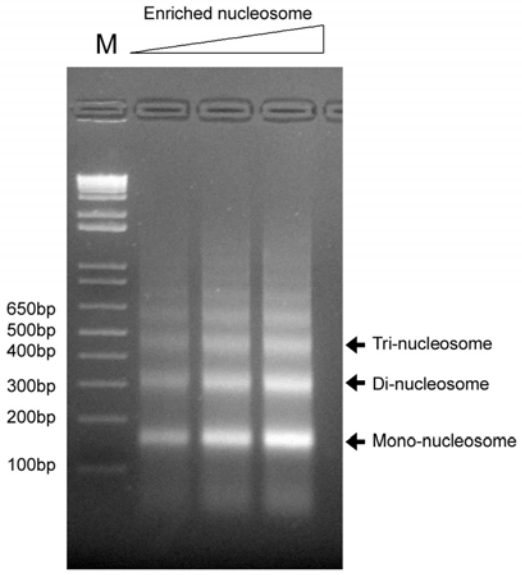

Figure 27: The enriched nucleosomes after protease K digestion presented on the agarose gel with ethidium bromide staining. M means DNA ladder marker. Triangle means the increasing of loading amount of digestion products. DNA fragments corresponding to mono-, di- and tri-nucleosomes are indicated.

Nucleosome binding abilities of *sir3* mutants that caused silencing defects were measured using the same assay. Three strong mutants (A136T, C177R and S204P), one moderate mutant (N80D) and two weak mutants (F94L and A181V) from the mutagenesis screen (Table 1) were purified from *E. coli* in the context of $Sir3^{1-219}$-GST. The nucleosome binding ability of the A2Q mutant which led a *HML* silencing defect was also tested.

Figure 29 showed the nucleosome binding results of the mutants. In the coomassie staining SDS PAGE gel, all upper bands were $Sir3^{1-219}$-GST fragments, and the lower bands were small proteins of $Sir3^{199-219}$ fused to entire GST. The negative control in this experiment was GST. The western data indicated that all the Sir3 fragments with mutations could not associate with nucleosomes any more, just

like the negative control, while WT still could bind.

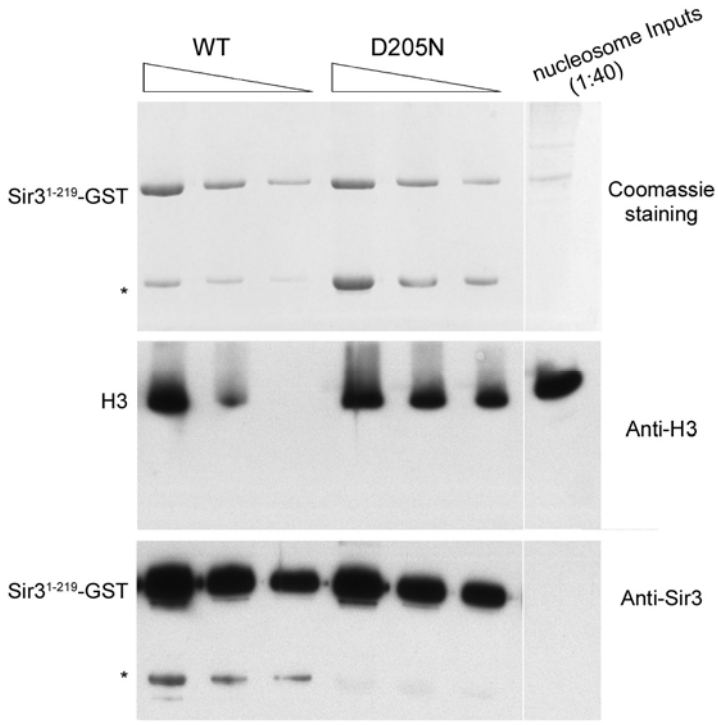

Figure 28: Sir3$^{1-219}$-GST and Sir3$^{1-219\ D205N}$-GST could associate with the nucleosomes. The upper part is a coomassie-stained SDS PAGE to indicate the amounts of Sir3$^{1-219}$-GST and Sir3$^{1-219\ D205N}$-GST used in the experiments. 5~20 μg of recombinant proteins were used. Star means a secondary product from protein purification. Middle part is an anti-H3 western. At low protein concentrations, Sir3$^{1-219\ D205N}$-GST could bind nucleosomes better than WT. Lower part is an anti-Sir3 western, which suggested that these proteins bands from nucleosome inputs shown in the coomassie staining were not Sir3. Asterisks represent the GST tag with a tiny Sir3 piece, aa 199-219 (unpublished data of J. Connelly).

All the recombinant proteins used in the nucleosome binding assay were purified from *E. coli*. One possibility of the nucleosome binding defects was because those fragments did not fold correctly and lost the functions. However, in the previous tests, Sir3$^{1-219\ A2Q}$-GST could change the mobility of naked DNA (Figure 26), and Sir3$^{1-219\ A136T}$-GST, Sir3$^{1-219\ C177R}$-GST and Sir3$^{1-219\ S204P}$-GST also

could (data not shown). This data suggested $Sir3^{1\text{-}219\ A2Q}$-GST, $Sir3^{1\text{-}219\ A136T}$-GST, $Sir3^{1\text{-}219\ C177R}$-GST and $Sir3^{1\text{-}219\ S204P}$-GST fragments from *E. coli* lost the nucleosome binding ability, but retained the DNA binding ability.

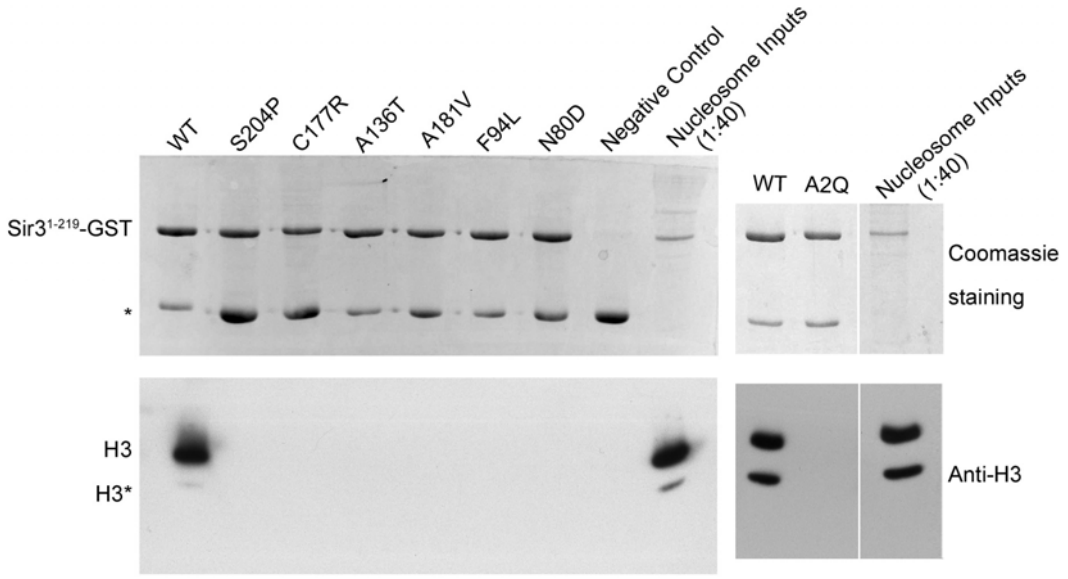

Figure 29: Nucleosome binding ability of $Sir3^{1\text{-}219}$-GST with various mutations. The upper part is coomassie-staining SDS PAGE to indicate the amounts of $Sir3^{1\text{-}219}$-GST, $Sir3^{1\text{-}219\ A2Q}$-GST $Sir3^{1\text{-}219\ N80D}$-GST, $Sir3^{1\text{-}219\ F94L}$-GST, $Sir3^{1\text{-}219\ A136T}$-GST, $Sir3^{1\text{-}219\ A181V}$-GST, $Sir3^{1\text{-}219\ C177R}$-GST, $Sir3^{1\text{-}219\ S204P}$-GST used in the experiments. 20 µg of each recombinant protein was used. Negative control was GST. Lower is the anti-H3 western. WT Sir3 still could associate with nucleosomes, while none of the mutants could. The asterisk in the coomassie gel represents the GST tag with a tiny Sir3 piece (aa 199-219), and the H3* indicates the degradation product of H3.

4. Orc1 BAH domain could bind to nucleosomes but not DNA

Since the Orc1 BAH domain bears a high similarity to the Sir3 BAH domain, we sought to determine whether the Orc1 BAH domain could associate with DNA and nucleosomes in a similar way. Because we obtained a good DNA binding result from $Sir3^{1\text{-}253}$-His and a good nucleosome binding from $Sir3^{1\text{-}219}$-GST, $Orc1^{1\text{-}253}$-His

was designed for the DNA binding test and Orc1$^{1-219}$-GST was used for the nucleosome binding test.

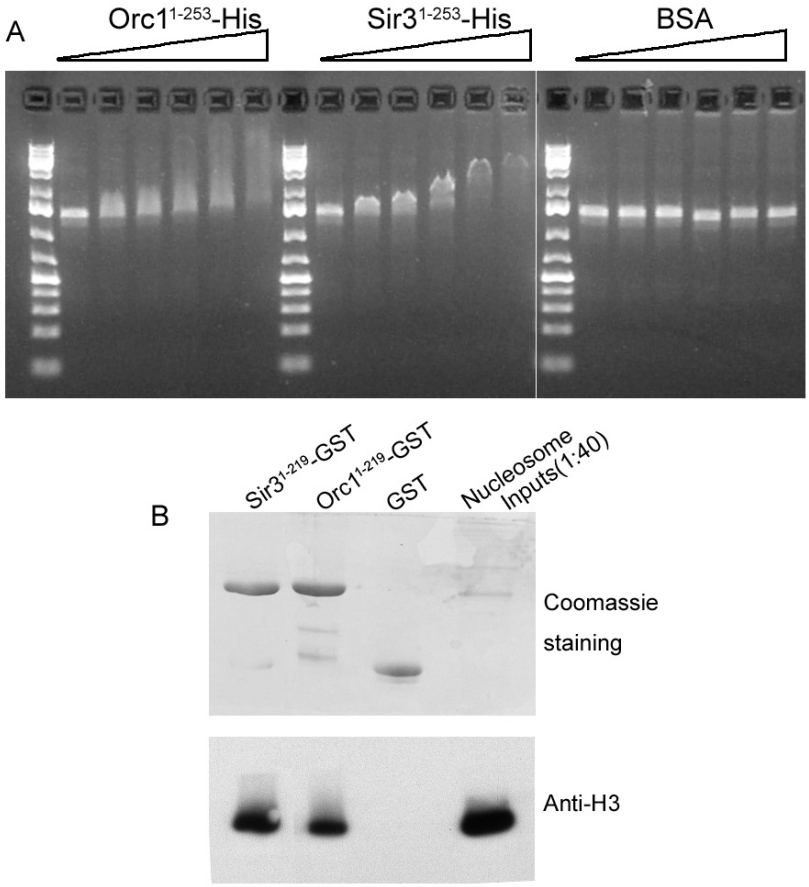

Figure 30: The Orc1 BAH domain could bind to nucleosomes and DNA. (A) DNA binding ability of Orc1$^{1-253}$-His fragment was examined in a gel retardation assay. 0~30 μg of recombinant proteins from *E. coli* and 1.3-kilobase DNA fragments of *HMR-E* were used. BSA was the negative control. Comparing with Sir3$^{1-253}$-His, Orc1$^{1-253}$-His only caused a weak mobility decrease (work of E. Prugar). (B) Nucleosome binding capability of Orc1$^{1-219}$-GST fragment was also measured by a standard GST pull-down assay. 20 μg of recombinant proteins from *E. coli* and enriched nucleosomes from W303-1a yeast strain were used. Histone H3 which bound to proteins was detected by western. Data showed that Orc1$^{1-219}$-GST could bind to nucleosomes, but a little weaker than Sir3$^{1-219}$-GST.

DNA binding ability of the Orc1$^{1-253}$-His fragment was examined in a gel retardation assay. 0~30 μg of recombinant proteins from *E. coli* and 1.3-kilobase

DNA fragments of *HMR-E* were used (work of E. Prugar). Comparing with Sir3$^{1-253}$-His (positive control) and BSA (negative control), Orc1$^{1-253}$-His only caused a weak mobility decrease. Since *sir3* mutants which caused *HML* silencing defects could also interact with DNA in the context of Sir3$^{1-253}$-His (Figure 25), we concluded that, compared with the Sir3 BAH domain, DNA binding ability of the Orc1 BAH domain was weak and perhaps not significant.

Nucleosome binding capability of the Orc1$^{1-219}$-GST fragment was also measured by a standard GST pull-down assay. 20 μg of recombinant proteins from *E. coli* and enriched nucleosomes from WT yeast strain (W303-1a) were used. Histone H3 which bound to proteins was detected by western. Data showed that Orc1$^{1-219}$-GST could bind to nucleosomes, but a little weaker than Sir3$^{1-219}$-GST. Based on the previous results that weak *sir3* mutants leading a telomeric silencing defect could not associate with nucleosomes any more (Figure 29), we conclude that the Orc1 BAH domain had an apparent nucleosome binding capability.

5. Some histone mutants could suppress some of *sir3* mutants

Acetylation of histone H4 on lysine 16 is a prevalent and reversible posttranslational chromatin modification in eukaryotes. Sir2 is a deacetylase which acts on histone H4 K16. A mutation of lysine 16 to arginine in histone H4 (H4 K16R) restored silencing at a defective *HMR* allele (Meijsing *et al*., 2001). The most direct explanation of this result is that H4 K16 is acetylated, which is

detrimental to silencing at a mutated *HMR* allele. Thus, when this position in the H4 tail is occupied by a positively charged amino acid, silencing is improved. Furthermore, H4 K16R caused derepression at *HML* in a *sir1*Δ strain and telomeric *URA3* (Meijsing *et al*., 2001). A recent paper indicated that the Sir3 BAH domain bound tightly to nucleosomes containing an H4 K16R mutation, suggesting that this domain efficiently recognized the charged, unacetylated state of H4 K16 (Onishi *et al*., 2007). Based on these discoveries, we sought to determine whether H4 K16R mutant could rescue any *sir3* mutants.

Yeast strains with an *hht1*Δ-*hhf1*Δ, *hht2*Δ-*hhf2*Δ and *sir3*Δ *sir1*Δ background were made and transformed with plasmids encoding either WT histones (VSY 29) or H4 K16R mutant (PPY12). A series of plasmids carrying *SIR3* with various *sir3* mutations which were studied in my previous work were transformed into the yeast cells and silencing of *HMR* tested by mating.

The result showed that in a *sir3*Δ *sir1*Δ strain all the *sir3* mutants could not lead to any silencing at *HMR* with WT histones which was consistent with my previous data (Figure 31A and Figure 17B).

As shown in Figure 31B, H4 K16R mutant could rescue silencing of some *sir3* mutants in a *sir3*Δ *sir1*Δ strain at *HMR,* including A181V, K209R and Y207C. In this case, H4 K16R also had a partial suppression effect to A2V, N80D, F94L and F123P at *HMR*. However, three strong mutants, A136T, C177R and S204P, still gave no silencing at *HMR* with H4 K16R mutant.

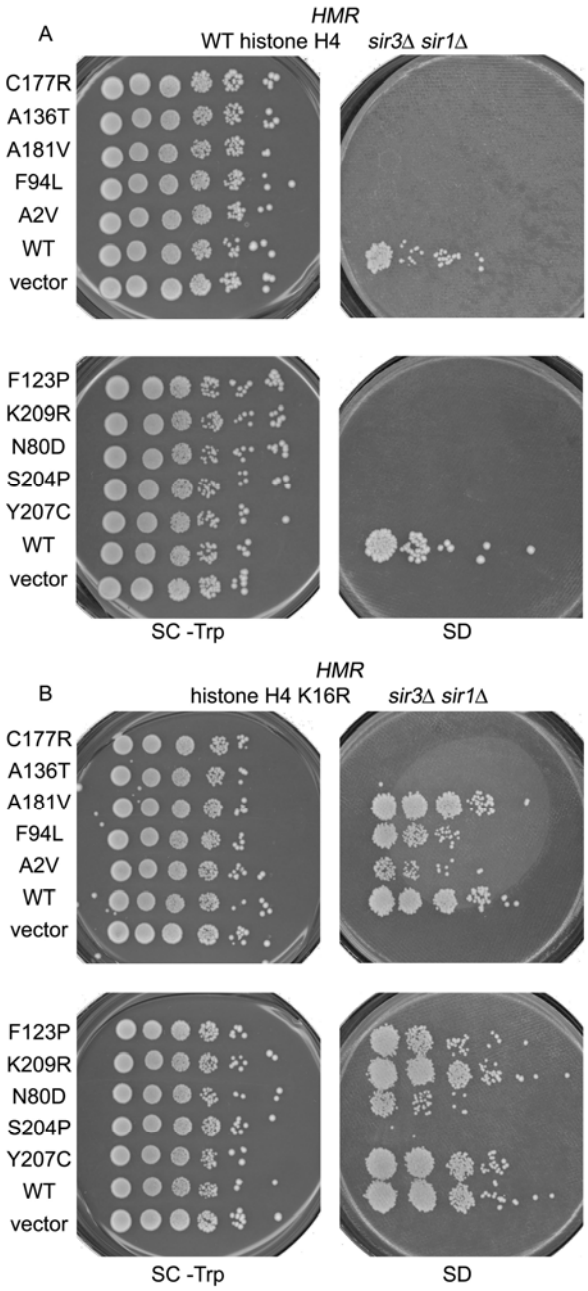

Figure 31: H4 K16R mutant could rescue some ***sir3*** mutants in a ***sir3***Δ ***sir1***Δ strain at ***HMR***. Yeast strains with an ***hht1***Δ-***hhf1***Δ, ***hht2***Δ-***hhf2***Δ and ***sir3***Δ***sir1***Δ background was made and transformed with plasmids encoding either WT histone (VSY 29) or H4 K16R mutant (PPY12). A series of plasmids carrying Sir3 with various mutations which were studied in my previous work were transformed into the yeast cells and silencing of ***HMR*** tested by mating. (A) In a ***sir3***Δ ***sir1***Δ strain, none of the ***sir3*** mutants could lead to any silencing at ***HMR*** with WT histones. (B) H4 K16R mutant could rescue some ***sir3*** mutants at ***HMR,*** including A181V, K209R and Y207C. H4

K16R had a partial suppression effect on A2V, N80D, F94L and F123P. However, three strong mutants, A136T, C177R and S204P, still gave no silencing at all even with H4 K16R mutant.

At *HML*, H4 K16R mutant caused no silencing with WT Sir3, which was consistent with previous study (Meijsing *et al*., 2001). None of the *sir3* mutant could be rescued by H4 K16R mutant at *HML* (data not shown).

	HML Silencing *sir3*Δ *sir1*Δ			*HMR* Silencing *sir3*Δ *sir1*Δ		
Sir3	H3/H4	H3 D77N/H4	H3/H4 K16R	H3/H4	H3 D77N/H4	H3/H4 K16R
A2V	-	-	-	-	-/+	+
N80D	-	-	-	-	-	+
F94L	-	+++	-	-	+++	++
F123P	-	+++	-	-	+++	++
A136T	-	-	-	-	-	-
C177R	-	-	-	-	-	-
A181V	-	+++	-	-	++	+++
S204P	-	-	-	-	-	-
Y207C	-	+++	-	-	+++	+++
K209R	-	+++	-	-	+++	+++
WT	+++	+++	-	+++	+++	+++
vector	-	-	-	-	-	-

Table 2: Compilation of phenotypes of the ***sir3*** mutants at ***HML*** and ***HMR*** in presence of suppressor mutations of histone H3 D77N (work of E. Prugar) or H4 K16R. +++=Good silencing; ++ to - =Different levels of defective silencing.

Our lab identified another histone mutant, a substitution of aspartic acid 77 to asparagine in histone H3 (H3 D77N), which could suppress the silencing defects of *sir3* A2G (work of V. Sampath). H3 D77 is located at the globular domain of histone H3. This histone mutant could also restore silencing of *sir3* A2V, F94L, F123P, A181V, K209R and Y207C in a *sir3*Δ *sir1*Δ yeast strain at *HMR*. N80D, A136T,

C177R and S204P still led no silencing at *HMR* in the same strain background (work of E. Prugar). At *HML*, the H3 D77N mutant could suppress *sir3* F94L, F123P, A181V, K209R and Y207C mutants. A2V, N80D, A136T, C177R and S204P could not be rescued with H3 D77N at *HML* (work of E. Prugar).

Phenotypes of the Sir3 BAH domain mutants in presence of suppressor mutations in histones H3 or H4 are summarized in Table 2. In conclusion, neither H3 D77N mutant nor H4 K16R mutant could suppress the three strong mutants, A136T, C177R and S204P. However, they could suppress weak *sir3* mutants in Group 1 (A181V, Y207C and K209R) and Group 3 (F94L and F123P).

III. Discussion

The results presented in this chapter showed that the Sir3 BAH domain was a nucleosome-binding domain. The DNA binding capability might also contribute to the association between Sir3 BAH domain and nucleosomes. In nucleosome binding assay as shown in Figure 28, the input molar ratio of nucleosome:Sir3 is 1:130 (13×10^{-12} mol of nucleosomes : 10 μg of $Sir3^{1-253}$-His) at the lowest protein concentration which shows nucleosome binding ability. However, as indicated in Figure 24A, the input molar ratio of DNA:Sir3 in the gel retardation assay is about 1:2800 (20 ng of 1.3 kb DNA fragments : 2 μg of $Sir3^{1-253}$-His) at the lowest protein concentration which shows DNA binding ability. And all the silencing defective mutants bond equally well. Therefore, comparing to nucleosome, the DNA binding

ability of the Sir3 BAH domain may not be biologically significant.

The suppression data with H4 K16R and H3 D77N suggested that the association of the Sir3 BAH domain with nucleosomes appeared to be regulated by distinct histone regions in the nucleosomes.

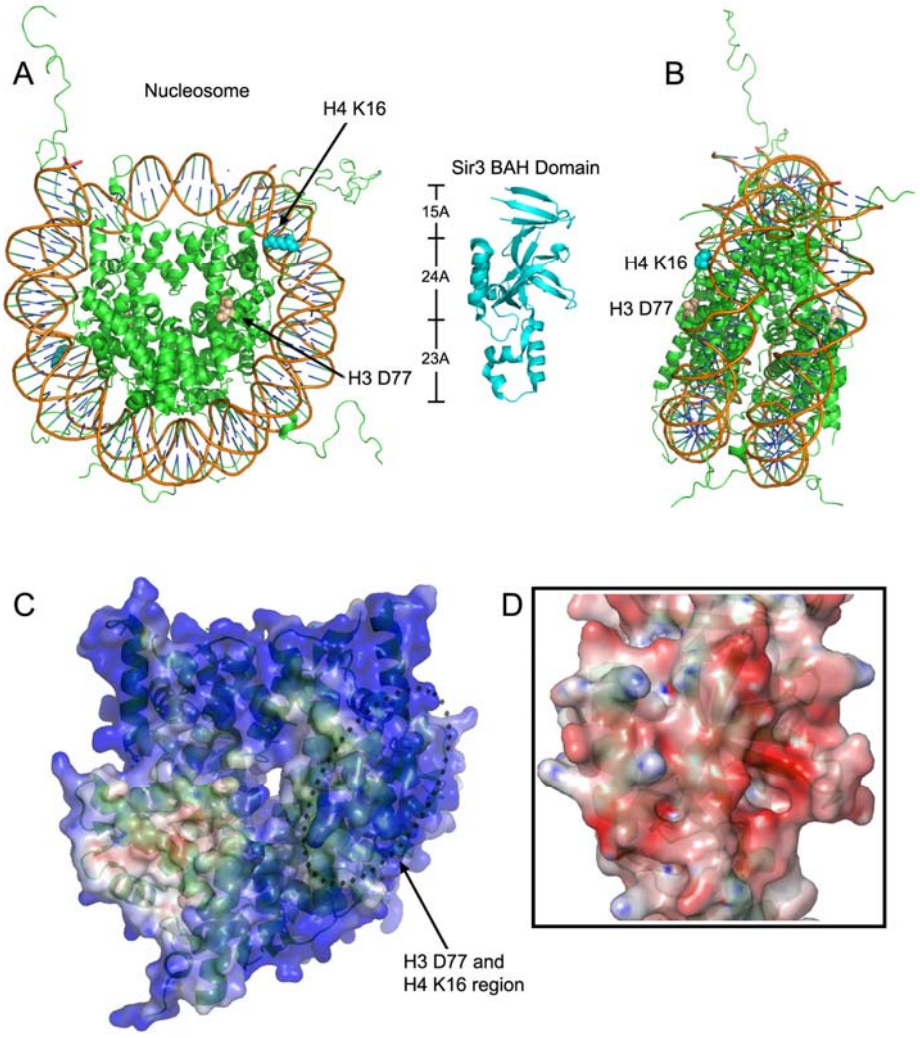

Figure 32: Structures of the nucleosome and the Sir3 BAH domain. (A) Images of the structure of a nucleosome from the *Xenopus laevis* (PDB: 1KX5) and the Sir3 BAH domain (PDB: 2FVU). H3 D77 is labeled in pink and H4 K16 is in cyan. (B) H3 D77(pink) and H4 K16(cyan) are both located on the surface of nucleosome.(C) Electrostatic surface of the chicken histone core (PDB: 1TZY). H3 D77 and H4 K16 region is indicated in a dashed circle. (D) Electrostatic surface of a Sir3 region around α-helix F and

core domain of Sir3^{BAH}. Electrostatic potential on the protein surfaces are indicated with red (negatively charged), blue (positively charged), or white (neutral). Protein structures of histone core and part of Sir3 BAH domain are visualized in a semi-transparent cartoon in green.

The first was composed of N-terminal tail of histone H4, containing K16. N-terminal residues 16, 17, 18, and 19 of H4 are crucial to silencing (Johnson *et al*., 1990). The H4 deletion, removing amino acids 4-23, reduced mating efficiency greatly at *HMR* (Durrin *et al*., 1991). Full-length Sir3 purified from yeast bound selectively to histone H4 peptides containing deacetylated histone H4 K16 (Liou *et al*., 2005). The association of the BAH domain with the nucleosome was tightly controlled by the acetylation state of lysine 16 within this domain (Onishi *et al*., 2007).

The second domain included Aspartic acid 77 of histone H3 and the residues around it. Moreover, lysine 79 in the globular domain of histone H3 was methylated by Dot1, and either deletion or overexpression of the *DOT1* gene, or a mutation of H3 K79 to alanine, resulted in defects in silencing (Ng *et al*., 2002; van Leeuwen *et al*., 2002). Additional support for the importance of this region came from genetic screens that identified histone H3 residues 68-83 as necessary for silencing (Park *et al*., 2002). However, the H3 D77N mutant didn't affect the methylation of H3 K79 (work of V. Sampath).

The N-terminus tail of H4 and the H3 D77 region are located on the same surface of the nucleosome (Figure 32B). The distance of Cα atoms between H4 K16

and H3 D77 was about 25Å. Therefore, the entire region around them is thought to be able to simultaneously contact a single BAH domain (Figure 32A). We propose that the surface of the nucleosome containing both H3 D77 and H4 K16 forms a composite binding site for the Sir3 BAH domain (Figure 32A-C).

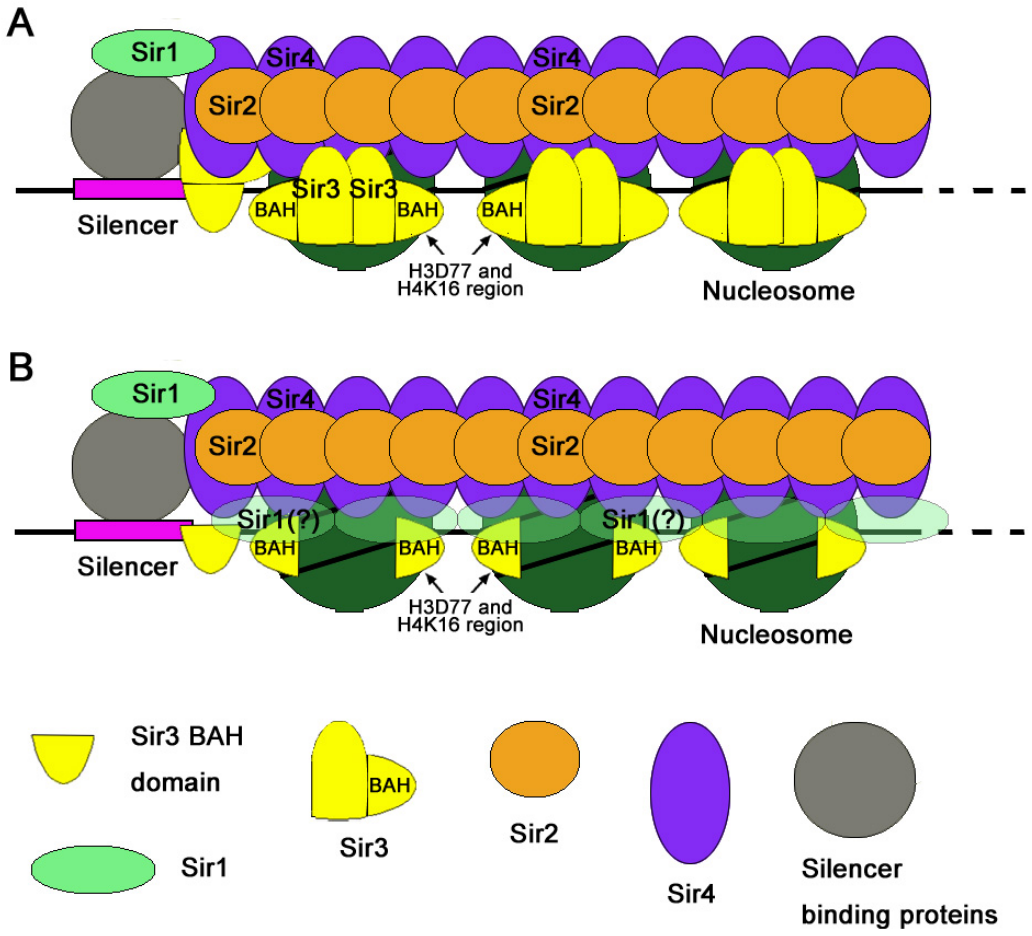

Figure 33: Models of yeast silencing maintenance with full-length Sir3 (A) or the Sir3 BAH domain (B). (A) The C-terminus of Sir3 associates with Sir2-Sir4 to form SIR complex and the spreading of Sir3 along the chromatin fiber requires interactions with both a deacetylated histone H4 K16 in the N-terminus of histone H4 and H3 D77 region in the globular domain of H3 located on the surface of the nucleosome. (B) In the case of Sir3 BAH silencing, Sir3 BAH domain still binds to the nucleosomes regions of H4 K16 and H3 D77, and spreads as well as the Sir2-Sir4 complex to maintain a silencing state. However, there should be a link to connect

the Sir2-Sir4 complex and the Sir3 BAH domain. Our hypothesis is that Sir1 is this bridge.

The genetic data implied that the regions around α-helix F and core domain of the Sir3 BAH domain were very important for the function of Sir3. Three strong *sir3* mutants (A136T, C177R and S204P) are all located within this region. A181V, Y207C and K209R which could be suppressed by H4 K16R mutant were also in this region. The electrostatic surface map suggested that the surface of the histone core is mostly positively charged, including the H3 D77 and H4 K16 region (Figure 32C). And the surface of the Sir3 region around α-helix F and core domain is mainly negatively charged (Figure 32D). We hypothesize that the Sir3 region around α-helix F and core domain should be one of the nucleosome binding sites.

Our hypothesis of yeast silencing maintenance is that the C-terminus of Sir3 associates with Sir2-Sir4 to form SIR complex and the spreading of Sir3 along the chromatin requires interactions with both a deacetylated histone H4 K16 in the N-terminus of histone H4 and H3 D77 region in the globular domain of H3 located on the surface of the nucleosome (Figure 33A).

The BAH silencing is caused just by Sir3 BAH fragments, in absence of full-length Sir3. The silencer binding proteins associate with the silencer and recruit the common Sir proteins to the chromatin. Sir3 BAH domain still binds to the nucleosome region of H4 K16 and H3 D77, and spreads as well as the Sir2-Sir4 complex to maintain a silencing state (Figure 33B).

The BAH silencing requires Sir2 and Sir4. But we don't know the relationship between Sir3 BAH and Sir2-Sir4 complex. Besides the nucleosome, we think the Sir3 BAH domain should have another binding partner which can bring the BAH fragment to the silent region and acts as a bridge to connect the Sir2-Sir4 complex and the Sir3 BAH domain. Since overexpression of *SIR1* allows the function of the Sir3 BAH fragments, and when *SIR1* is deleted, certain *sir3* mutants show a stronger phenotype, our hypothesis is that Sir1 also binds to the Sir3 BAH domain. As shown in the Figure 33B, when Sir1 is overexpressed, we hypothesize that Sir1 interacts with both the Sir2-Sir4 complex and the Sir3 BAH domain, and also spreads along the nucleosomes. The spreading of Sir1 helps the Sir3 BAH to bind with nucleosome and establish silencing. However, this hypothesis needs further study to test if it correct.

CHAPTER FIVE

Study of Sir3 Extreme N-terminus

I. Introduction

Previous work from our lab suggested that the extreme N-terminus of Sir3 is important for the function of the protein and this region is highly conserved among *Saccharomyces* (Figure 34A). We noted that a GBD-Sir3 hybrid protein was only partially functional when GBD was at the N-terminus of the protein, but was fully functional when GBD was at the C-terminus (Chien *et al*. 1993). The same was true for LexA-Sir3 and GBD-Sir3 hybrids (work of J. Connelly). Another lab also noted that N-terminal fusions of Sir3 were not functional (Gotta *et al*. 1998). These results suggested that the N-terminus of Sir3 needed to be exposed and not blocked by fusion to other proteins for full function.

It is thought that N-terminal acetylation of one or more proteins involved in silencing is important for their function. This is based on the observation that mutations in either *ARD1* or *NAT1*, genes that encode subunits of the N -acetyltransferase now called NatA, cause a noticeable silencing defect (Whiteway *et al*., 1987; Mullen *et al*., 1989). Our lab showed directly that Sir3 was N-terminally acetylated by NatA (Figure 34B; Wang *et al*., 2004). Our lab described

a mutational analysis of the N-terminal alanine 2 residue of Sir3, tested the acetylation state of these mutant proteins, and showed that such mutants could have a profound negative effect on silencing (Wang *et al*., 2004). These mutations demonstrated that the N-terminus of Sir3 was important for its function.

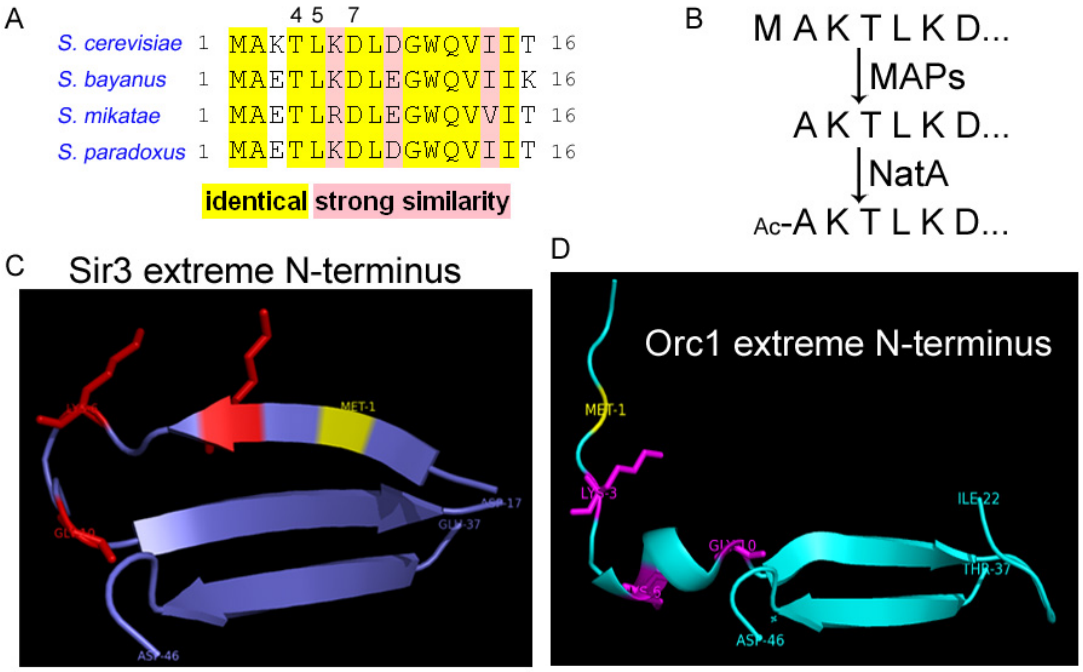

Figure 34: Background of the Sir3 extreme N-terminus. (A) Protein sequences alignment shows that the extreme N-terminus of Sir3 is highly conserved among *Saccharomyces.* (B) Sir3 is N-terminally acetylated by NatA. (C) Structure of the extreme N-terminus of Sir3. First methionine of Sir3 is indicated in yellow. Residues K3, K6 and G10 of Sir3 are shown in a stick representation and colored in red. (D) Structure of the extreme N-terminus of Orc1. First methionine of Orc1 is indicated in yellow. Residues K3, K6 and G10 of Orc1 are shown in a stick representation and colored in purple.

The Orc1^{BAH} (aa 1-219) used for crystallography contained four extra amino acids, MHMT, that resulted from thrombin digestion of the His-tagged protein. For the crystal structure of Sir3^{BAH}, these same extra four amino acids were also

designed before the first methionine of Sir3 because they were used for the previous successful crystallization of $Orc1^{BAH}$.

Significant conformational differences are found at the extreme N-terminus of Sir3 and Orc1. Residues 1 to 5 of $Sir3^{BAH}$ form an antiparallel β-strand with residues 11 to 15. In the $Orc1^{BAH}$ structure, the N-terminal tail projects out of the core domain and interacts with a neighboring molecule. It is interesting that the N-terminal tails of $Sir3^{BAH}$ and $Orc1^{BAH}$ have significantly different conformations, despite 100% sequence identity of the first eight residues. In the $Orc1^{BAH}$ structure, the N-terminal tail is involved in interacting with neighboring molecules (Zhang *et al*., 2002). This region in $Sir3^{BAH}$ is important for silencing (Wang *et al*., 2002), and in the structure, it is involved in protein-protein interactions between the two molecules within the same asymmetric unit.

II. Results

1. A mutational analysis of the N-terminal T4, L5 and D7 residues of Sir3

A protein sequence alignment indicated that the extreme N-terminus of Sir3 was highly conserved among *Saccharomyces.* Therefore, we chose residue, threonine 4, leucine 5 and aspartic acid 7 for mutational analysis. T4G, T4F (work of F. Anwar), L5A, D7K, D7N and D7A mutants were created by site-directed mutagenesis. *SIR3* plasmids with the various mutations driven by the *SIR3* promoter were transformed into yeast strains for silencing tests.

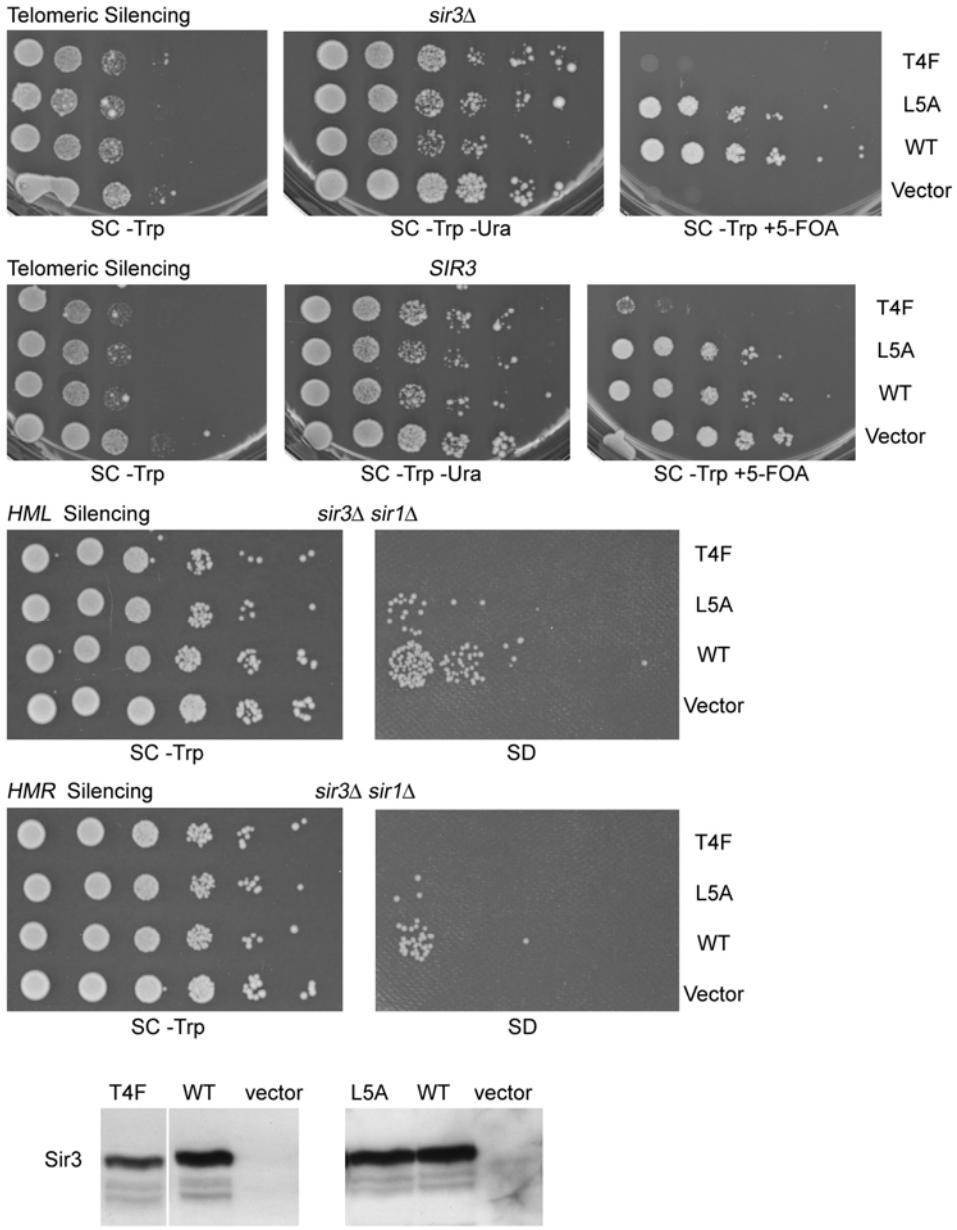

Figure 35: Silencing and protein expression levels of *sir3* T4F and L5A mutants. *SIR3* plasmids with T4F or L5A mutation were transformed into yeast strains for silencing tests. WT *SIR3* plasmids and pRS314 were used as the positive and negative controls. XRY16 (*sir3*Δ, telomeric *URA3*) and RS1045 (*SIR3*, telomeric *URA3*) was used for telomeric silencing; JCY8 (*MAT***a**, *sir3*Δ*sir1*Δ) was used for *HML* silencing; JCY9 (*MAT*α, *sir3*Δ*sir1*Δ) was used for *HMR* silencing. Anti-Sir3 western was used to detect the protein levels of T4F and L5A mutants in a *MAT***a** *sir3*Δ (JCY3) strain.

The T4F mutant could not complement a deletion of *SIR3* at telomere, and it

also led to a silencing defect in a *sir3*Δ *sir1*Δ strain at both *HML* and *HMR*. It showed a dominant effect at a telomere. L5A had no telomeric silencing defect, only led to a partial silencing defect in a *sir3*Δ *sir1*Δ strain at either *HML* or *HMR*. The anti-Sir3 western suggested that both T4F and L5A gave similar Sir3 protein levels to that of the WT. T4F and L5A could restore silencing at both *HML* and *HMR* in a *sir3*Δ strain in presence of Sir1 (data not shown). T4G, D7K, D7N and D7A always acted as well as WT at both telomere and *HM* loci, even in the *sir3*Δ *sir1*Δ strains (data not shown).

Genotype	Telomeric *sir3*Δ	*HML* *sir3*Δ	*HMR* *sir3*Δ	*HML* *sir3*Δ *sir1*Δ	*HMR* *sir3*Δ *sir1*Δ	Dominant at Telo.	Expression Levels
T4G	+	+++	+++	+++	+++	No	N. D.
T4F	-	+++	+++	-	-	Yes	+++
L5A	+	+++	+++	-/+	-/+	No	+++
D7K	+	+++	+++	+++	+++	No	N. D.
D7N	+	+++	+++	+++	+++	No	N. D.
D7A	+	+++	+++	+++	+++	No	N. D.
WT	+	+++	+++	+++	+++	-	+++
Null	-	-	-	-	-	-	-

N.D.=Not Determined

Table 3: Summary of the results from T4G, T4F, L5A, D7K, D7N and D7A mutants with LexA tags. Yeast strains XRY16 (***sir3***Δ, telomeric ***URA3***) and RS1045 (***SIR3***, telomeric ***URA3***) were used for telomeric silencing; JCY3 (***MAT*****a**, ***sir3***Δ) and JCY8 (***MAT*****a**, ***sir3***Δ***sir1***Δ) were used for ***HML*** silencing; JCY4 (***MAT*****α**, ***sir3***Δ) and JCY9 (***MAT*****α**, ***sir3***Δ***sir1***Δ) were used for ***HMR*** silencing. An anti-Sir3 western was used to detect the protein levels of T4F and L5A mutants in a ***MAT*****a** ***sir3***Δ (JCY3) strain. +++=Good silencing; ++ to - =Different levels of defective silencing.

At first, all the mutant plasmids mentioned above were constructed with a LexA tag fused at the Sir3 C-terminus, and silencing functions were examined. Only

T4F and L5A caused some phenotypes. Later, these two mutations were swapped to a *SIR3* plasmid with no LexA tag, which was also driven by the *SIR3* promoter, in order to mimic the natural condition. Comparing untagged mutants with LexA-tagged mutants, we found no difference in their silencing functions at telomere and *HM* loci. Data of T4F and L5A without tag were shown in Figure 35. Table 3 summarized the results from T4G, T4F, L5A, D7K, D7N and D7A mutants with LexA tags.

2. *sir3* Δ3-6 and *sir3* Δ3-10 mutants affected the protein's stability

We also designed two more drastic mutations: *sir3* Δ3-6 (deletion of residues 3-6) and *sir3* Δ3-10 mutants (deletion of residues 3-10), as indicated in Figure 36A. According to the crystal structure, residues leucine 6 and glycine 10 are located in the loop before β-sheet 2 of the Sir3 BAH domain (Figure 34C). In the mature WT Sir3 protein, the first methionine is removed by MAPs (methionine aminopeptidases) and alanine 2 is exposed at the N-terminus and acetylated by NatA (Figure 34B). In the *sir3* Δ3-6 and *sir3* Δ3-10 mutants, the second alanine was retained, so mutations probably would not change the acetylation of the N-terminal alanine. These two mutants were generated by PCR and constructed in a plasmid in context of full-length *SIR3* driven by its own promoter. A LexA tag was fused at the C-terminus. Yeast strains, *MAT***a** *sir3*Δ (JCY3) and *MAT***α** *sir3*Δ (JCY4) were used for silencing measurement at *HM* loci.

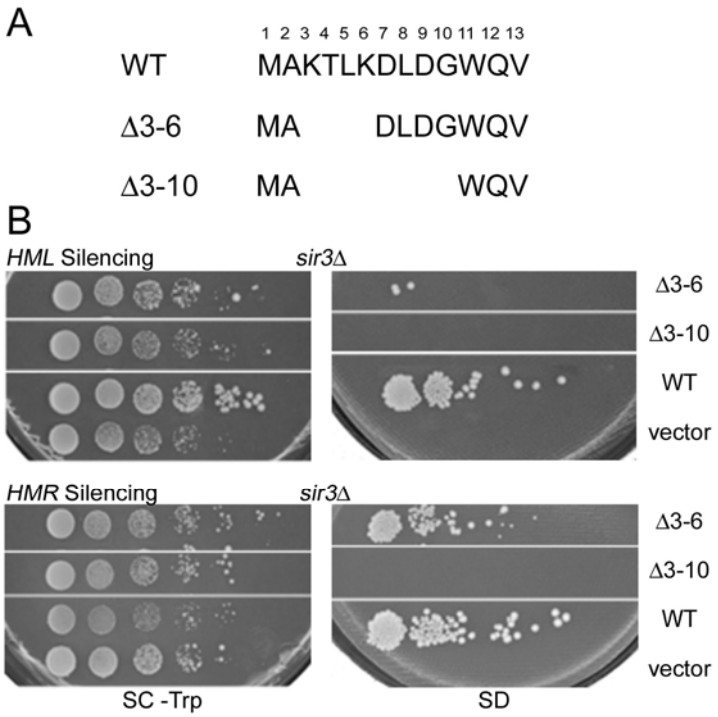

Figure 36: Silencing of *sir3* Δ3-6 and *sir3* Δ3-10 at *HM* loci. The mutant plasmids in context of full-length *SIR3* were driven by the *SIR3* promoter. Yeast strains, *MAT***a** *sir3*Δ (JCY3) and *MAT*α *sir3*Δ (JCY4) were used for silencing measurement at *HML* (A) and *HMR* (B). Neither Δ3-6 nor Δ3-10 mutants could restore silencing at *HML*. Even at *HMR*, Δ3-10 mutant also caused a complete silencing defect.

The data showed that neither Δ3-6 nor Δ3-10 mutants could restore silencing at *HML*. At *HMR*, Δ3-10 mutant also caused a complete silencing defect.

Western blot with both anti-Sir3N and anti-LexA antibodies demonstrated that the Δ3-10 mutant made no Sir3 proteins at all (Figure 37A). We thought that this was the reason that Δ3-10 mutant led to a complete derepression of the mating loci. Δ3-6 mutant gave some Sir3 protein but less than WT.

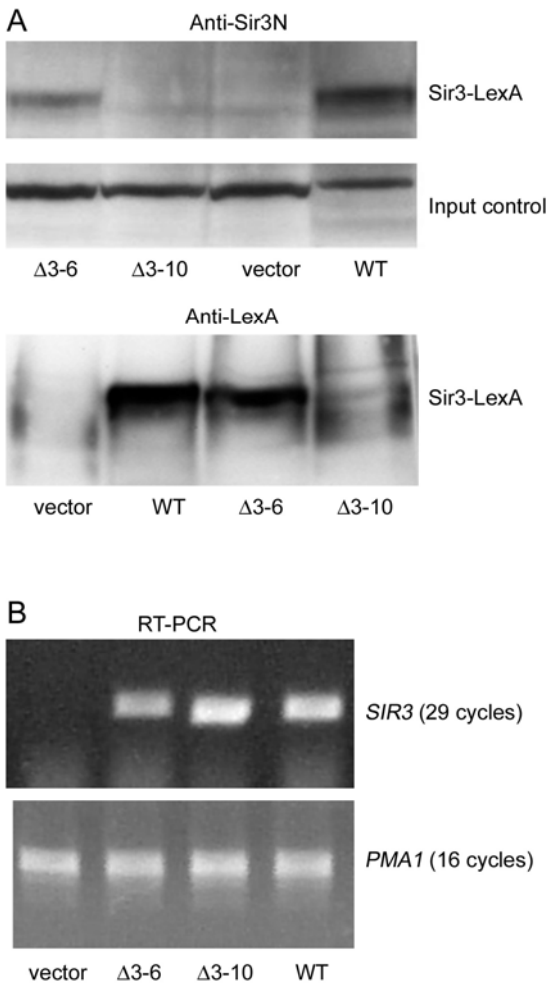

Figure 37: Protein and mRNA levels of Sir3, ***sir3*** Δ3-6 and ***sir3*** Δ3-10 mutants. (A) Sir3 protein levels of WT, Δ3-6 and Δ3-10 mutants were monitored by using western blot. Both anti-Sir3N and anti-LexA antibodies were used. Δ3-6 mutant gave some Sir3 protein but a little less than WT. Δ3-10 mutant made no Sir3 protein at all. (B) mRNA levels of ***SIR3*** WT, Δ3-6 and Δ3-10 mutants were monitored by using RT-PCR. RNA was isolated from a ***sir3***Δ yeast strain (JCY3) with plasmids encoding Sir3, ***sir3*** Δ3-6 and Δ3-10 mutants. ***SIR3*** 337-850 bp fragments were generated from cDNA template after 29 PCR cycles. PCR of ***PMA1*** fragments was used as an input control.

RT-PCR was used to monitor mRNA levels of *SIR3*, *sir3*Δ3-6 and Δ3-10 mutants. With a template of cDNA, *SIR3*, *sir3* Δ3-6 and Δ3-10 mutants gave PCR products of *SIR3* fragments (337-850 bp) after 29 cycles, while the vector had no

products at all (Figure 37B). PCR of *PMA1* fragments in 16 cycles was used as an input control. Without the process of reverse transcription, RNA extracts led to no PCR products of *PMA1* in the same cycles (data not shown), which suggests that the DNA in the RNA extracts was completely digested and the PCR products shown in Figure 37B were all from cDNA.

The results of RT-PCR indicated that *sir3* Δ3-6 and *sir3* Δ3-10 mutants could be transcribed equal to the WT. But *sir3* Δ3-10 mutant protein was not detected.

3. Mutations of alanine 2 of Sir3 showed dominance at telomere

Our lab described that a mutational analysis of the N-terminal alanine 2 residue of Sir3. The results showed that the A2S mutant was very slightly defective at telomere in a *sir3*Δ strain while the other three mutants, A2G, A2T, and A2Q, gave no silencing (Wang *et al*., 2004).

We were also interested in whether these mutants were dominant at telomere. To assess telomeric silencing, plasmids expressing Sir3 and the various Ala2 mutants also were transformed into a $SIR3^{+}$ strain with an *URA3* reporter gene placed near a telomere (RS1045). The results (Figure 38) showed A2G and A2Q gave no silencing, while A2S led to full silencing. The A2T mutant was partially dominant at this locus.

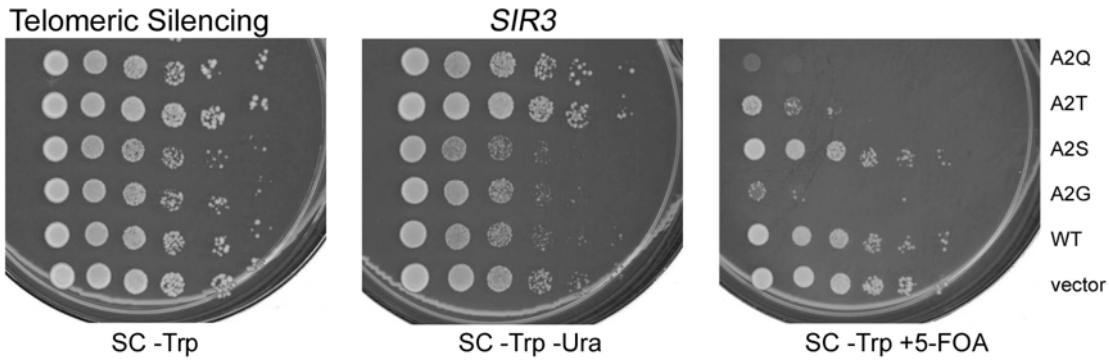

Figure 38: Mutants of alanine 2 of Sir3 showed dominance at telomere. To assess telomeric silencing, plasmids expressing Sir3 and the various Ala2 mutants also were transformed into a ***SIR3***$^{+}$ strain with an ***URA3*** reporter gene placed near a telomere (RS1045). All the plasmids were ***CEN***-based low-copy plasmids, driven by ***SIR3*** own promoter and without tags. The results showed that A2G and A2Q were dominant, while A2S led full silencing. The A2T mutant was partially dominant at this locus.

The dominance results suggested that these mutants of alanine 2 residue could compete with WT Sir3. One possible reason was these mutants would form nonfunctional complexes with WT Sir3 and other silencing proteins, thereby interfering with WT Sir3 silencing at telomeres.

III. Discussion

The *sir3* T4G mutant led to full silencing, but the *sir3* T4F mutant caused a silencing defect at telomere. These data suggested that a large residue at this position weakens protein function. D7N, D7K and D7A all gave full silencing, suggesting that the charge of this residue was not crucial.

It was reported that expression in *trans* of the N- (aa 1-503) and C-terminal (aa 568-978) fragments of Sir3 could restore *HML* repression in a *sir3*Δ strain (Gotta *et*

al., 1998). Also elevated levels of Sir3C (aa 108-978) led to derepression of a telomeric *URA3* (Le *et al*., 1997). These data demonstrated that even without the entire Sir3 BAH domain, the rest of Sir3 could exist and be functional. However, *sir3* Δ3-10 mutant showed no protein at all. Our hypothesis was that the extreme N-terminal region of Sir3 might be able to stabilize the structure of the whole protein. In the Sir3 N-terminus, there is probably a degradation signal which can regulate the stability of full-length Sir3. In normal condition, this signal is inhibited by the extreme Sir3 N-terminus. If the entire N-terminus is cleaved, the rest of protein still can exist. But when the extreme N-terminus of Sir3 is deleted, the degradation signal will be exposed and the rest of protein will disappear.

A2Q and A2G mutants were dominant at a telomere. They could also cause a telomeric silencing defect in a *sir3*Δ strain. One possibility is the extreme N-terminus of WT Sir3 binds to a certain partner directly, but A2Q and A2G mutants could not. The other possibility is mutation at the extreme N-terminus does not bind to anything, but affects the folding of whole BAH domain. The mutations can cause a misfolding of some binding regions in the rest of Sir3. Therefore, the N-terminal mutants lose their functions and the C-terminus of Sir3 still binds to Sir4 and Sir3 itself to form a SIR complex. However, this SIR complex cannot be functional like the WT Sir3, and therefore silencing is lost.

CHAPTER SIX

Conclusions and Future Work

I. Conclusions

The Sir3 BAH domain contains the Sir3 N-terminal residues from 1 to 219. It can partially silence *HM* loci in a *sir3*Δ strain, when *SIR1* is overexpressed. The *sir3* D205N mutant enhances silencing at *HML* and *HMR* compared to the WT BAH fragment and even gives some silencing without extra Sir1. The BAH silencing depends on common silencing factors, including Sir1, Sir2, Sir4. The ChIP experiment indicates that the Sir3 N-terminal fragment spread from silencer to the silent region.

In the random mutagenesis screen, a series of single *sir3* mutants within the BAH domain was identified. A136T, C177R and S204P are the most severe mutations; they cause both telomeric and *HML* silencing defects. Based on the structure, we find that these three mutations are located in the same region of $Sir3^{BAH}$. They are all located in the groove between helix F and the core domain. In addition to these three strong mutations, positions of some weak *sir3* mutations which lead to a telomeric silencing defect, A181V, Y207C and K209R, also are in this region. We think this groove of Sir3 must play an important role in yeast

silencing.

Biochemical data show that the Sir3 BAH fragment can associate with nucleosomes. The *sir3* mutants with silencing defects lost nucleosome binding ability. The D205N mutant that can suppress some kinds of silencing defects binds nucleosomes more tightly than WT. Histone mutants, either H4 K16R or H3 D77N, can suppress some silencing defective *sir3* point mutants. We hypothesize that the nucleosome region containing both H3 D77 and H4 K16 forms a composite binding site for the Sir3 BAH domain, and the groove in the Sir3 BAH domain between helix F and the core domain is one of the specific nucleosome binding regions of Sir3.

The extreme N-terminal region of Sir3 is highly conserved among *Saccharomyces*. Accordingly, mutations of conserved residues T4, L5 and D7 were built, and the result indicated that the residues T4 and L5 have effects on the full length protein function. The *sir3* Δ3-6 mutant and *sir3* Δ3-10 mutant show lower protein levels than WT, but the same mRNA levels. These data suggest that the extreme N terminus of Sir3 might be involved in stabilization of the whole protein.

II. Future work

I presented evidence that the Sir3 BAH domain bind to nucleosomes and DNA (Chapter Four). The Sir3 BAH fragments with various silencing defective mutation lost nucleosome binding ability but retained DNA binding capability (Chapter Four).

Therefore, in an attempt to understand the role of the Sir3 BAH domain, it is very important to learn: (i) whether it can bind free histones; (ii) if it does, then which kind of free histones it can bind, for example H3, H4 or H3-H4 tetramer. I tested the interaction between the Sir3 BAH domain and recombinant histone H3-H4 tetramers (a gift of R. Xu). However, because of some technical problems (the recombinant histone H3-H4 tetramers precipitated on the glutathione beads) I didn't get meaningful results. In the future, we should figure out a proper condition for histone-Sir3^{BAH} binding tests and find the answers.

The widely accept view is that at *HM* loci and telomere the histone tails are deacetylated through the action of Sir2, creating a binding surface on nucleosomes for Sir3 and Sir4 (Rusche *et al*., 2002). However, this view is about the Sir3 C-terminus and we don't know whether the same would be true for the Sir3 BAH domain. It is interesting to examine that whether the Sir3^{BAH}-nucleosome association is dependent on Sir2, Sir4 or other silencing factors.

The function of the extreme N-terminal Sir3 is not clear. Since certain histone mutants can suppress a *sir3* A2G mutant allele (work of V. Sampath), we think the extreme N-terminus of Sir3 should be one of the nucleosome binding regions of the Sir3 BAH domain. But due to some technical problems, we don't have good biochemical data to support this hypothesis. In the future, we should improve conditions of the experiments and solve the problems (a post-doc in our lab, V. Sampath, is working on this project).

We think in the Sir3 BAH domain there are at least two nucleosome binding regions: (i) the groove between helix F and the core domain; (ii) the extreme Sir3 N-terminus. In the nucleosomes, we think both H4 K16 region and H3 D77 region can interact with the Sir3 BAH domain. Our study show that the Sir3 BAH domain interacts with nucleosomes, probably through multiple points of interaction. X-ray crystallography data will be needed for delineating the exact contact points between the Sir3 BAH domain and nucleosomes.

In BAH silencing, overexpression of *SIR1* allows Sir3 BAH fragments to partially silence *HML* and *HMR* in absence of full-length Sir3 (Chapter Two). Some *sir3-eso* mutants also infer a genetic interaction between $Sir3^{BAH}$ and Sir1 (Chapter Three). Although we don't have any convincing data to prove that $Sir3^{BAH}$ can bind any part of Sir1, we still think it is possible that the two proteins do interact. Additional experiments should be done to address this issue. Because extra Sir1 leads to the restoration of silencing of several mating defective mutants (Stone *et al*., 1991) and because of my work, we are very interested to test if Sir1 can spread along nucleosomes when overexpressed (a graduate student in our lab, J. Ren, is working on this project).

CHAPTER SEVEN

Material and Methods

Plasmids and yeast strains

A list of plasmids used and details on their construction can be found in Appendix A. All plasmids constructed for these studies were sequenced to confirm that the insert did not contain mutations and, in the cases where a mutation was made, sequenced to confirm that mutation.

Site-directed mutagenesis was performed using Stratagene's QuickChange Site-Directed Mutagenesis protocol.

A list of yeast strains used can be found in Appendix B. All deletions were confirmed by PCR analysis of the deleted locus and in the cases where a phenotype should result from the deletion, that phenotype was measured.

Mating assays

For patch mating assays, cells transformed with the indicated plasmids were patched on to the appropriate SC selective medium. Patches were grown for 1 day and transferred to YPD by replica plating along with the appropriate mating tester strain. After one day, these cells were transferred by replica plating to SD plates to

select for diploids. Diploids were allowed to grow for 2 days.

For quantitative mating assays, cells transformed with the indicated plasmids were grown in the appropriate liquid selective medium to exponential phase. Dilutions were made in YPD and plated onto YPD to count the total number of cells. Appropriate dilutions were also plated to SD after mixing with 10^7 cells of exponentially growing mating tester. Mating efficiency is calculated as the fraction of cells that mated. In all cases, data was normalized to a wild-type value of 1. All values are the mean of three independent assays.

For semi-quantitative mating assays, cells transformed with the indicated plasmids were grown in the appropriate liquid selective medium to exponential phase. Mating was assayed by monitoring the growth of 10-fold serial dilutions of cells. Culture were diluted to the equal concentration and spotted (5 µl per spot) onto a lawn of mating tester on YPD plate. After incubated overnight at 30˚C, cells were duplicated to a SD plate to get diploid. Diploids spots were allowed to grow for 2 days.

Recombinant protein purification from *E. coli*

All the recombinant proteins were expressed from corresponding plamids (Appendix A) in *BL21 (DE3)* codon$^+$. Expression was induced by addition of 1 mM IPTG and 3% ethanol for 5 or 6 hours at room temperature. The His-tagged proteins were purified using Novagen His Bind resin according to the manufacturer's

instruction. The GST-tagged proteins were purified using GE Healthcare Glutathione Sepharose^{TM} 4 Fast Flow resin by following the manufacturer's instruction. Purified proteins were dialyzed against a buffer containing: 50 mM HEPES pH 7.5, 25 mM KCl, 1mM EDTA, 1 mM EGTA, 5 mM magnesium acetate. Protein concentrations were estimated by comparing Coomassie Blue staining of samples to BSA standards, as well as quantitated using a Bio-Rad Bradford assay.

Immunoprecipitation of chromatin from fixed yeast

20 OD_{600} of cells were cross-linked with formaldehyde for 30 minutes. Cells were collected and washed in PBS buffer. Pellets were lysed in IP lyses buffer as in Co-IP methods. After lyses, the insoluble debris was resuspended in the supernatant and sonicated 18×10 sec (ice in between) at level 2 with an Ultrasonics, Inc. sonicator (model W-220F). This sheared the chromatin to an average length of 500 bp. After sonication, the extract was cleared by centrifugation at 14,000 rpm for 10 minutes. Total protein was measure by Biorad Bradford assay. 2 mg of protein was added to a total volume of 300 µl of IP lyses buffer. The Biorad Bradford assay was performed on extracts to determine protein concentration. 2 mg of protein was added to a total volume of 300 µl of IP buffer. 10 µl of α-LexA (Santa Cruz D-19) was added and incubated at 4˚C overnight with rotation for $Sir3^{1-380}$-LexA immunoprecipitation. 50 µl of protein-G agarose was equilibrated in IP Buffer (25 mM HEPES-KOH pH 7.5, 12.5 mM magnesium chloride, 150 mM potassium

chloride, 1mM EDTA pH 8.0, 0.1% NP-40, and protease inhibitors) and added to precipitate antibody bound protein complex. Precipitation was performed at 4˚C with rotation for 2 hours. Supernatant was removed from the protein-G beads and the beads were washed 4×15 minutes in cold IP buffer. The immunoprecipitated chromatin was eluted in 100 µl of IP elution buffer (50 mM Tris, pH 8.0, 10 mM EDTA, 1% SDS) by incubation at 65˚C for 30 minutes. Eluted material was removed from beads to a new tube and the beads were eluted again as described with 50 µl IP elution buffer. The elution was combined and incubated overnight at 65˚C to reverse the crosslinks. DNA was isolated from the eluant by purification over a QiaQuick PCR column (Qiagen) following the manufacturer's protocol. The DNA was eluted from the column in 50 µl of Qiagen elution buffer. Input material (5 µl of extract) was subjected to the same protocol without immunoprecipitation. PCR was performed with the following primer pairs: JCP107/JCP108 (*HMR***a**), JCP113/JCP114 (*HMR-E*) and JCP121/JCP122 (*ACT1*). Primers were as follows:

*HMR***a**: 5'CAGTTTCCCCGAAAGAACAA and 5' CCATCCGCCGATTTATTT

HMR-E: 5'ACCAGGAGTACCTGCGCTTA and 5'TGCAAAAACCCATCAACCTGG

PCR reactions were performed using Herculase Polymerase (Stratagene) and the following reaction components: 0.5 mM dNTPs, 0.5 µM of each primer, and 1 µl of Herculase. Amplification conditions were: 1 cycle of 95˚C for 5 minutes, 26 cycles of 95˚C for 30 seconds, 56˚C for 30 seconds and 72˚C for 1 minute. These reactions were run on a 1.8% agarose gel to resolve the amplified products. Each

reaction always contained a primer set for the locus of interest (*HMR-E* or *HMR***a**) and the non-specific primer set (*ACT1*).

PCR random mutagenesis screen

Plasmid pPY41 (Sir3-LexA) was constructed as described in Figure 13. BAH fragments for the random mutagenesis were created by PCR following common condition: 5 mM $MgCl_2$, 25 pmol of each primer, 0.5 mM of dNTP mix, 1×PCR buffer (Invitrogen) and 1U of Platinum® Taq polymerase (Invitrogen). A linearized plasmid was generated by digestion with by BamHI and PstI. In order to increase the efficiency of transformation, pPY17 was transformed into PYY4 first, and then the PCR products and the linearized pPY41 were co-transformed into yeast with to construct a *sir3* mutant library through gap repair, as illustrated in Figure 14. Cells were plated on SC-Trp-Leu first and then duplicated to SC-Trp-Leu, SC-Trp-Leu-Ura, SC-Trp-Leu+5-FOA plates. A β-gal assay was performed on the SC-Trp-Leu plate to look for two hybrid interaction. Colonies which were β-gal$^+$ and cannot grow on SC-Trp-Leu+5-FOA plates were chosen for further analysis. After further purification, candidates of *sir3* mutant plasmids are isolated and retested. Candidates are then sequenced.

Urea lysis of whole cell extract

200 ml of cells culture grew to exponential phase (OD_{600}=1.0~1.2) and

collected by spinning at 6K for 6min. Pallet was resuspended in 5 ml of 50 mM Tris·HCl pH 8.0 and transferred to 12ml-volumed tube. The bottle was rinsed with 5 ml of 50 mM Tris·HCl pH 8.0 and the liquid was transferred to the tube to mix with previous slurry. Supernatant was poured off by Spin at 3K for 5 min.

Fresh 8 M Urea solution(2.4 g Urea was dissolved in 50 mM Tris·HCl pH 8.0, final volume is 5ml PMSF, Aprotinin, Pepstatin and Leupeptin were added) was prepared. The pellet was resuspended with 900 μl Urea solution by pipetting. The final volume of the mixture was about ~1.5 ml. 1 ml mixture was transferred to 2 ml-volume tube with screw cap. 750 μl of glass beads were added and vortexed briefly. The mixture was beat by bead-beater processing for 1min at 4 ºC and cooled in machine for 1min. 2 more times were repeated. The tube was puncture at the bottom by burned needle. The tube was placed in Falcon 2059 tube and spin at 3K for 5 min. Supernatant was transferred to fresh Epp tube. Slurry was spin in the tube at 13.2K rpm for 30 min at 4 ºC. The final supernatant was transferred to chilled Epp tube. The protein concentration in the whole cell extract was measured by Bio-rad Bradford assay. Samples were stored at -20 ºC after boiling.

Nucleosome isolation

Yeast nuclei were prepared as described in (Edmondson *et al*., 1996). Yeast nuclei were washed with MSB (20 mM HEPES pH 7.5, 400 mM NaCl, 1 mM EDTA, 1 mM β-mercaptoethanol, 0.5 mM PMSF, 5% glycerol, 2 mg/ml leupeptine,

2 mg/ml pepstatin, 5 mg/ml aprotinin, 5 mM sodium butyrate, 5 mM β-glycerophosphate, 0.5 mM spermidine, 0.15 mM spermine) and extracted with HSB (20 mM HEPES pH 7.5, 650 mM 85 NaCl, 1 mM EDTA, 340 mM sucrose, 1 mM beta-mercaptoethanol, 0.5 mM PMSF, 2 mg/ml leupeptine, 2 mg/ml pepstatine, 5 mg/ml aprotinin , 5 mM sodium butyrate, 5 mM beta- glycerophosphate, 0.5 mM spermidine, 0.15 mM spermine). The extract was dialyzed against LSB (20 mM HEPES pH 7.5, 100 mM NaCl, 1mM EDTA, 1 mM beta-mercaptoethanol, 0.5 mM PMSF, 2 mg/ml leupeptine, 2 mg/ml pepstatine, 5 mg/ml aprotinin , 5 mM sodium butyrate, 5 mM beta- glycerophosphate, 0.5 mM spermidine, 0.15 mM spermine). Calcium chloride was added to 3 mM final concentration and the chromatin was digested with 0.1 U/ml micrococcal nuclease for 5 minutes at 37˚C. The reaction was stopped by addition of 50 mM EDTA, and NaCl was added to a final concentration of 0.6 M. The digested chromatin was concentrated to 2 ml on a centriprep 30 (Amicon) column and injected on a superose6 column (Pharmacia) gel filtration column. This column was equilibrated with HSB without sucrose prior to sample loading. 0.5 ml fractions were collected and analyzed for purity and oligo-nucleosome sizes. Appropriate sized nucleosomes were pooled, concentrated, and dialyzed against 20 mM HEPES pH 7.5, 1 mM EDTA, 1 mM β-mercaptoethanol, and protease inhibitors. Samples were stored at -80˚C.

Enrichment of yeast nucleosomes

The 1 liter culture of yeast was grown to OD_{600} of approximately 1.5-2. Harvest cells were spin down at 5000rpm for 5min (Cells can be frozen at this point or used immediatel). Cells were resuspend in 100ml of prespheroplasting buffer (100 mM Tris.HCl pH 7.9, 60 mM β-mercaptoethanol) and incubated at room temperature for 15 min with occasional stirring. Cells was pelleted by centrifugation in 250ml bottles at 5000 rpm for 6 min and resuspend in 50 ml spheroplasting buffer (0.7 M sorbitol, 0.75% yeast extract, 1.5% peptone, 10 mM Tris·HCl pH 7.5, 40 mM β-mercaptoethanol). 4000 units of lyticase (β-1,3-endoglucanase) per gram of yeast cells were added and incubated in a 30˚C water bath with occasional swirling for 60 min. Spheroplasts were palleted at 5000 rpm for 6min and washed with 50ml YEPD/Sorbitol (1% yeast extract, 2% peptone, 2% dextrose, 1 M Sorbitol, 10 mM Tris.HCl pH 6.8, 2 mM EDTA, 1 mM PMSF, 2 mM benzamidine, 2 mM sodium metabisulfite) once at room temperature, then washed with 50 ml Sorbitol Wash Buffer (1 M Sorbitol, 10 mM Tris.HCl pH 6.8, 2 mM EDTA, 1 mM PMSF, 2 mM benzamidine, 2 mM sodium metabisulfite) at 4˚C twice. Spheroplasts were resuspend in 50 ml of ice-cold Lysis buffer (10 mM Tris·HCl pH 7.5, 18% Ficoll 400, 20 mM KCl, 5 mM $MgCl_2$, 1 mM EDTA, 0.25 mM EGTA, 0.5 mM spermidine, 3 mM DTT, 2 mM benzamidine, 2 mM sodium metabisulfite, 1 mM PMSF, 1 μg per ml each pepstatin, leupeptin, and bestatin), then lysed with 10-20 strokes in a Dounce homogenizer with a type B pestle at 4˚C. The homogenate was diluted with 50 ml of 2.4 M Sorbitol Buffer (10 mM Tris·HCl pH 7.5, 18% Ficoll 400, 20 mM

KCl, 5 mM $MgCl_2$, 1 mM EDTA, 0.25 mM EGTA, 0.5 mM spermidine, 3 mM DTT, 2 mM benzamidine, 2 mM sodium metabisulfite, 1 mM PMSF, 1 μg per ml each pepstatin, leupeptin, and bestatin, 18% Ficoll 400) and spin at 9000 rpm for 20 min at 4˚C. Nuclei was washed by 10 ml of buffer A with NP-40(10 mM Tris·HCl pH 7.5, 75 mM NaCl, 1 M Sorbitol, 2 mM benzamidine, 2 mM sodium metabisulfite, 1 mM PMSF, 1 μg per ml each pepstatin, leupeptin, and bestatin. 0.5% NP-40) and centrifuged at 9000 rpm for 20 min at 4˚C as above. Nuclei was washed by 10ml of buffer A without NP-40 (10 mM Tris·HCl pH 7.5, 75 mM NaCl, 1 M Sorbitol, 2 mM benzamidine, 2 mM sodium metabisulfite, 1 mM PMSF, 1 μg per ml each pepstatin, leupeptin, and bestatin)and centrifuged at 9000 rpm for 20 min at 4˚C as above. Nuclei was resuspended in 10 ml per gram cells of MNase buffer (10 mM Tris·HCl pH 8.0, 150 mM NaCl, 5 mM KCl, 1 mM EDTA, 1 mM PMSF, 2 mM benzamidine, 1 μg per ml each pepstatin, leupeptin, and bestatin). Then $CaCl_2$ was added up to 5 mM and mixture was preincubated for 2 min at 37˚C. MNase was added (45 U/μl of Worthington, in ddH_2O) to 200U per ml and mixture was incubated for 15 min at 37˚C with occasional stirring. Reaction was stopped by adding EGTA to 20 mM. Supernatant from spinning at 12000 rpm in SA-600 at 4˚C was enriched in nucleosomes. Glycerol was added up to 10% for stock at -80˚C.

Agarose gel retardation assays

40 ng of yeast mononucleosomes or 15~20 ng of 146-base pair DNA were

incubated without Sir3 protein(0~30 μg) in 20 mM Tris·HCl pH 8.0, 4 mM EDTA pH 8.0, 0.5 mM DTT, and 1 mM PMSF for 30 minutes at room temperature. The reactions were fractionated using electrophoresis at room temperature on a 2 % agarose gel (containing ethidium bromide) for 30 minutes at 100 volts.

Native gel electrophoresis

5% native PAGE gel was made following the standard SDS-PAGE gel recipe without SDS. Proteins samples were prepared by using standard loading buffer without β-mercaptoethanol. The gel was powered up at a constant voltage of 120~130 volts at 4˚C. The gel was run until the bromophenol blue dye front reached the bottom (about three hours) and stained as a standard Coomassie gel. The protocol can also be found at http://www.proteinchemist.com/tutorial/natpage.html

Nucleosome binding assay

10~20 μg of recombinant proteins were reloaded on 20 μl of Glutathione beads (GE Healthcare) and mixed with 400 μl of enriched nucleosome, which was stocked at -80˚C. Slurry was incubated at 4˚C for one hour. Beads were collected by spinning at 4000 rpm for 1 min. Supernatant was removed by syringe with 30G needle. Beads were washed by 300 μl of B3 buffer (20 mM Tris·HCl pH 8.0, 25 mM NaCl, 1 mM DTT) three times and collected by spinning at 4000rpm for 1min. Samples were eluted with 20 μl of 1×SD loading buffer with boiling 5 min.

Filter binding assay

^{32}P-labeled DNA was produced by PCR with ^{32}P-labeled ATP. PCR condition followed the manuscript of Invitrogen™ platinum *Taq* DNA Polymerase High Fidelity. DNA fragments were 1.3 kb amplified from *HMR-E* region (Figure 39). Primers were as follows:

HMR-E 292133: 5' TATAGGCTAGATCGTAATCCACTA

HMR-E 293489: 5' AAAATAAATCGGCGGATGGGTTGG

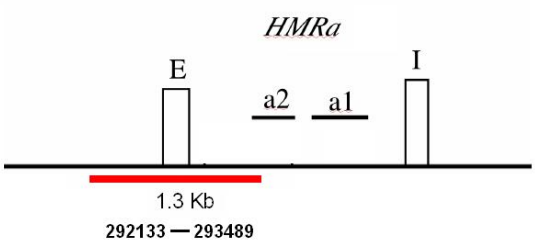

Figure 39: 1.3 kb DNA fragments used in a gel retardation assay and a filter binding assay. 1.3 kb DNA fragments were amplified from *HMR-E* region. Primers were designed according to Zhang *et al.*, 2002 as figure shows.

Pore size of the nitrocellulose membrane (Schleicher& Schuell) was 0.45 μm. To reduce retention of free DNA, nitrocellulose membrane was presoaked for 10 min in 0.4 M KOH followed by three 5 min washes in distilled water to bring the pH to neutral. Nitrocellulose membrane were then equilibrated in the washing buffer(50 mM HEPES pH 7.5, 25 mM KCl, 1 mM EDTA, 1 mM EGTA, 5 mM magnesium acetate) at room temperate for a minimum of 1 hour before use.

20~40 ng of ^{32}P-labeled 1.3 kb DNA was incubated with various quantities of

recombinant Sir3 proteins in 20 μl of a buffer containing 20 mM Tris·HCl pH 8.0, 4 mM EDTA pH 8.0, 0.5 mM DTT, and 1 mM PMSF, for 30 min at room temperature. The reaction mixtures were then loaded on a nitrocellulose membrane by using a hybridot device. After three times washing with 50 μl washing buffer, the labeled probe retained on the membrane was quantified with a PhosphoImager or scintillation counter.

RT-PCR

Overnight culture was dilute into fresh medium and grew till exponential growth. 3×10^8 cells were collect by spinning at 3000 rpm for 5 min. Pallet was washed by DEPC water once and transferred to EPP tube. The supernatant was removed thoroughly after spinning at 13.2K rpm for 2 min. 480 μl Lyses Buffer (Ambion RiboPure^{TM} Yeast Kit), 48 μl 10% SDS and 480 μl Phenol:Chloroform:IAA (Ambion RiboPure^{TM} Yeast Kit) was added in order. Mixture was vortexed 10-15 sec to suspend the cells, and then transferred into 1.5 ml screw cap tube with 700 μl cold Zirconia Beads. Horizontal vortex mixer was used to beat 10min at the maximal speed to lyses the cells. 400 μl of aqueous phase was transferred into 4-15 ml capacity tubes after spinning at 13.2K rpm for 5 min at room temperature. 1.4 ml of binding buffer (Ambion RiboPure^{TM} Yeast Kit) and 940 μl 100% ethanol was added in order and mixed thoroughly. 750 μl of mixture was applied into Filter Cartridge (Ambion RiboPure^{TM} Yeast Kit) assembled in

collection tube. Flow through was discarded after spinning at 13.2K rpm for 1 min. The process was repeated to pass the entire sample through Filter Cartridge. 700 µl of Wash Solution 1 (Ambion RiboPure^{TM} Yeast Kit) was added to wash the Filter Cartridge. 450 µl of Wash Solution 2/3 (Ambion RiboPure^{TM} Yeast Kit) was added to wash the Filter Cartridge. The flow through was discarded after spinning at 13.2K rpm for 1 min and the washing process was repeated once. The excess wash solution was removed from the filter after spinning at 13.2K rpm for 2 min. The Filter Cartridge was transferred a fresh collection tube. RNA was eluted with 30~50 µl of 100 ºC pre-heated Elution Solution (Ambion RiboPure^{TM} Yeast Kit), by spinning at 13.2K rpm for 1 min.

1/10 volume of 10×DNase Buffer (Ambion) and 1~2 µl of DNase I (Roche) was added to the eluted RNA and treated for 30 min at 37 ºC. Sample was resuspend by adding the DNase I Inactivation Reagent (Ambion) and set at room temperate for 5 min. The supernatant was taken to a fresh tube after spinning at 13.2K rpm for 3 min. RNA concentration was measured by A_{260}.

1 ug of Oligo $(dT)_{15,}$ 1~5 µg of DNAse I digested RNA, 1 µl of 10mM dNTP Mix was added into a nuclease-free tube, DEPC H_2O was added up 13 µl. Mixture was heated at 65 ºC for 5 min in PCR machine and quickly chilled on ice. 4 µl of 5×First-Strand Buffer (Invitrogen) and 2 µl of 0.1 M DTT, 1 µl (200 units) of SuperScript II RT (Invitrogen) was added into mixture in order and mixed by pipetting gently. The final volume was 20 µl. The 20 µl of mixture was incubated at

42ºC for 1 hr and 70 ºC for 15 min. Then 2 µl of mixture was used as PCR template.

Appendix A: Plasmids List

Name	Construct	Construction	Marker
pPY12	$Sir3^{FL}$-LexA A2R	$Sir3^{1-162}$ released from pXR11 with digestion of BamHI/ClaI and cloned into pBC8 at BamHI/ClaI	*ADH1*^{P} 2 micron *TRP1* *Amp*^{r}
pPY13	$Sir3^{FL}$-LexA A2Q	$Sir3^{1-162}$ released from pXR12 with digestion of BamHI/ClaI and cloned into pBC8 at BamHI/ClaI	*ADH1*^{P} 2 micron *TRP1* *Amp*^{r}
pPY14	LexA	pFBL23 digested with PstI and refilled by klenow to delete PstI	*ADH1*^{P} 2 micron *TRP1* *Amp*^{r}
pPY15	$Sir3^{FL}$-LexA WT	$Sir3^{FL}$ released from pBC8 with digestion of EcoRI/SalI and cloned into pPY14 at EcoRI/SalI	*ADH1*^{P} 2 micron *TRP1* *Amp*^{r}
pPY17	$Rad7^{94-566}$-GAD	$Rad7^{94-566}$ released pH11.1	*LEU2*

		with digestion of EcoRI/PstI and cloned into pGAD424 at EcoRI/PstI	*Amp*^{r} 2 micron
pPY32	Sir3^{FL}-LexA F105L	Sir3^{FL}-LexA-*ADH1*^{term} released from pBC8 with digestion of BamHI/SpeI and cloned into pRS314 at BamHI/SpeI; *SIR3* promoter -300bp - -1 released from pJC38 and cloned into pRS314 at SalI/BamHI	*SIR3*^{P} *CEN* *TRP1* *Amp*^{r}
pPY41	Sir3^{FL}-LexA WT	Sir3$^{1-253}$ released from pBC8 with digestion of BamHI/PstI and cloned into pPY32 at BamHI/PstI	*SIR3*^{P} *CEN* *TRP1* *Amp*^{r}
pSTM1b.1	Sir3^{FL}-LexA K209R	Obtained from random mutagenesis screen	*SIR3*^{P} *CEN* *TRP1* *Amp*^{r}

pSTM2b.1	Sir3^{FL}-LexA S204P	Obtained from random mutagenesis screen	*SIR3*^{P} *CEN* *TRP1* *Amp*^{r}
pSTM7b.1	Sir3^{FL}-LexA Y207C	Obtained from random mutagenesis screen	*SIR3*^{P} *CEN* *TRP1* *Amp*^{r}
pSTM64b	Sir3^{FL}-LexA A181V	Obtained from random mutagenesis screen	*SIR3*^{P} *CEN* *TRP1* *Amp*^{r}
pSTM65b	Sir3^{FL}-LexA N80D	Obtained from random mutagenesis screen	*SIR3*^{P} *CEN* *TRP1* *Amp*^{r}
pSTM67a	Sir3^{FL}-LexA F94L	Obtained from random mutagenesis screen	*SIR3*^{P} *CEN* *TRP1* *Amp*^{r}

pSTM75c	$Sir3^{FL}$-LexA C177R	Obtained from random mutagenesis screen	*SIR3*^{P} *CEN* *TRP1* *Amp*^{r}
pSTM78c	$Sir3^{FL}$-LexA A136T	Obtained from random mutagenesis screen	*SIR3*^{P} *CEN* *TRP1* *Amp*^{r}
pPY64	$Sir3^{1-253}$	$Sir3^{1-253}$ released from pBC8 with digestion of BamHI/PstI and cloned into pBluescript IISK at BamHI /PstI	*Amp*^{r}
pPY65	$Sir3^{1-253}$ D205K	Site-directed mutagenesis PCR on pPY64 to change Sir3 D205 to K	*Amp*^{r}
pPY71	$Sir3^{FL}$-LexA D205K	$Sir3^{1-253}$ released from pPY65 with digestion of BamHI/PstI and cloned into pPY41 at BamHI/PstI	*SIR3*^{P} *CEN* *TRP1* *Amp*^{r}

pJ#1	$Sir3^{FL}$-LexA F123P	Site-directed mutagenesis PCR on pPY41 to change Sir3 F123 to P	$SIR3^{P}$ *CEN* *TRP1* Amp^{r}
pPY82	$Sir3^{FL}$-LexA A2V	$Sir3^{1-253}$ fragments amplified from pPY41 by primers with mutation A2V and cloned into pPY41 at BamHI/PstI	$SIR3^{P}$ *CEN* *TRP1* Amp^{r}
pFA2	$Sir3^{FL}$-LexA T4F	$Sir3^{1-253}$ fragments amplified from pPY41 by primers with mutation T4F and cloned into pPY41 at BamHI/PstI	$SIR3^{P}$ *CEN* *TRP1* Amp^{r}
pPY96	$Sir3^{FL}$-LexA T4G	$Sir3^{1-253}$ fragments amplified from pPY41 by primers with mutation T4G and cloned into pPY41 at BamHI/PstI	$SIR3^{P}$ *CEN* *TRP1* Amp^{r}

pPY84	$Sir3^{FL}$-LexA L5A	$Sir3^{1-253}$ fragments amplified from pPY41 by primers with mutation L5A and cloned into pPY41 at BamHI/PstI	*SIR3*^{P} *CEN* *TRP1* *Amp*^{r}
pPY86	$Sir3^{FL}$-LexA D7K	$Sir3^{1-253}$ fragments amplified from pPY41 by primers with mutation D7K and cloned into pPY41 at BamHI/PstI	*SIR3*^{P} *CEN* *TRP1* *Amp*^{r}
pPY97	$Sir3^{FL}$-LexA D7A	$Sir3^{1-253}$ fragments amplified from pPY41 by primers with mutation D7A and cloned into pPY41 at BamHI/PstI	*SIR3*^{P} *CEN* *TRP1* *Amp*^{r}
pPY98	$Sir3^{FL}$-LexA D7N	$Sir3^{1-253}$ fragments amplified from pPY41 by primers with mutation D7N and cloned into pPY41 at BamHI/PstI	*SIR3*^{P} *CEN* *TRP1* *Amp*^{r}

pPY107	$Sir3^{FL}$-LexA Δ3-6	$Sir3^{1-253}$ fragments amplified from pPY41 by primers with mutation Δ3-6 and cloned into pPY41 at BamHI/PstI	*SIR3*^{P} *CEN* *TRP1* *Amp*^{r}
pPY108	$Sir3^{FL}$-LexA Δ3-10	$Sir3^{1-253}$ fragments amplified from pPY41 by primers with mutation Δ3-10 and cloned into pPY41 at BamHI/PstI	*SIR3*^{P} *CEN* *TRP1* *Amp*^{r}
pPY110	$Sir3^{1-214}$-LexA D205K	$Sir3^{1-214}$ D205K fragments amplified from pPY71 and cloned into pFBL23 at BamHI/SalI	*ADH1*^{P} *CEN* *TRP1* *Amp*^{r}
pPY117	$Sir3^{FL}$ C177R	$Sir3^{1-253}$ released from pSTM75c with digestion of BamHI/PstI and cloned into pXR58 backbone at BamHI/PstI	*SIR3*^{P} *CEN* *TRP1* *Amp*^{r}

pPY118	$Sir3^{FL}$ A136T	$Sir3^{1-253}$ released from pSTM78c with digestion of BamHI/PstI and cloned into pXR58 backbone at BamHI/PstI	$SIR3^{P}$ *CEN* *TRP1* Amp^{r}
pPY119	$Sir3^{FL}$ A181V	$Sir3^{1-253}$ released from pSTM64b with digestion of BamHI/PstI and cloned into pXR58 backbone at BamHI/PstI	$SIR3^{P}$ *CEN* *TRP1* Amp^{r}
pPY120	$Sir3^{FL}$ F94L	$Sir3^{1-253}$ released from pSTM67a with digestion of BamHI/PstI and cloned into pXR58 backbone at BamHI/PstI	$SIR3^{P}$ *CEN* *TRP1* Amp^{r}
pPY121	$Sir3^{FL}$ D205K	$Sir3^{1-253}$ released from pPY71 with digestion of BamHI/PstI and cloned into pXR58 backbone at BamHI/PstI	$SIR3^{P}$ *CEN* *TRP1* Amp^{r}

pPY122	$Sir3^{FL}$ A2V	$Sir3^{1-253}$ released from pPY82 with digestion of BamHI/PstI and cloned into pXR58 backbone at BamHI/PstI	$SIR3^{P}$ *CEN* *TRP1* Amp^{r}
pPY123	$Sir3^{FL}$ F123P	$Sir3^{1-253}$ released from pJ#1 with digestion of BamHI/PstI and cloned into pXR58 backbone at BamHI/PstI	$SIR3^{P}$ *CEN* *TRP1* Amp^{r}
pPY124	$Sir3^{FL}$ K209R	$Sir3^{1-253}$ released from pSTM1b.1 with digestion of BamHI/PstI and cloned into pXR58 backbone at BamHI/PstI	$SIR3^{P}$ *CEN* *TRP1* Amp^{r}
pPY125	$Sir3^{FL}$ N80D	$Sir3^{1-253}$ released from pSTM65b with digestion of BamHI/PstI and cloned into pXR58 backbone at BamHI/PstI	$SIR3^{P}$ *CEN* *TRP1* Amp^{r}

pPY126	$Sir3^{FL}$ S204P	$Sir3^{1-253}$ released from pSTM2b.1 with digestion of BamHI/PstI and cloned into pXR58 backbone at BamHI/PstI	$SIR3^{P}$ *CEN* *TRP1* Amp^{r}
pPY127	$Sir3^{FL}$ Y207C	$Sir3^{1-253}$ released from pSTM7b.1 with digestion of BamHI/PstI and cloned into pXR58 backbone at BamHI/PstI	$SIR3^{P}$ *CEN* *TRP1* Amp^{r}
pPY128	$Sir3^{FL}$ T4F	$Sir3^{1-253}$ released from pFA2 with digestion of BamHI/PstI and cloned into pXR58 backbone at BamHI/PstI	$SIR3^{P}$ *CEN* *TRP1* Amp^{r}
pPY129	$Sir3^{FL}$ L5A	$Sir3^{1-253}$ released from pPY84 with digestion of BamHI/PstI and cloned into pXR58 backbone at BamHI/PstI	$SIR3^{P}$ *CEN* *TRP1* Amp^{r}

pPY138	$Sir3^{FL}$ T4G	$Sir3^{1-253}$ released from pPY96 with digestion of BamHI/PstI and cloned into pXR58 backbone at BamHI/PstI	$SIR3^{P}$ *CEN* *TRP1* Amp^{r}
pPY139	$Sir3^{FL}$ D7A	$Sir3^{1-253}$ released from pPY97 with digestion of BamHI/PstI and cloned into pXR58 backbone at BamHI/PstI	$SIR3^{P}$ *CEN* *TRP1* Amp^{r}
pPY140	$Sir3^{FL}$ D7K	$Sir3^{1-253}$ released from pPY86 with digestion of BamHI/PstI and cloned into pXR58 backbone at BamHI/PstI	$SIR3^{P}$ *CEN* *TRP1* Amp^{r}
pPY141	$Sir3^{FL}$ D7N	$Sir3^{1-253}$ released from pPY98 with digestion of BamHI/PstI and cloned into pXR58 backbone at BamHI/PstI	$SIR3^{P}$ *CEN* *TRP1* Amp^{r}

pPY54	$Sir3^{1-253}$-His	$Sir3^{1-253}$ fragments amplified from pPY41 and cloned into pET28b at NcoI/BamHI	$T7^{P}$ Kan^{r}
pPY58	$Sir3^{1-253}$-His K209R	$Sir3^{1-253}$ fragments amplified from pSTM1b.1 and cloned into pET28b at NcoI/BamHI	$T7^{P}$ Kan^{r}
pPY59	$Sir3^{1-253}$-His N80D	$Sir3^{1-253}$ fragments amplified from pSTM65b and cloned into pET28b at NcoI/BamHI	$T7^{P}$ Kan^{r}
pPY60	$Sir3^{1-253}$-His F94L	$Sir3^{1-253}$ fragments amplified from pSTM67a and cloned into pET28b at NcoI/BamHI	$T7^{P}$ Kan^{r}
pPY61	$Sir3^{1-253}$-His C177R	$Sir3^{1-253}$ fragments amplified from pSTM75c and cloned into pET28b at NcoI/BamHI	$T7^{P}$ Kan^{r}

pPY62	$Sir3^{1-253}$-His A136T	$Sir3^{1-253}$ fragments amplified from pSTM78c and cloned into pET28b at NcoI/BamHI	*T7* promoter *Kan*^{r}
pPY103	$Sir3^{1-253}$-His S204P	$Sir3^{1-253}$ fragments amplified from pSTM2b.1 and cloned into pET28b at NcoI/BamHI	*T7*^{P} *Kan*^{r}
pPY69	$Sir3^{1-253}$-His A181V	$Sir3^{1-253}$ fragments amplified from pSTM64b and cloned into pET28b at NcoI/BamHI	*T7*^{P} *Kan*^{r}
pPY101	$Sir3^{1-253}$-His A2V	$Sir3^{1-253}$ fragments amplified from pPY82 and cloned into pET28b at NcoI/BamHI	*T7*^{P} *Kan*^{r}
pPY102	$Sir3^{1-253}$-His D205N	$Sir3^{1-253}$ fragments amplified from pJC61 and cloned into pET28b at NcoI/BamHI	*T7*^{P} *Kan*^{r}

pPY104	$Sir3^{1-253}$-His F123P	$Sir3^{1-253}$ fragments amplified from pJ#1 and cloned into pET28b at NcoI/BamHI	$T7^{P}$ Kan^{r}
pPY109	$Sir3^{1-253}$-GST	$Sir3^{1-253}$ fragments amplified from pPY41 and cloned into pJC82 at NcoI/BamHI	$T7^{P}$ Kan^{r}
pPY111	$Sir3^{1-219}$-GST D205N	$Sir3^{1-219}$ fragments amplified from pJC61 and cloned into pJC82 at NcoI/BamHI	$T7^{P}$ Kan^{r}
pEP14	$Sir3^{1-219}$-GST	$Sir3^{1-219}$ cloned into pJC82	$T7^{P}$ Kan^{r}
pVS32	$Sir3^{1-219}$-GST A2Q	$Sir3^{1-219}$ A2Q cloned into pJC82	$T7^{P}$ Kan^{r}
pPY114	$Sir3^{1-219}$-GST S209P	$Sir3^{1-219}$ fragments amplified from pSTM2b.1 and cloned into pJC82 at NcoI/BamHI	$T7^{P}$ Kan^{r}

pPY115	$Sir3^{1-219}$-GST C177R	$Sir3^{1-219}$ fragments amplified from pSTM75c and cloned into pJC82 at NcoI/BamHI	$T7^{P}$ Kan^{r}
pPY116	$Sir3^{1-219}$-GST A136T	$Sir3^{1-219}$ fragments amplified from pSTM78c and cloned into pJC82 at NcoI/BamHI	$T7^{P}$ Kan^{r}
pPY133	$Sir3^{1-219}$-GST F123P	$Sir3^{1-219}$ fragments amplified from pPY123 and cloned into pJC82 at NcoI/BamHI	$T7^{P}$ Kan^{r}
pPY134	$Sir3^{1-219}$-GST A181V	$Sir3^{1-219}$ fragments amplified from pPY119 and cloned into pJC82 at NcoI/BamHI	$T7^{P}$ Kan^{r}
pPY135	$Sir3^{1-219}$-GST F94L	$Sir3^{1-219}$ fragments amplified from pPY120 and cloned into pJC82 at NcoI/BamHI	$T7^{P}$ Kan^{r}

pPY136	Sir3$^{1-219}$-GST N80D	Sir3$^{1-219}$ fragments amplified from pPY125 and cloned into pJC82 at NcoI/BamHI	*T7* promoter *Kan*^{r}
pPY55	Sir3$^{1-219}$-His	Sir3$^{1-219}$ fragments amplified from pPY41 and cloned into pET28b at NcoI/BamHI	*T7*^{P} *Kan*^{r}
pPY137	Sir3$^{1-219}$-His D205N	Sir3$^{1-219}$ fragments amplified from pPY102 and cloned into pET28b at NcoI/BamHI	*T7*^{P} *Kan*^{r}
pEP23	Orc1$^{1-219}$-GST	Orc1$^{1-219}$ fragments cloned into pJC82 at NcoI/BamHI	*T7*^{P} *Kan*^{r}
pEP24	Orc1$^{1-253}$-His	Orc1$^{1-253}$ fragments cloned into pET28b at NcoI/BamHI	*T7*^{P} *Kan*^{r}

P (superscript) =Promoter

r (superscript) =resistance

Appendix B: Yeast Strains List

Strains	Genotype	Source
W303-1a	*MAT***a** *ade2-1 can1-100 his3-11, 15 leu2-3,112 ura3-1 trp1-1*	R.Rostein
W303-1b	*MAT***α** *ade2-1 can1-100 his3-11, 15 leu2-3,112 ura3-1 trp1-1*	R.Rostein
PYY4	*MAT***a** *his3Δ200 trp1-901 leu2-3, 112 ade2 lys2-801am ura3 sir3Δ::KAN ppr1Δ::natR LYS::(lexAop)$_8$:HIS3 URA3::(lexAop)$_8$:LacZ adh4::URA3-TEL-VII*	This study
JCY3	W303-1a *sir3Δ:: kanMX6*	J. Connelly
JCY4	W303-1b *sir3Δ:: kanMX6*	J. Connelly
JCY8	W303-1a *sir3Δ:: kanMX6 sir1Δ::his5*$^+$	J. Connelly
JCY9	W303-1b *sir3Δ:: kanMX6 sir1Δ::his5*$^+$	J. Connelly
XRY2	W303-1a *ard1Δ:: kanMX6 sir3Δ::his5*$^+$	X. Wang
JCY42	W303-1a *sir3Δ:: kanMX6 sir2Δ::his5*$^+$	J. Connelly
JCY17	W303-1a *sir3Δ:: kanMX6 sir4Δ::his5*$^+$	J. Connelly
XRY16	RS1045 *sir3Δ:: kanMX6*	X. Wang

RS1045	W303-1b *adh4::URA3-(C_{1-3}-A)*	C. Chien
PYY5	*MAT***a** *leu2-3,112 ura3 his3 ade2 trp1 hhf1*::*HIS3 hhf2*::*LEU2 sir3*Δ::*kanMX6 HHF2* on a *URA3 CEN* plasmid	This study
PYY6	*MAT*α *leu2-3,112 ura3 his3 ade2 trp1 hhf1*::*HIS3 hhf2*::*LEU2 sir3*Δ::*kanMX6 HHF2* on a *URA3 CEN* plasmid	This study
PYY7	*MAT***a** *leu2-3,112 ura3 his3 ade2 trp1 hhf1*::*HIS3 hhf2*::*LEU2 sir3*Δ::*kanMX6 hhf2*Δ*4-14* on a *URA3 CEN* plasmid	This study
PYY8	*MAT*α *leu2-3,112 ura3 his3 ade2 trp1 hhf1*::*HIS3 hhf2*::*LEU2 sir3*Δ::*kanMX6 hhf2*Δ*4-14* on a *URA3 CEN* plasmid	This study
PYY9	*MAT***a** *leu2-3,112 ura3 his3 ade2 trp1 hhf1*::*HIS3 hhf2*::*LEU2 sir3*Δ::*kanMX6 hhf2*Δ*4-23* on a *URA3 CEN* plasmid	This study
PYY10	*MAT*α *leu2-3,112 ura3 his3 ade2 trp1 hhf1*::*HIS3 hhf2*::*LEU2 sir3*Δ::*kanMX6 hhf2*Δ*4-23* on a *URA3 CEN* plasmid	This study

VSY29	*MAT***α** *hml::URA3 lys2-801 ade2-101 trp*Δ*63 his*Δ*200 leu2*Δ*1 ura3-52 ppr1*::*LYS2 sir3*Δ*::kanMX6 sir1*Δ*::natR hhf1-hht1::S.p.his5*$^{+}$ *hhf2-hht2::hphMX VR:ADE2:TEL HHF2-HHT2* on a *LEU2, CEN* plasmid	V. Sampath
PYY12	*MAT***α** *hml::URA3 lys2-801 ade2-101 trp*Δ*63 his*Δ*200 leu2*Δ*1 ura3-52 ppr1*::*LYS2 sir3*Δ*::kanMX6 sir1*Δ*::natR hhf1-hht1::S.p.his5*$^{+}$ *hhf2-hht2::hphMX VR:ADE2:TEL hhf1*(K16R)-*HHT1* on a *LEU2, CEN* plasmid	This study

References

1. **Aparicio, O. M., B. L. Billington, and D. E. Gottschling.** 1991. Modifiers of position effect are shared between telomeric and silent mating-type loci in S. cerevisiae. Cell **66:**1279-87.

2. **Baur, J. A., Y. Zou, J. W. Shay, and W. E. Wright.** 2001. Telomere position effect in human cells. Science **292:**2075-7.

3. **Bell, S. P., J. Mitchell, J. Leber, R. Kobayashi, and B. Stillman.** 1995. The multidomain structure of Orc1p reveals similarity to regulators of DNA replication and transcriptional silencing. Cell **83:**563-8.

4. **Berger, S. L.** 2007. The complex language of chromatin regulation during transcription. Nature **447:**407-12.

5. **Bi, X., M. Braunstein, G. J. Shei, and J. R. Broach.** 1999. The yeast HML I silencer defines a heterochromatin domain boundary by directional establishment of silencing. Proc Natl Acad Sci U S A **96:**11934-9.

6. **Boscheron, C., L. Maillet, S. Marcand, M. Tsai-Pflugfelder, S. M. Gasser, and E. Gilson.** 1996. Cooperation at a distance between silencers and proto-silencers at the yeast HML locus. Embo J **15:**2184-95.

7. **Bourns, B. D., M. K. Alexander, A. M. Smith, and V. A. Zakian.** 1998. Sir proteins, Rif proteins, and Cdc13p bind Saccharomyces telomeres in vivo. Mol Cell Biol **18:**5600-8.

8. **Brand, A. H., G. Micklem, and K. Nasmyth.** 1987. A yeast silencer contains sequences that can promote autonomous plasmid replication and transcriptional activation. Cell **51:**709-19.

9. **Braunstein, M., A. B. Rose, S. G. Holmes, C. D. Allis, and J. R. Broach.** 1993. Transcriptional silencing in yeast is associated with reduced nucleosome acetylation. Genes Dev **7:**592-604.

10. **Braunstein, M., R. E. Sobel, C. D. Allis, B. M. Turner, and J. R. Broach.** 1996. Efficient transcriptional silencing in Saccharomyces cerevisiae requires a heterochromatin histone acetylation pattern. Mol Cell Biol **16:**4349-56.

11. **Brower-Toland, B., D. A. Wacker, R. M. Fulbright, J. T. Lis, W. L. Kraus, and M. D. Wang.** 2005. Specific contributions of histone tails and their acetylation to the mechanical stability of nucleosomes. J Mol Biol **346:**135-46.

12. **Bryan, T. M., and T. R. Cech.** 1999. Telomerase and the maintenance of chromosome ends. Curr Opin Cell Biol **11:**318-24.

13. **Callebaut, I., J. C. Courvalin, and J. P. Mornon.** 1999. The BAH (bromo-adjacent homology) domain: a link between DNA methylation, replication and transcriptional regulation. FEBS Lett **446:**189-93.

14. **Carmen, A. A., L. Milne, and M. Grunstein.** 2002. Acetylation of the yeast histone H4 N terminus regulates its binding to heterochromatin protein SIR3. J Biol Chem **277:**4778-81.

15. **Chien, C. T., S. Buck, R. Sternglanz, and D. Shore.** 1993. Targeting of SIR1 protein establishes transcriptional silencing at HM loci and telomeres in yeast. Cell **75:**531-41.

16. **Chikashige, Y., D. Q. Ding, Y. Imai, M. Yamamoto, T. Haraguchi, and Y. Hiraoka.** 1997. Meiotic nuclear reorganization: switching the position of centromeres and telomeres in the fission yeast Schizosaccharomyces pombe. Embo J **16:**193-202.

17. **Cockell, M., F. Palladino, T. Laroche, G. Kyrion, C. Liu, A. J. Lustig, and S. M. Gasser.** 1995. The carboxy termini of Sir4 and Rap1 affect Sir3 localization: evidence for a multicomponent complex required for yeast telomeric silencing. J Cell Biol **129:**909-24.

18. **Connelly, J. J., P. Yuan, H. C. Hsu, Z. Li, R. M. Xu, and R. Sternglanz.** 2006. Structure and function of the Saccharomyces cerevisiae Sir3 BAH domain. Mol Cell Biol **26:**3256-65.

19. **Davey, C. A., D. F. Sargent, K. Luger, A. W. Maeder, and T. J. Richmond.** 2002. Solvent mediated interactions in the structure of the nucleosome core particle at 1.9 a resolution. J Mol Biol **319:**1097-113.

20. **Durrin, L. K., R. K. Mann, P. S. Kayne, and M. Grunstein.** 1991. Yeast histone H4 N-terminal sequence is required for promoter activation in vivo. Cell **65:**1023-31.

21. **Edmondson, D. G., M. M. Smith, and S. Y. Roth.** 1996. Repression domain of the yeast global repressor Tup1 interacts directly with histones H3 and H4. Genes Dev **10:**1247-59.

22. **Gardner, K. A., J. Rine, and C. A. Fox.** 1999. A region of the Sir1 protein dedicated to recognition of a silencer and required for interaction with the Orc1 protein in saccharomyces cerevisiae. Genetics **151:**31-44.

23. **Geissenhoner, A., C. Weise, and A. E. Ehrenhofer-Murray.** 2004. Dependence of ORC silencing function on NatA-mediated Nalpha acetylation in Saccharomyces cerevisiae. Mol Cell Biol **24:**10300-12.

24. **Georgel, P. T., M. A. Palacios DeBeer, G. Pietz, C. A. Fox, and J. C. Hansen.** 2001. Sir3-dependent assembly of supramolecular chromatin structures in vitro. Proc Natl Acad Sci U S A **98:**8584-9.

25. **Ghidelli, S., D. Donze, N. Dhillon, and R. T. Kamakaka.** 2001. Sir2p exists in two nucleosome-binding complexes with distinct deacetylase activities. Embo J **20:**4522-35.

26. **Goodwin, G. H., and R. H. Nicolas.** 2001. The BAH domain, polybromo and the RSC chromatin remodelling complex. Gene **268:**1-7.

27. **Gotta, M., F. Palladino, and S. M. Gasser.** 1998. Functional characterization of the N terminus of Sir3p. Mol Cell Biol **18:**6110-20.

28. **Gottschling, D. E., O. M. Aparicio, B. L. Billington, and V. A. Zakian.** 1990. Position effect at S. cerevisiae telomeres: reversible repression of Pol II transcription. Cell **63:**751-62.

29. **Grunstein, M.** 1997. Histone acetylation in chromatin structure and transcription. Nature **389:**349-52.

30. **Grunstein, M.** 1998. Yeast heterochromatin: regulation of its assembly and inheritance by histones. Cell **93:**325-8.

31. **Hecht, A., T. Laroche, S. Strahl-Bolsinger, S. M. Gasser, and M. Grunstein.** 1995. Histone H3 and H4 N-termini interact with SIR3 and SIR4

proteins: a molecular model for the formation of heterochromatin in yeast. Cell **80:**583-92.

32. **Hecht, A., S. Strahl-Bolsinger, and M. Grunstein.** 1996. Spreading of transcriptional repressor SIR3 from telomeric heterochromatin. Nature **383:**92-6.

33. **Hoppe, G. J., J. C. Tanny, A. D. Rudner, S. A. Gerber, S. Danaie, S. P. Gygi, and D. Moazed.** 2002. Steps in assembly of silent chromatin in yeast: Sir3-independent binding of a Sir2/Sir4 complex to silencers and role for Sir2-dependent deacetylation. Mol Cell Biol **22:**4167-80.

34. **Hou, Z., D. A. Bernstein, C. A. Fox, and J. L. Keck.** 2005. Structural basis of the Sir1-origin recognition complex interaction in transcriptional silencing. Proc Natl Acad Sci U S A **102:**8489-94.

35. **Hsu, H. C., B. Stillman, and R. M. Xu.** 2005. Structural basis for origin recognition complex 1 protein-silence information regulator 1 protein interaction in epigenetic silencing. Proc Natl Acad Sci U S A **102:**8519-24.

36. **Jenuwein, T., and C. D. Allis.** 2001. Translating the histone code. Science **293:**1074-80.

37. **Johnson, A. D.** 1995. Molecular mechanisms of cell-type determination in budding yeast. Curr Opin Genet Dev **5:**552-8.

38. **Johnson, L. M., P. S. Kayne, E. S. Kahn, and M. Grunstein.** 1990. Genetic evidence for an interaction between SIR3 and histone H4 in the repression of the silent mating loci in Saccharomyces cerevisiae. Proc Natl Acad Sci U S A **87:**6286-90.

39. **Kayne, P. S., U. J. Kim, M. Han, J. R. Mullen, F. Yoshizaki, and M. Grunstein.** 1988. Extremely conserved histone H4 N terminus is dispensable for growth but essential for repressing the silent mating loci in yeast. Cell **55:**27-39.

40. **Kimmerly, W., A. Buchman, R. Kornberg, and J. Rine.** 1988. Roles of two DNA-binding factors in replication, segregation and transcriptional repression mediated by a yeast silencer. Embo J **7:**2241-53.

41. **Landry, J., A. Sutton, S. T. Tafrov, R. C. Heller, J. Stebbins, L. Pillus, and R. Sternglanz.** 2000. The silencing protein SIR2 and its homologs are NAD-dependent protein deacetylases. Proc Natl Acad Sci U S A **97:**5807-11.

42. **Laurenson, P., and J. Rine.** 1992. Silencers, silencing, and heritable transcriptional states. Microbiol Rev **56:**543-60.

43. **Le, S., C. Davis, J. B. Konopka, and R. Sternglanz.** 1997. Two new S-phase-specific genes from Saccharomyces cerevisiae. Yeast **13:**1029-42.

44. **Levis, R., T. Hazelrigg, and G. M. Rubin.** 1985. Effects of genomic position on the expression of transduced copies of the white gene of Drosophila. Science **229:**558-61.

45. **Lieb, J. D., X. Liu, D. Botstein, and P. O. Brown.** 2001. Promoter-specific binding of Rap1 revealed by genome-wide maps of protein-DNA association. Nat Genet **28:**327-34.

46. **Liou, G. G., J. C. Tanny, R. G. Kruger, T. Walz, and D. Moazed.** 2005. Assembly of the SIR complex and its regulation by O-acetyl-ADP-ribose, a product of NAD-dependent histone deacetylation. Cell **121:**515-27.

47. **Liu, C., and A. J. Lustig.** 1996. Genetic analysis of Rap1p/Sir3p interactions in telomeric and HML silencing in Saccharomyces cerevisiae. Genetics **143:**81-93.

48. **Loo, S., C. A. Fox, J. Rine, R. Kobayashi, B. Stillman, and S. Bell.** 1995. The origin recognition complex in silencing, cell cycle progression, and DNA replication. Mol Biol Cell **6:**741-56.

49. **Luger, K., A. W. Mader, R. K. Richmond, D. F. Sargent, and T. J. Richmond.** 1997. Crystal structure of the nucleosome core particle at 2.8 A resolution. Nature **389:**251-60.

50. **Luger, K., and T. J. Richmond.** 1998. The histone tails of the nucleosome. Curr Opin Genet Dev **8:**140-6.

51. **Luo, K., M. A. Vega-Palas, and M. Grunstein.** 2002. Rap1-Sir4 binding independent of other Sir, yKu, or histone interactions initiates the assembly of telomeric heterochromatin in yeast. Genes Dev **16:**1528-39.

52. **Lustig, A. J.** 1998. Mechanisms of silencing in Saccharomyces cerevisiae. Curr Opin Genet Dev **8:**233-9.

53. **Mahoney, D. J., and J. R. Broach.** 1989. The HML mating-type cassette of Saccharomyces cerevisiae is regulated by two separate but functionally equivalent silencers. Mol Cell Biol **9:**4621-30.

54. **Meijsing, S. H., and A. E. Ehrenhofer-Murray.** 2001. The silencing complex SAS-I links histone acetylation to the assembly of repressed chromatin by CAF-I and Asf1 in Saccharomyces cerevisiae. Genes Dev **15:**3169-82.

55. **Merrick, C. J., and M. T. Duraisingh.** 2006. Heterochromatin-mediated control of virulence gene expression. Mol Microbiol **62:**612-20.

56. **Moazed, D., A. Kistler, A. Axelrod, J. Rine, and A. D. Johnson.** 1997. Silent information regulator protein complexes in Saccharomyces cerevisiae: a SIR2/SIR4 complex and evidence for a regulatory domain in SIR4 that inhibits its interaction with SIR3. Proc Natl Acad Sci U S A **94:**2186-91.

57. **Moretti, P., K. Freeman, L. Coodly, and D. Shore.** 1994. Evidence that a complex of SIR proteins interacts with the silencer and telomere-binding protein RAP1. Genes Dev **8:**2257-69.

58. **Moretti, P., and D. Shore.** 2001. Multiple interactions in Sir protein recruitment by Rap1p at silencers and telomeres in yeast. Mol Cell Biol **21:**8082-94.

59. **Mullen, J. R., P. S. Kayne, R. P. Moerschell, S. Tsunasawa, M. Gribskov, M. Colavito-Shepanski, M. Grunstein, F. Sherman, and R. Sternglanz.** 1989. Identification and characterization of genes and mutants for an N-terminal acetyltransferase from yeast. Embo J **8:**2067-75.

60. **Nelson, C. J., H. Santos-Rosa, and T. Kouzarides.** 2006. Proline isomerization of histone H3 regulates lysine methylation and gene expression. Cell **126:**905-16.

61. **Ng, H. H., Q. Feng, H. Wang, H. Erdjument-Bromage, P. Tempst, Y. Zhang, and K. Struhl.** 2002. Lysine methylation within the globular domain of histone H3 by Dot1 is important for telomeric silencing and Sir protein association. Genes Dev **16:**1518-27.

62. **Nimmo, E. R., G. Cranston, and R. C. Allshire.** 1994. Telomere-associated chromosome breakage in fission yeast results in variegated expression of adjacent genes. Embo J **13:**3801-11.

63. **Noguchi, K., A. Vassilev, S. Ghosh, J. L. Yates, and M. L. DePamphilis.** 2006. The BAH domain facilitates the ability of human Orc1 protein to activate replication origins in vivo. Embo J **25:**5372-82.

64. **Onishi, M., G. G. Liou, J. R. Buchberger, T. Walz, and D. Moazed.** 2007. Role of the conserved Sir3-BAH domain in nucleosome binding and silent chromatin assembly. Mol Cell **28:**1015-28.

65. **Paetkau, D. W., J. A. Riese, W. S. MacMorran, R. A. Woods, and R. D. Gietz.** 1994. Interaction of the yeast RAD7 and SIR3 proteins: implications for DNA repair and chromatin structure. Genes Dev **8:**2035-45.

66. **Park, E. C., and J. W. Szostak.** 1992. ARD1 and NAT1 proteins form a complex that has N-terminal acetyltransferase activity. Embo J **11:**2087-93.

67. **Park, J. H., M. S. Cosgrove, E. Youngman, C. Wolberger, and J. D. Boeke.** 2002. A core nucleosome surface crucial for transcriptional silencing. Nat Genet **32:**273-9.

68. **Pillus, L., and J. Rine.** 1989. Epigenetic inheritance of transcriptional states in S. cerevisiae. Cell **59:**637-47.

69. **Rusche, L. N., A. L. Kirchmaier, and J. Rine.** 2002. Ordered nucleation and spreading of silenced chromatin in Saccharomyces cerevisiae. Mol Biol Cell **13:**2207-22.

70. **Stone, E. M., C. Reifsnyder, M. McVey, B. Gazo, and L. Pillus.** 2000. Two classes of sir3 mutants enhance the sir1 mutant mating defect and abolish telomeric silencing in Saccharomyces cerevisiae. Genetics **155:**509-22.

71. **Stone, E. M., M. J. Swanson, A. M. Romeo, J. B. Hicks, and R. Sternglanz.** 1991. The SIR1 gene of Saccharomyces cerevisiae and its role as an extragenic suppressor of several mating-defective mutants. Mol Cell Biol **11:**2253-62.

72. **Strahl, B. D., and C. D. Allis.** 2000. The language of covalent histone modifications. Nature **403:**41-5.

73. **Strahl-Bolsinger, S., A. Hecht, K. Luo, and M. Grunstein.** 1997. SIR2 and SIR4 interactions differ in core and extended telomeric heterochromatin in yeast. Genes Dev **11:**83-93.

74. **Suka, N., Y. Suka, A. A. Carmen, J. Wu, and M. Grunstein.** 2001. Highly specific antibodies determine histone acetylation site usage in yeast heterochromatin and euchromatin. Mol Cell **8:**473-9.

75. **Thorne, A. W., D. Kmiciek, K. Mitchelson, P. Sautiere, and C. Crane-Robinson.** 1990. Patterns of histone acetylation. Eur J Biochem **193:**701-13.

76. **Triolo, T., and R. Sternglanz.** 1996. Role of interactions between the origin recognition complex and SIR1 in transcriptional silencing. Nature **381:**251-3.

77. **van Leeuwen, F., P. R. Gafken, and D. E. Gottschling.** 2002. Dot1p modulates silencing in yeast by methylation of the nucleosome core. Cell **109:**745-56.

78. **Wallace, J. A., and T. L. Orr-Weaver.** 2005. Replication of heterochromatin: insights into mechanisms of epigenetic inheritance. Chromosoma **114:**389-402.

79. **Wang, X., J. J. Connelly, C. L. Wang, and R. Sternglanz.** 2004. Importance of the Sir3 N terminus and its acetylation for yeast transcriptional silencing. Genetics **168:**547-51.

80. **Weiler, K. S., and B. T. Wakimoto.** 1995. Heterochromatin and gene expression in Drosophila. Annu Rev Genet **29:**577-605.

81. **Whiteway, M., R. Freedman, S. Van Arsdell, J. W. Szostak, and J. Thorner.** 1987. The yeast ARD1 gene product is required for repression of cryptic mating-type information at the HML locus. Mol Cell Biol **7:**3713-22.

82. **Wotton, D., and D. Shore.** 1997. A novel Rap1p-interacting factor, Rif2p, cooperates with Rif1p to regulate telomere length in Saccharomyces cerevisiae. Genes Dev **11:**748-60.

83. **Wright, J. H., D. E. Gottschling, and V. A. Zakian.** 1992. Saccharomyces telomeres assume a non-nucleosomal chromatin structure. Genes Dev **6:**197-210.

84. **Zakian, V. A.** 1996. Structure, function, and replication of Saccharomyces cerevisiae telomeres. Annu Rev Genet **30:**141-72.

85. **Zhang, Z., M. K. Hayashi, O. Merkel, B. Stillman, and R. M. Xu.** 2002. Structure and function of the BAH-containing domain of Orc1p in epigenetic silencing. Embo J **21:**4600-11.